Loughborough University

Pilkington Library

Author/Filing Title .. EAGLES

Vol. No. ..... Class Mark T

Please note that fines are charged on ALL overdue items.

OPEN SHELF COPY

~~NON-REFERENCE ONLY~~

0402391446

INTERACTIONS BETWEEN MACROMOLECULES AND MEMBRANES: THEIR EFFECTS ON BEER QUALITY.

A Doctoral thesis.

Submitted by WARREN PAUL EAGLES
in partial fulfilment of the requirements
for the award of Doctor of Philosophy of
Loughborough Unviersity.

September 2000.

© Warren Eagles 2000

Loughborough University
Library
Date Oct 01
Class
Acc No. 040239 144

ACKNOWLEDGEMENT

Firstly, may I thank my family for their support and encouragement during my years of education. Without that help I would never have reached this stage.

I would also like to thank my supervisor, Professor R.J. Wakeman for his guidance throughout this project. His strong encouragement towards the end ensured that the thesis was completed on time.

To all my friends around the department that have helped and supported me. Special thanks to Mel, Andy, Simon, Sion, Suella, Crazy, Jon, Alan and Matt, they were always willing to listen and offer advice when it was most needed.

Many thanks must also go to Zubin, Justin and Mr C.J. Manning, fellow workers in the separations laboratory whose help during this project proved invaluable.

I am most grateful to the Department of Chemical Engineering for giving me the opportunity to do a Ph.D. and to the Biotechnology and Biological Sciences research council for funding. The use of the Brewing Research library was much appreciated during the preparation of the literature review.

Finally, I must thank the department for its technical support especially Paul for solving the computing problems and Dave for his extensive help with HPLC.

Cheers to you all.

ABSTRACT

When filtering beer at pore sizes of 0.45 μm and below, some desirable components may be lost, even though they are orders of magnitude smaller than the pores. In this work, a model beer solution of pure components has been filtered through 0.2 μm membranes to investigate this problem. Starch (a model for the long chain carbohydrates) at a concentration of 1500 mg $l^{-1}$and casein (a model for the protein fraction) at a concentration of 150 mg l^{-1} were found to result in reduced permeate fluxes in the region of 20-40 l m^{-2} h^{-1}.

Both starch and casein suffered high/total rejections. Citric acid suffered a 50% rejection, but this was reduced/eliminated in the presence of casein, possibly due to the surface charge on the protein. At lower fluxes there was a slight rejection of ethanol (≈3%) and a 20% rejection of ethyl acetate. In systems containing both starch and casein, changes in starch concentration were shown to dominate the permeate flux behaviour, whilst casein played an important role in molecule rejection.

Casein was found to be responsible for greatly influencing the level of catechin and maltose rejection. With catechin the permeate flux was also found to increase. This has been attributed to the formation of insoluble complexes between the protein and the polyphenol, as is widely acknowledged in the brewing industry. The increased rejection with maltose was further investigated with a range of mono/disaccharides. The disaccharides displayed twice the rejection of the monosaccharides. This may be explained by the adsorption of a single sugar ring to the protein. Hence, twice the mass of disaccharide may be adsorbed at a protein site. Calcium ions were found to inhibit the trends in rejection shown by casein, as they cause some casein fractions to precipitate.

CONTENTS

ACKNOWLEDGEMENTS		i
ABSTRACT		ii
CONTENTS		iii
LIST OF FIGURES		viii
LIST OF TABLES		x
CHAPTER 1	**INTRODUCTION**	1
1.1	OUTLINE OF THE BREWING PROCESS	1
1.1.1	Malting	1
1.1.2	Mashing	2
1.1.3	Wort separation	3
1.1.4	Fermentation	3
1.1.5	Conditioning	4
1.2	PROJECT RATIONALE	4
CHAPTER 2	**BEER MICROFILTRATION – LITERATURE REVIEW**	
2.1	CURRENT BEER FILTRATION PRACTISE	6
2.2	CROSSFLOW MICROFILTRATION OF BEER	7
2.2.1	Permeate composition	8
2.2.2	Economics	14
2.2.3	Crossflow velocity	17
2.2.4	Transmembrane pressure	19
2.2.5	Temperature	22
2.2.6	Feed type	24
2.2.7	Membrane material	29
2.2.8	Pore size	33
2.2.9	Reduction of fouling	35
2.2.10	The "gel" layer and fouling mechanisms	39

CHAPTER 3 PROTEIN CROSSFLOW FILTRATION 42

3.1 PROTEIN CONCENTRATION 42

3.2 PROTEIN TYPE 44

3.3 MEMBRANE PORE SIZE AND STRUCTURE 45

3.4 MEMBRANE MATERIAL 46

3.5 TRANSMEMBRANE PRESSURE 47

3.6 CROSSFLOW VELOCITY 48

3.7 TEMPERATURE 51

3.8 pH 51

3.9 IONIC STRENGTH 52

3.10 MECHANISMS 54

CHAPTER 4 EXPERIMENTAL MATERIALS AND METHODS 59

4.1 CHOICE OF MATERIALS 59

4.1.1 Beer composition 59

4.1.2 Ethanol 64

4.1.3 Glycerol 64

4.1.4 Maltose 64

4.1.5 Citric acid 65

4.1.6 Starch 65

4.1.7 Casein 66

4.1.8 Calcium sulphate 68

4.1.9 Catechin 69

4.1.10 Ethyl acetate 69

4.1.11 Structures of components 70

4.2 EXPERIMENTAL MATERIALS 71

4.2.1 Chemicals 71

4.2.2 Membranes 72

4.3 EXPERIMENTAL APPARATUS 74

4.3.1 Description 74

4.3.2 Calibration 77

4.4 FEED PREPARATION 80
4.4.1 Starch 80
4.4.2 Casein 81
4.4.3 Calcium sulphate 81
4.4.4 Catechin 81
4.4.5 Feed composition 82
4.4.6 Experimental feed 82
4.5 EXPERIMENTAL PROCEDURE 83
4.5.1 Preparation 83
4.5.2 Filtration 83
4.5.3 Cleaning 84

CHAPTER 5 ANALYTICAL TECHNIQUES 85
5.1 HIGH PRESSURE LIQUID CHROMATOGRAPHY (HPLC) 85
5.1.1 Apparatus 86
5.1.1.1 Column 88
5.1.1.2 Detector 88
5.1.2 Eluent preparation 88
5.1.3 Sample preparation 89
5.1.4. Acid/alcohol/carbohydrate analysis 89
5.1.4.1 Without maltose 89
5.1.4.2 With maltose 90
5.1.5 Ethyl acetate analysis 91
5.1.6 Calibration 92
5.2 STARCH ANALYSIS 93
5.2.1 Enzymatic hydrolysis 93
5.2.2 Iodine binding 94
5.3 CALCIUM ANALYSIS 95
5.4 PROTEIN ANALYSIS 97
5.5 CATECHIN ANALYSIS 99

CHAPTER 6 RESULTS AND DISCUSSION 101
6.1 FEED SOLUTION 101
6.2 EFFECT OF ACID TYPE 103
6.3 STARCH ADDITION 106
6.3.1 Effect of starch concentration 107
6.3.2 Effect of crossflow velocity 109
6.3.3 Effect of transmembrane pressure 111
6.4 CASEIN ADDITION 111
6.4.1 Effect of casein concentration 114
6.4.2 Effect of crossflow velocity 115
6.4.3 Effect of transmembrane pressure 117
6.5 STARCH AND CASEIN ADDITION 118
6.6 EFFECT OF SUGAR TYPE 119
6.7 CALCIUM ADDITION 121
6.7.1 Effect on feed containing starch 121
6.7.2 Effect on feed containing casein 123
6.7.3 Effect on feed containing both starch and casein 124
6.8 CATECHIN ADDITION 126
6.8.1 Effect on feed containing starch 127
6.8.2 Effect on feed containing casein 127
6.8.3 Effect on feed containing both starch and casein 128
6.8.4 Effect on feed containing starch, casein and calcium 129
6.9 ETHYL ACETATE ADDITION 129
6.9.1 Effect on feed containing starch 129
6.9.2 Effect on feed containing casein 130
6.9.3 Effect on feed containing both starch and casein 131
6.9.4 Effect on feed containing all components 131
6.10 EFFECT OF MEMBRANE TYPE 132
6.11 EFFECT OF PERMEATE FLUX ON REJECTION 135
6.12 FOULING MECHANISMS 137

CHAPTER 7	**CONCLUSIONS**	142
REFERENCES		145
APPENDIX 1	ANALYTICAL METHODS	I
APPENDIX 2	CALCULATIONS	XX
APPENDIX 3	MEMBRANE CHARACTERISATION	XXVII
APPENDIX 4	DEFINITION OF UNITS	XXX

LIST OF FIGURES

Figure no.

1.1:	An outline of the brewing process.	2
2.1:	The effect of crossflow velocity on steady state filtrate flux.	18
2.2:	Effect of transmembrane pressure on maturation vessel bottoms.	20
2.3:	Effect of membrane type on filtrate flux - Kieselguhr filtrate.	31
2.4:	Effect of membrane type on filtrate flux - cellar beer.	32
2.5:	Effect of backflush.	37
2.6:	Effect of backflush on bitterness and present gravity (pilot scale)	38
2.7:	Proposed gel layer of Lenoel *et al.* (1994).	40
3.1:	Effect of protein precipitate concentration on permeate flux (Taylor *et al.* (1994)).	43
3.2:	The effect of crossflow velocity on permeate flux (Taylor *et al.* (1994)).	50
4.1:	Schematic of experimental rig.	75
4.2:	Photograph of the apparatus.	76
4.3:	Diagram of membrane cell and dimensions.	78
4.4:	Photograph of the filtration cell.	79
5.1:	Schematic of HPLC apparatus.	87
5.2:	A typical chromatogram.	91
5.3:	A typical chromatogram.	92
5.4:	Starch analysis calibration data.	95
5.5:	AA calibration data.	97
5.6:	Protein analysis calibration data.	98
5.7:	Catechin analysis calibration data.	100
6.1:	Flux decline with base solution.	102
6.2:	Citric acid rejection.	103
6.3:	Rejection of different acid types.	104
6.4a:	Effect of pH on acetic acid species.	105
6.4b:	Effect of pH on succinic acid species.	105

6.4c: Effect of pH on citric acid species. 106
6.5: Effect of starch addition (1000mgl^{-1}) on flux. 107
6.6: Effect of starch concentration on flux. 108
6.7: Effect of crossflow velocity on flux. 110
6.8: Effect of casein addition (200mgl^{-1}) on flux. 112
6.9: Effect of casein addition (200mgl^{-1}) on ethanol and maltose rejection. 112
6.10: Zeta potential vs. pH plot for starch and casein. 113
6.11: Effect of casein concentration on flux. 115
6.12: Effect of crossflow velocity on flux. 116
6.13: Effect of transmembrane pressure on flux. 117
6.14: Rejections of different sugars. 120
6.15: Suggested mechanism for sugar rejection with casein. 121
6.16: Effect of calcium ions on filtrate flux in the presence of starch. 122
6.17: Effect of calcium ions on filtrate flux in the presence of casein. 123
6.18: Effect of calcium ions on ethanol rejection in the presence of casein. 124
6.19: Effect of calcium ions on filtrate flux in the presence of starch and casein. 125
6.20: Effect of membrane type on flux. 133
6.21: Dependence of permeate flux on rejection of sugars with casein. 136
6.22: A typical standard blocking model plot for casein experiments. 138
6.23 A typical cake filtration plot for casein experiments. 138
6.24 Cake filtration plot for increases in casein concentration. 140
6.25: Cake filtration plot for casein in the presence of calcium. 141
6.26 Cake filtration plot for increases in starch concentration. 141

LIST OF TABLES

Table no.

2.1:	Analysis of filtered beer.	9
2.2:	Analysis of beer recovered from spent yeast.	9
2.3:	GC analysis of beer recovered from spent yeast.	10
2.4:	Comparison of unfiltered/filtered fermentation bottoms.	11
2.5:	Comparison of unfiltered/filtered fermentation bottoms (volatiles).	12
2.6:	Beer analyses with time.	13
2.7:	Economics for a 1.8mm internal membrane.	14
2.8:	Economics for a 3mm internal membrane.	15
2.9:	Economical fluxes for filtration of two beer types.	16
2.10:	Effect of crossflow velocity on filtrate flux.	18
2.11:	Effect of crossflow velocity on beer component transmission.	19
2.12:	Effect of transmembrane pressure on filtrate flux.	21
2.13:	Effect of TMP on beer component transmission and flux.	21
2.14:	Effect of temperature on beer component transmission and flux.	23
2.15:	Filtration characteristics of different feeds.	24
2.16:	Comparison of non-volatiles and method of separation (microfiltration and centrifugation).	24
2.17:	Comparison of volatiles and method of separation (microfiltration and centrifugation).	25
2.18:	Beer analysis data for increasing yeast concentrations.	26
2.19:	Analyses of different beer types.	28
2.20:	Beer/membrane interactions.	30
2.21:	Effect of membrane type on beer quality - Kieselguhr filtrate.	31
2.22:	Effect of membrane type on beer quality - cellar beer.	32
2.23:	Beer analyses with pore size.	33
2.24:	Optimisation of the backflushing process.	36
2.25:	Optimised multi-stage backflushing.	37
3.1:	Constants for the generalised blocking model.	56

4.1: Beer composition given by Hough *et al.* (1982a, 1982b). 60
4.2: Basic beer composition given by René and Maingonnat (1993). 61
4.3: Typical beer composition of a Pilsen beer given by Moll (1991). 62
4.4: Amino acid composition of casein and two beer proteins. 68
4.5: Organic components in model feed stream: Their role and structure. 70
4.6: Beer component suppliers and purity. 72
4.7: Membrane materials and pore sizes. 73
4.8: Structures of membrane materials. 73
4.9: Example of feed composition calculation. 82
5.1: HPLC operating parameters for acid/alcohol/carbohydrate analysis without maltose. 90
5.2: HPLC operating parameters for acid/alcohol/carbohydrate analysis. 90
5.3: HPLC operating parameters for ethyl acetate analysis. 92
5.4: Operating conditions for the atomic adsorption spectrophotometer. 96
6.1: Effect of acid type on flux and rejection. 103
6.2: Fraction and charge density of acid species. 104
6.3: Effect of starch on steady state rejection. 108
6.4: Effect of crossflow velocity on steady state rejection. 110
6.5: Effect of transmembrane pressure on steady state rejection. 111
6.6: Effect of casein concentration on steady state rejection. 115
6.7: Effect of crossflow velocity on steady state rejection. 116
6.8: Effect of transmembrane pressure on steady state rejection. 117
6.9: Effect of casein concentration on steady state rejection in the presence of both starch and casein. 118
6.10: Steady state rejection/flux for different sugars. 120
6.11: Effect of calcium on steady state rejections in the presence of starch. 122
6.12: Effect of calcium on steady sate rejections in the presence of casein. 123
6.13: Effect of calcium on steady state rejections in the presence of starch and casein. 126
6.14: Effect of catechin on steady state rejection on base solution only. 126
6.15: Effect of catechin on steady state rejections in the presence of starch. 127
6.16: Effect of catechin on steady state rejections in the presence of casein. 128

6.17: Effect of catechin on steady state rejections in the presence of both starch and casein. 128

6.18: Effect of catechin on steady state rejections in the presence of starch, casein and calcium. 129

6.19: Effect of ethyl acetate on steady state rejections in the presence of starch. 130

6.20: Effect of ethyl acetate on steady state rejections in the presence of casein. 130

6.21: Effect of ethyl acetate on steady state rejections in the presence of both starch and casein. 131

6.22: Effect of ethyl acetate on steady state rejections with all components present. 132

6.23: Effect of membrane type on steady state rejection. 133

6.24: Properties of 0.2μm membranes. 134

6.25 Effect of concentration and crossflow velocity on the specific cake resistance of casein deposits. 139

CHAPTER 1
INTRODUCTION

This section contains an outline of the brewing process, introducing brewing terminology used throughout this work, providing an understanding of the origin of components and also identifying the stages at which crossflow microfiltration may be used in the brewing process. The rationale for this work is then discussed.

1.1 OUTLINE OF THE BREWING PROCESS

The sources of reference for this first section are Hough *et al.* (1982a, 1982b), Hough (1985), Pollock (1981) and Moll (1991).

In order to produce beer, five basic ingredients are required: barley, water, sugar, hops, yeast. Barley may, however, be replaced by some other cereal crop such as maize, wheat, rice, etc. The production route also requires five main steps: malting, mashing, wort separation, fermentation and conditioning. The end result of the processing is a coloured liquid containing hundreds of different compounds. Each compound is vital in order to obtain the desired colour/flavour/aroma/head characteristics. To this end, the modern day plant requires close process control. Beer production is traditionally a batch operation. Continuous processes are now available which reduce downtime but lead to a greater risk of yeast infection. The five process steps are detailed below. An outline of the beer production process is shown in Figure 1.1.

1.1.1 Malting

The raw cereal is steeped (soaked) in water at 10-15°C and then kept in air at a controlled humidity until it begins to germinate. This produces enzymes that are capable of converting starches to fermentable sugars. The cereal is then kilned, initially below 100°C to stop the reactions present and reduce the moisture content.

Higher temperature roasting results in distinctive colours and flavours that are carried through to the final product. The final dry product is called malt. This is then milled prior to mashing.

1.1.2 Mashing

Mashing is the step in which the wanted chemicals are removed from the barley and taken up by the process liquor (brewing water). Modern mashing vessels are jacketed, for steam heating, containing a large impeller rotating at 5-50 revs./minute. The milled malt (grist) and water at 40-45°C are mixed, prior to heating at 1°C/minute to a final temperature of around 70°C. This allows the enzymes to break down longer chain molecules for fermentation. There are variations on this procedure where the cereal is cooked or the temperature profile is programmed.

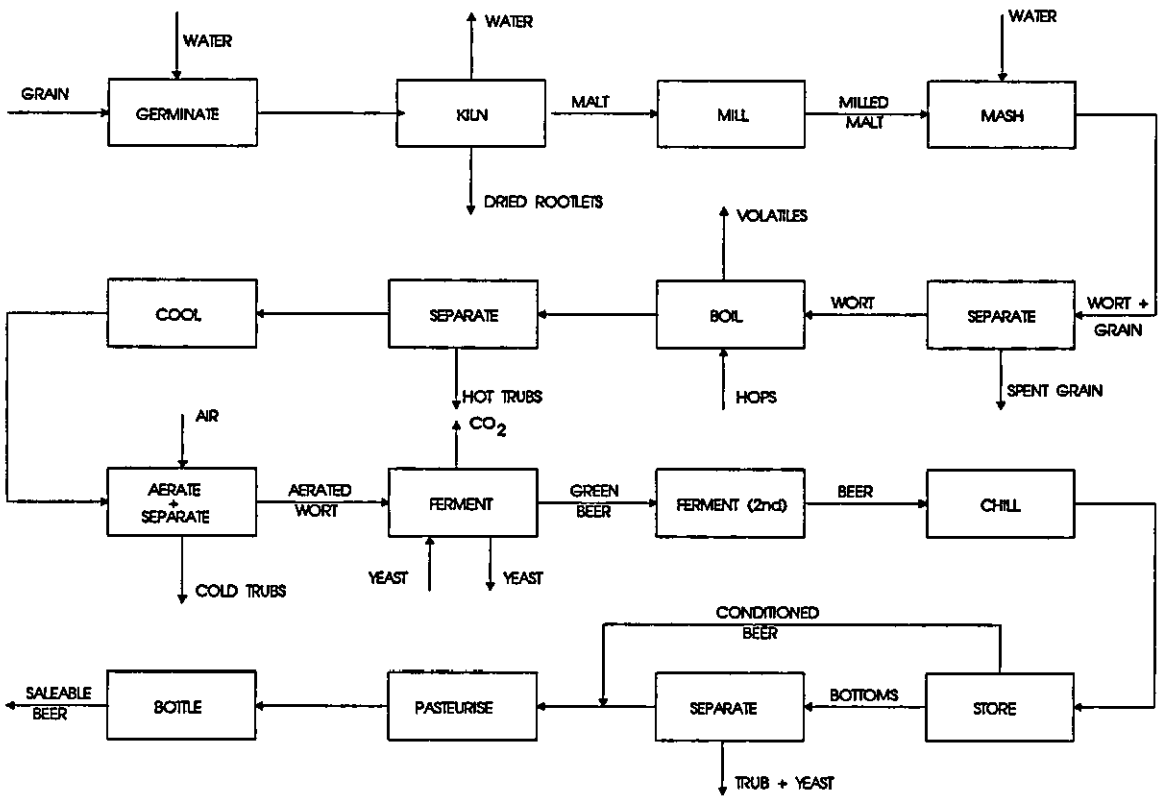

Figure 1.1: An outline of the brewing process.

1.1.3 Wort separation

The mash is then transferred to a lauter tun (although in some cases remains in the mashing vessel) containing a slotted bottom. The spent grains form a permeable layer at the base of the vessel. A series of rotating rakes are then used to avoid the build up of too high a pressure drop across the grain bed. The resulting sugar laden solution (wort) is then drained by gravity and recycled until the turbidity reaches a suitable level. The wort is drained off and the bed is washed (sparged) with brewing liquor to wash out any remaining sugars.

An alternative modern process is to use a mash filter. The mash is fed to chambers between permeable plates where it may later be compressed and washed.

The wort is boiled in a vessel with either a heated jacket or an external heat exchanger (calandria). During boiling, hops are added. The boiling promotes wort/hop reactions, distils volatiles, coagulates protein and tannins (trubs), sterilises the mixture and degrades enzymes. The coagulated matter may then be removed by centrifugation or by a whirlpool. Crossflow microfiltration may be an alternative here. Prior to fermentation the wort is cooled to 15°C, usually in a plate and frame heat exchanger, and aerated.

1.1.4 Fermentation

During fermentation, fermentable carbohydrate matter is converted to alcohol (and some other metabolic by-products) using yeast. Other carbohydrate matter remains relatively untouched. Generally, two types of tank are used. Either an open top square tank or an enclosed cylindro-conical vessel. In either case the temperature must be controlled to ensure that the yeast remains viable and produces the compounds required. Fermentation typically takes 4-7 days at 12°C. After this time the yeast is removed by skimming it from the top of an open tank or collecting from the bottom of a cylindro-conical tank. This yeast contains entrained beer and is known as

fermentation tank bottoms. Crossflow filtration may be used to recover the beer from an otherwise waste stream.

1.1.5 Conditioning

On leaving the fermenter, beer is passed into a closed vessel where it is conditioned. The small amount of remaining yeast and carbohydrate continue to react at 10°C for several days. This enhances flavour and aroma and allows CO_2 to dissolve. Finings are then added to coagulate the yeast and trub. Along with entrained beer, these are the tank bottoms. It is expensive to send this waste down the drain and hence it is filtered. The usual methods of filtration are the leaf filter, rotary vacuum and the plate and frame filter. Due to the relatively large pore sizes of cloth and small particle sizes remaining in beer, a filtration aid is required. Crossflow filtration is an alternative.

By this stage all that remains to be done is to pasteurise the beer and package it. If the beer is bottled it may be pasteurised within the bottle.

1.2 PROJECT RATIONALE

In this work, we are concerned with the use of crossflow filtration for beer clarification. It may be used to recover valuable beer from waste fermentation bottoms, or clarify conditioned beer and sterilise it in one operation. The use of pore sizes of 0.2 μm or less would ensure a sterile product. However, even though the pore sizes are many times greater than the molecules present, compounds essential to the final taste/aroma/head forming properties have been reported to be removed.

The aim of this work is therefore to investigate this exclusion of molecules from the permeate stream. There are several ways in which this could be achieved. Beers of differing, but known, composition could be filtered and the permeate stream analysed. Due to the complex composition of beer, it would be difficult to ascertain the effects of individual components. An alternative approach (Gan *et al.* 1997) is to enzymatically breakdown specific components. This then leads to confusion as to

whether changes in the system are due to the removal of the component or the presence of enzymes and their by-products. The approach used in this work is to build a model beer solution, based on a knowledge of the components present. In this way the action of specific components may be assessed and the subsequent analysis of the permeate is simplified.

CHAPTER 2

BEER MICROFILTRATION - LITERATURE REVIEW

A summary of the current methods of beer filtration/pasteurisation is included in this section, along with alternative technologies. It should be noted that this work is only concerned with the filtration of beer after the fermentation stage, although crossflow filtration methods could be applied to earlier separation steps in the brewing process, such as the separation of trub from wort. Beer microfiltration research is reviewed, but it should be noted that much of the literature is written from an industrial viewpoint and, as such, is of a more commercial nature than a fundamental one.

2.1 CURRENT BEER FILTRATION PRACTISE

Most beer filtration is carried out with the filter aid kieselguhr (diatomaceous earth) or perlite, generally on either plate and frame or leaf and candle type filters. Beer is mixed with the filter aid, in slurry form, and pumped into the filter. It is the introduction of the filter aid that reduces the effective pore size to produce the required bright product. The filter aid particles contain fine pores, although these are not thought to greatly influence the process. It is the void spaces in the particle bed that effectively sieve out the unwanted solids (Reed, 1989b). Often, the filtrate may later require the removal of fines (polishing) and this may typically be performed by means of a cartridge filter.

The greatest problems with this method are the use of the filter aid. It is a fine powder and must therefore be treated with care. It cannot be regenerated and large quantities must therefore be disposed. Due to the cost of disposing of this material, the filtration process has been optimised over time. More recently the use of automatic dosing systems has been introduced, a thorough study of which has been carried out recently by Freeman *et al.* (1995) to produce a means of modelling the process in order to minimise cost. In order to continue the use of current methods and equipment, alternative body feeds have been sought (Bamforth and Reed (1994), McKechnie

(1995)), such as a regenerable cellulose/polyvinylpyrollidone, along with methods of regenerating kieselguhr.

Other developments have been reviewed by McKechnie (1995) and O'Shaughnessy and McKechnie (1996). Some methods are alternatives, whilst others reduce the solids loading on subsequent separation stages. For example deep bed filters containing sand (Reed *et al.* (1983), Atkinson *et al.* (1985)) or compressed fibres may be used as an alternative but would require a subsequent "polishing stage". The use of hydrocyclones or ultrasonics may also be used to reduce the solids. Coagulation or flocculation may be employed to reduce the quantity of fine material prior to filtration or in order to aid settling.

2.2 CROSSFLOW MICROFILTRATION OF BEER

Despite developments in other areas of beer filtration, crossflow filtration has the potential to be more economical and has recently been the subject of further research. It may potentially be used in three areas. They are trub separation from wort, yeast separation from fermentation tank bottoms and a combination of the removal of suspended matter from conditioned beer with sterilisation and polishing. Here, we are only concerned with the latter parts of the brewing process, i.e. the fermented product. The removal of suspended matter may be achieved in several ways, as given in the previous section. Conventional brewing techniques dispose of most beer-laden tank bottoms. Crossflow filtration allows valuable beer to be recovered. For the removal of suspended matter from conditioned beer, the advantage of beer microfiltration is that it negates the need to use kieselguhr or other filter aids and may produce a beer that does not require subsequent pasteurisation. Hence it does not create waste that requires dumping in a landfill site. It provides a system where air exclusion is easy to achieve which is desirable to maintain the quality of the finished product. When performed, the sterilisation of beer is generally carried out by heat treating the bottles or kegs or by means of cartridge filters and this process may also save on a costly heating process.

Most papers on the subject tend to look at beer crossflow filtration from an industrial viewpoint and are therefore more concerned with the economics and optimum operating conditions of the process than an understanding of the fouling processes. The effects of changing process parameters have been explored by several researchers and are relatively well established in all areas of crossflow microfiltration but often the behaviour of the individual components has not been closely examined. Unlike the filtration of proteins, there is not an abundance of published fundamental literature on the crossflow filtration of beer.

As is the problem with crossflow microfiltration, flux decays with time. For example, Le (1987) filtered maturation tank bottoms at 2 ms^{-1}, 140 kPa through a range of pore sizes. In each case there was a sharp drop in flux over the first 20 minutes followed by a much smaller decline over several hours, irrespective of whether fresh or recycled feed was used.

Buhler *et al.* (1993), Burrell *et al.* (1994a) and Ryder *et al.* (1988) have all shown that filtration of beer through membrane pores of 0.5 μm or less is capable of rendering the permeate stream sterile. However, filtration at these pore sizes may lead to the removal of components that are important for bitterness, haze and foam retention.

2.2.1 Permeate composition.

Leeder and Girr (1994) filtered a yeast-laden beer through a 0.9 μm ceramic membrane (90 kPa, 3-4.6 m s^{-1}, 10°F). The analysis of the permeate and retentate is shown in Table 2.1. In the table O.G. is the original gravity, a measure of nonfermented extract combined with the amount of extract required to produce the ethanol present, and the P.G. is the present gravity, a measure of the nonfermented extract remaining in the beer. (Other units used throughout this section are defined in Appendix 4). A viscosity decrease of 50% was identified (possibly due to β-glucan losses), along with a fall of 10-15% in total nitrogen, although the amino nitrogen remained unchanged. The concentration of the aroma substances (higher alcohols,

acetate esters, fatty acids, fatty acid esters and hop oil constituents) remained the same or decreased.

Parameter	Standard. bright beer	Permeate	Retentate
O.G. (°Pl)	11.2	10.9	11.6
P.G. (°Pl)	3.4	2.9	3.7
Alcohol (vol. %)	5.1	5.2	5.2
Colour (EBC)	7.4	7.8	10.5
pH	4.23	4.55	4.62
Bitterness (EBC)	24.4	19.6	29.6
Haze	0.4	0 2	1.5
Yeast (/100ml)	<5	0	>10

Table 2.1: Analysis of filtered beer.

Similar studies by Muller (1992) and Schlenker (1998) filtered a yeast-laden beer through a 0.2 μm ceramic membrane. Table 2.2 shows the standard analyses of the feed and permeate streams, whilst Table 2.3 shows the analysis of the volatiles in the streams. The high decrease in real extract may be explained by a 6% protein reduction and an 87% β-glucan reduction (amongst others).

	Spent yeast	Recovered beer	Yield of substances
Orig. extract	11.91%	11.36%	95.4%
App. extract	2.22%	1.77%	
Real extract	4.05%	3.58%	88.4%
Alcohol	4.05%	4.00%	98.8%
Bitterness EBC	34	34	100%
pH	5.03	4.95	
Colour EBC	14.6	9.6	

Table 2.2: Analysis of beer recovered from spent yeast.

	Recovered	Blended	Original
	mg l^{-1}		
Ethyl acetate	24.5	10.5	14.7
i-amyl acetate	2.43	4.13	4 41
2-phenylethyl acetate	0.11	0.40	0.27
Ethyl capronate	0.31	0.43	0.48
Ethyl caprylate	0.38	0.32	0.38
i-butanol	11.3	14.6	15.4
i-amyl alcohol	56.5	71.8	79.2
2-phenyl ethanol	41.2	37.0	35.0
Caprylic acid	12.2	4.1	3.6

Table 2.3: GC analysis of beer recovered from spent yeast.

Most components are less concentrated in the recovered beer than in the original beer. However the concentration of ethyl acetate, 2-phenyl ethanol and caprylic acid increase. This may possibly be due to extra material being leached from the yeast cells. The concentration of ethyl caprylate remains unchanged.

The analytical values of beer recovered from yeast compared to the beer recovered from the fermenter are shown in Tables 2.4 and 2.5 (volatiles), following work by Walla (1994). It may be seen that reductions in original gravity, soluble nitrogen, polyphenol, antocyanogens, β-glucans and viscosity have occurred. Bearing in mind the difference in alcohol levels, it is suggested that dilution has occurred. The drop in β-glucans suggests that they are retained by the membrane, as they are present in colloidal form. Increases in bitter substances and some volatile components are probably due to secondary fermentation during filtration or leaching from the yeast cells.

	Filtered	Unfiltered
Original gravity (GG%)	10.97	11.91
Alcohol (GG%)	3.42	3.82
Apparent extract (GG%)	3.46	3.94
Specific gravity at 20°C	1.01355	1.01545
Apparent attenuation (%)	69	68
pH	4.71	4.69
Bitterness (EBU)	23.5	24.7
Polyphenols (mg l^{-1})	23.1	229
Anthocyanogens (mg l^{-1})	96	98
β-glucans	249	435
Viscosity (mPa s)	1.60	1.62

Table 2.4: Comparison of unfiltered/filtered fermentation bottoms.

Filtering yeast slurries and tank bottoms through a 0.45 μm ceramic membrane, Lenoël (1990) reported that the recovered beer could be blended with normal beer up to 5% without a significant change in quality, in terms of taste analysis. However, analytically, the filtrate was found to be higher in alcohols and bitterness, yet lower in extract and foam retention, the later two suggesting the retention of proteins and dextrins. An optimum operating temperature was found to be around 5°C with a velocity of 3 m s^{-1} and a pore size of 0.8 μm. Treatment of the membrane was found to be of slight benefit over no treatment, but treatment with caustic had a significantly deleterious effect.

	Filtered	Unfiltered
	mg l^{-1}	
Acetic acid ethyl ester	18.60	10.40
Acetic acid butyl ester	0.12	0.10
Acetic acid isopentyl ester	2.10	1.30
Acetic acid phenyl ethyl ester	0.77	0.58
Octanoic acid ethyl ester	0.12	0.28
Decanoic acid ethyl ester	0.11	0.15
n-propyl alcohol	12.90	8.10
i-butyl alcohol	10.20	6.10
Amyl alcohols	59.20	37.30
2-phenyl ethanol	21.07	16.61
Hexanoic acid	2.40	1.61
Octanoic acid	5.09	3.12
Nonanoic acid	0.54	0.42
Decanoic acid	0.51	1.22
Total diacetyl	0.24	0.15
Total 2,3-pentanedione	0.13	0.10

Table 2.5: Comparison of unfiltered/filtered fermentation bottoms (volatiles).

Unfined conditioned beer has been filtered (<0.5 μm, 6 m s^{-1}, -1°C) by Noble (1988). The changes in permeate (Perm.) and retentate (Ret.) quality with time are shown in Table 2.6.

The data suggests that the analyses for the permeate and feed are somewhat similar after 140 minutes of filtration. The data for P.G., % alcohol and bitters suggest that although these values are initially lower than the feed, they reach similar values with time. This has been confirmed for bitters by Mylius and Reiter (1988).

	Feed	Ret.	Perm.	Ret	Perm.	Ret.	Perm.	Ret.	Perm.
Time (mins)	0	Start		+20		+100		+140	
O.G.	1060 2	1057 0	1056 1	1059 7	1059.0	1060 3	1060.3	1060.7	1060.5
P.G	6.5	6 2	6 0	6 6	6.3	6 7	6 6	6 8	6 6
% Alcohol	7 07	6 68	6.58	6 99	6.94	7.06	7.07	7.11	7.10
Colour	14		13.5		13		13 5		13
Bitters	48 2	43.5	42.4	49.0	46.0	52.0	47 8	52.7	48.7
Haze (EBC)	o/s		1 4		1 6		1.8		1.85
Flux		140		160		130		120	

Table 2.6: Beer analyses with time.

In a review, Peachey (1991) mentions the fate of β-glucan on filtration. Generally, β-glucan and carbohydrate material is seen as being potentially responsible for extract removal. He states that Oechsle found lower β-glucan levels in the permeate. Cantrell *et al.* (1985) and Ryder *et al.* (1988) reported the retention of β-glucan, dextrins, proteins and polymeric materials, whilst Hansen (1989) showed complete rejection of β-glucan.

Conclusion

Long chain carbohydrate and protein matter appear to be retained by microfiltration membranes with a pore size of less than 0.45 μm. Generally, components tend to be lost under these circumstances. However, when large amounts of yeast are present, concentrations of the metabolic by-products (alcohols, esters, acids, etc.) may increase as they are leached from the yeast cells.

2.2.2 Economics

For any new process to be accepted, it must be economical. Early economic evaluations need to be promising before time and money is invested in development work. Initial estimates tend to use limited laboratory data with a wide range of assumptions. Clearly, the actual economics of the process become clearer as more work is carried out and the process is scaled up. Beer filterability may change from beer to beer and this would have an effect on the economics.

Economic evaluations carried out at full scale by Kiefer (1991) highlighted the importance of flux requirement and module design. If a system provides a lower flux then a larger filtration area is required to clarify a given volume in a given time. The size of the channel and module configuration also have a bearing on the cost. Tables 2.7 and 2.8 indicate the costs of running plants in both a series and parallel mode with membrane channels of 1.8 mm and 3 mm. The underlying assumptions are that the beer has to be processed at 250 hl h^{-1} at a viscosity of 3 mPa s with optimum operating conditions of a Reynolds number of 3000 and a maximum pressure drop across the module of 1.5 bar.

The recirculation volumes and hence power consumption are large. Clearly, running membrane modules in series looks somewhat unattractive.

	Series	Parallel
Flux rate	20 l m^{-2} h^{-1}	35 l m^{-2} h^{-1}
Membrane area	1250 m^2	715 m^2
Recirculation	202500 hl h^{-1}	116000 hl h^{-1}
Number of pumps	104	59
Power	1750 kW	990 kW
Total cost	5.70 SFr hl^{-1}	3.34 SFr hl^{-1}

Table 2.7: Economics for a 1.8 mm internal membrane.

It should be noted, however, that it is unclear whether the series configuration here is a straightforward series or cascade system. It is also somewhat surprising that the recirculation volumes are greater for the smaller diameter channel, as there would be a greater membrane surface area per volume and lower recirculation volumes would therefore be expected.

	Series	Parallel
Flux rate	20 l m^{-2} h^{-1}	35 l m^{-2} h^{-1}
Membrane area	1250 m^2	715 m^2
Recirculation	42500 hl h^{-1}	24300 hl h^{-1}
Number of pumps	21	12
Power	352 kW	202 kW
Total cost	2.67 SFr hl^{-1}	1.62 SFr hl^{-1}

Table 2.8: Economics for a 3 mm internal membrane.

Operating costs for the recovery of beer from yeast, given the experience of operating a plant for two years, have been given by Müller (1992). 6 mm ceramic membranes were used in a parallel configuration. The operating costs are equivalent to 66 p hl^{-1}, which is close to the value given Kiefer (1991) for a 3 mm internal diameter membrane in a parallel configuration (69 p hl^{-1}). After a payback period of 3 years and assuming a value of £3.90 /hl^{-1} of recovered beer, the saving would be in the region of £3.25 /hl^{-1}.

The economics of beer filtration have also been shown to be dependant on the beer type by Bühler *et al.* (1993), Burrell and Reed (1994a) and Burrell *et al.* (1994b). The economical fluxes required to filter two different beers are given in Table 2.9. Each beer was then filtered through a 0.5 μm alumina membrane with 2 mm channels. Beer A showed economical fluxes (still above 20 l m^{-2} h^{-1} after 20 hours), whilst beer B would only have been economical for short runs of less than 5 hours with very short down times. In this case the crossflow filtration of beer B would not have been economical. Further work was carried out on tank bottoms (7% w/w dry solids) on a

1.3 μm alumina membrane, as this gave a greater flux, although the clarity was poorer. The clarity was still acceptable for blending the beer.

To replace:	Economical flux ($l\ m^{-2} h^{-1}$)	
	Beer A	Beer B
Kieselguhr filtration (KGF)	25.8	14.9
KGF + pasteurisation (P)	17.4	11.9
KGF + P + bottoms filtration (BF)	13.8	9.9
KGF + P + BF + reduced beer losses	12.4	9.2

Table 2.9: Economical fluxes for filtration of two beer types.

Le (1987) showed that crossflow microfiltration could be economically viable for beer recovery. It was assumed that 7 days worth of bottoms could be processed in 24 hours, achieving an effluent of 150 g l^{-1} solids. Projected recovery costs of 90 p hl^{-1} for fermentation vessel bottoms and £6 /hl for maturation vessel bottoms were stated. Assuming a value of the recovered beer in the region of £3.90 /hl, then crossflow filtration of fermentation bottoms would save £3 /hl. However, it would appear that the processing of maturation bottoms would be uneconomical. Czech (1995) also stated the use of crossflow as an alternative to kieselguhr was not economical. O'Reilly (1987) suggested that crossflow microfiltration would be unsuitable for use on fined conditioned tank bottoms.

Leeder and Houldsworth (1988) predicted the potential savings for a beer leaving the maturation vessel. The system was assumed to operate 14 h day^{-1}, 4 days $week^{-1}$, 45 weeks $year^{-1}$ for a plant producing 1,000,000 hl yr^{-1}. The potential savings were stated as 47 p hl^{-1}. This is in agreement with work by Reed et al. (1989) and Reed (1989). They calculated savings of 51 p hl^{-1} for a plant handling 1,600,000 hl per year.

For a brewery producing 1.5 million barrels of beer, Leeder and Girr (1994) projected the saving in recovering 17,000 barrels per year from maturation vessel bottoms, as

approximately £3 63 /hl. This figure appears to be somewhat higher than most other studies.

Conclusion

These economic estimates of the process suggest that the process is viable in some cases, where fluxes are high enough. The potential savings appear to be of the order of £3 /hl in the recovery of beer from yeast and 50 p hl^{-1} when processing maturation vessel bottoms.

2.2.3 Crossflow velocity

The importance of crossflow velocity has been demonstrated theoretically by Leeder and Girr (1994). An increase in Reynolds number results in a subsequent thinning of the gel layer. The Reynolds number may be increased by decreasing the feed stream viscosity but clearly the viscosity of the stream will increase as it is concentrated during processing. The only alternative way of increasing the Reynolds number is to increase the crossflow velocity, although this is at the cost of power consumption. Kiefer (1991) states that a Reynolds number should be greater than 3000 to ensure turbulent flow and thus minimise concentration polarisation.

Le (1987) filtered both fermentation vessel bottoms and maturation vessel bottoms through a 0.45 µm ASYPOR (Domnick Hunter Filters Ltd.) membrane. Figure 2.1 shows a plot of log (crossflow velocity) against steady state flux. Clearly an increase in velocity, over the range 0.2 to 5.6 m s^{-1}, results in an increase in flux. The gradients of the two lines indicate that fermentation vessel bottoms are more suited to this process. This effect of crossflow has been agreed by Ryder *et al.* (1988) and Mylius and Reiter (1988) for the recovery of beer from tank bottoms.

Little effect on filtrate flux with a change in crossflow velocity in the range 2.2 -7.93 m s^{-1} has been observed by Burrell *et al.* (1994b) filtering a beer through a 0.5 µm laboratory scale ceramic membrane. This was corroborated by pilot scale data (Table

2.10), which showed lower fluxes at 1.5 m s^{-1} and 3.5 m s^{-1}, giving an optimum at about 2.2 m s^{-1}, although interpretation of the data was made difficult by the fluctuating solids present.

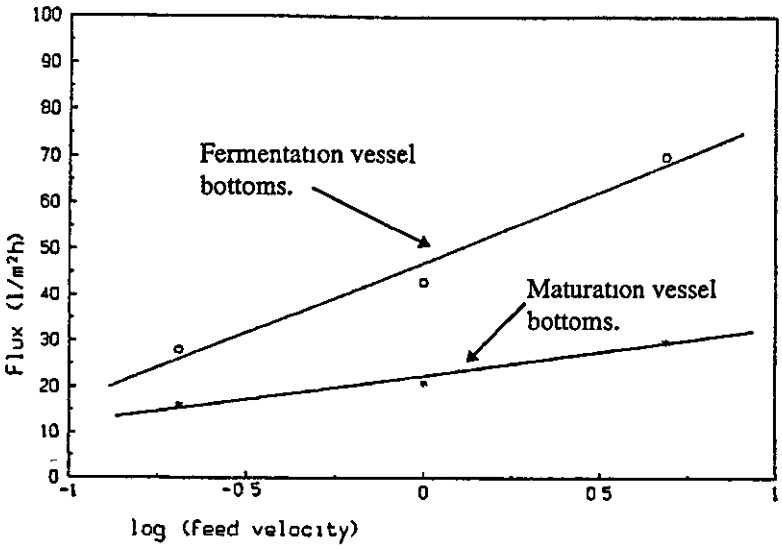

Figure 2.1: The effect of crossflow velocity on steady state filtrate flux.

Crossflow velocity (m s^{-1})	Average flux (l m^{-2} h^{-1})	Solids in rough beer (g l^{-1})	Filtrate haze sampled at 1hr (EBC)
1.5	5.1	3.9	0.25
2.2	13.2	5.0	0.6
2.2	36.0	0.64	0.35
3.5	23.5	1.0	0.55

Table 2.10: Effect of crossflow velocity on filtrate flux.

Walla (1994) showed an almost linear increase in specific flux with velocity over the range 2-4 m s^{-1} when filtering a lager cellar beer through a 0.45 μm alumina membrane and reported the differences in filtrate quality over this range (Table 2.11). This data suggests that a thinner fouling layer increases the transmission of beer components.

	Unfiltered	2 m s^{-1}	4 m s^{-1}	6 m s^{-1}
Orig. gravity (GG%)	12.26	11.80	12.08	12.11
Alcohol (GG%)	4 28	4.27	4.28	4.28
pH	4 78	4.77	4.78	4.78
Bitterness (EBU)	25.9	21.6	24.1	24.5
Polyphenols (mg l^{-1})	223	195	205	209
Anthocyanogens (mg l^{-1})	85	78	81	81
Foam R&C	136	122	130	131
Viscosity (mPa s)	1.57	1.48	1.53	1.54
Soluble nitrogen (mg l^{-1})	1040	986	1001	1009

Table 2.11: Effect of crossflow on beer component transmission.

Conclusion

It has been generally accepted, in other fields as well as for beer, that an increase in crossflow velocity generates higher shear near the membrane surface, removing the upper layers of the deposit on the membrane, resulting in a thinner deposit, reducing the total resistance to flow and increasing the filtrate flux. This also appears to be the case with beer microfiltration. Data also suggests that a thinner gel layer results in similar or possibly better passage of beer components.

2.2.4 Transmembrane pressure

Work by Le (1987) demonstrated the effect changes in transmembrane pressure may have. The effect of doubling the system pressure whilst filtering a 50 g solid per litre maturation vessel feed on a 0.45 µm and 0.8 µm membrane at 2 m s^{-1} was compared (Figure 2.2). In raising the pressure from 140 kPa to 280 kPa, it was observed that the flux of the finer membrane was reduced whilst the flux of the coarser membrane almost doubled. This increased flux was also accompanied by an increase in turbidity, which reached a maximum after 60 minutes of filtration. This suggests that part of the

fouling may be due to pore bridging, which may disintegrate under higher pressures, allowing larger particles to pass through the membrane.

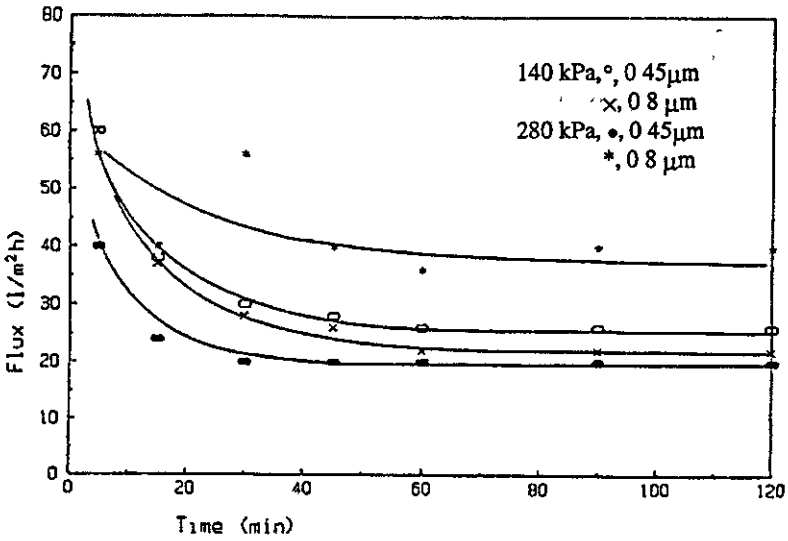

Figure 2.2: Effect of transmembrane pressure on maturation vessel bottoms.

Filtering a lager beer through a 0.2 μm PET cyclopore membrane in a stirred cell (850 rpm), the data of Lenoel *et al.*(1993) suggested that an increase in transmembrane pressure from 10 to 100 kPa resulted in an increase in initial flux from 160 l m^{-2} h^{-1} to 850 l m^{-2} h^{-1}, although steady state fluxes were somewhat similar. Gan *et al.* (1997) filtered a rough beer through a 0.5 μm alumina membrane, varying the TMP from 0.11 to 1.15 bar. Generally, higher pressures resulted in higher initial fluxes but somewhat similar steady state fluxes. However, fluxes over 0.8 bar resulted in lower steady state flux. This is in agreement with Mylius and Reiter (1988).

An optimum TMP has been observed by Burrell *et al.* (1994b). They filtered a commercial beer at a range of pressures (0.7-2.75 bar) on the laboratory scale (0.5 μm, 2.2 m s^{-1}) using a ceramic membrane (Table 2.12). Although the feed solids fluctuate, it is quite clear that 1.3 bar is the optimum transmembrane pressure tested. This was later confirmed at the pilot scale under similar conditions. Ryder *et al.* (1988) also point to an optimum flux for recovery from tank bottoms. They state that an increase in pressure increases flux but high TMP may be responsible for compaction of yeast on the membrane surface.

Transmembrane pressure (bar)	Solids in feed (ml solids/ml beer × 10^6)	Average flux over 5 h. ($l\ m^{-2}\ h^{-1}$)
0.75	146	7.6
1.3	195	20.7
2.75	200	10.0

Table 2.12: Effect of transmembrane pressure on filtrate flux.

Work by Walla (1994) showed not only an optimum in flux but also an optimum in beer component transmission with TMP when filtering a lager beer through a 0.45 μm alumina membrane (Table 2.13). The optimum TMP lies in the region 1.5±0.5 bar.

	Unfiltered	0.5 bar	1.0 bar	1.5 bar	2.0 bar	2.5 bar
Orig. gravity (GG%)	12.26	11.80	12.02	12.08	12.01	11.75
Alcohol (GG%)	4.28	4.27	4.27	4.28	4.28	4.28
pH	3.97	3.51	3.74	3.78	3.72	3.44
Bitterness (EBU)	4.78	4.71	4.77	4.78	4.78	4.70
Polyphenols ($mg\ l^{-1}$)	25.9	20.1	22.0	24.1	22.5	19.5
Anthocyanogens ($mg\ l^{-1}$)	223	190	200	205	199	192
Foam R&C	136	115	120	130	126	109
Viscosity (mPa s)	1.57	1.50	1.52	1.53	1.51	1.49
Flux ($l\ m^{-2}\ h^{-1}$)		24.03	32.90	37.25	30.31	20.82

Table 2.13: Effect of TMP on beer component transmission and flux.

Conclusion

During the microfiltration of beer, an increase in transmembrane pressure may have somewhat different results depending on the system. It may lead to both increases and decreases in filtrate flux and it appears possible that specific systems may display an optimum transmembrane pressure. Beer component transmission may also display an optimum TMP.

2.2.5 Temperature

At ambient temperature, Finnigan *et al.* (1989) showed that it was possible to concentrate a maturation vessel bottoms stream containing 2-6% w/w solids up to 26% w/w solids at a pressure of 4 bar. At lower temperatures (0-4°C) a build up of solids occurred and the temperature had to be raised. Ceramic membranes (0.12-0.18 μm) were used.

An increase in filtration temperature has been shown to enhance filtration rate by Burrell *et al.* (1994c) and Mylius and Reiter (1988). In raising the temperature from 0°C to above 15°C, the steady state flux was increased by 100%. This was thought to be as a consequence of reduced viscosity (also Ryder *et al.* (1988), Walla (1994)), increasing both the permeation rate and the back diffusion of molecules in the fouling layer. Filtration of a beer through a 0.5 μm ceramic membrane at 15°C gave a beer with acceptable haze characteristics, as shown by forced haze analysis. A further increase to 20°C showed few additional benefits, apart from the obvious reduction in cooling duty.

Crossflow filtration of a yeast suspension through a 0.45 μm alumina membrane has been shown to benefit from the use of elevated temperatures by Walla (1994). Table 2.14 shows that filtration at 5°C (opposed to 0°C) increases the flux and transmission of some components such as sugars, foaming proteins and anthocyanogens.

Kieselguhr filtration provides an effective pore size of about 0.6 μm whilst membrane pore sizes of 0.5 μm may provide even tighter effective pore sizes of <0.1 μm according to McKechnie (1995) and O'Shaughnessy and McKechnie (1996). As current practise requires the chilling of the feed to precipitate haze materials and facilitate their subsequent removal, the use of temperatures above 3°C may allow haze material to re-dissolve and pass through traditional filters (Freeman *et al.* (1995)). The use of microfiltration may remove these larger macromolecules without the need for chilling, increasing throughputs and reducing energy usage. However, Meier (1990) states that for the recovery of beer from yeast, the use of temperatures above 10°C

may affect the taste of the product as the levels of total nitrogen, colour, organic acids and fatty acids increases.

	Unfiltered	0°C	3°C	5°C
Orig. gravity (GG%)	12.26	12.08	12.08	12.14
Alcohol (GG%)	4.28	4.28	4.29	4.28
pH	3.97	3.78	3.79	3.85
Bitterness (EBU)	4.78	4.78	4.78	4.78
Polyphenols (mg l^{-1})	7.55	7.25	7.25	7.25
Anthocyanogens (mg l^{-1})	25.9	24.1	24.2	24 9
Foam R&C	223	205	207	217
Viscosity (mPa s)	136	130	130	133
Soluble nitrogen (mg l^{-1})	1.57	1.53	1.53	1.55
Flux (l m^{-2} h^{-1})	37.25	37.91	41.13	52.61

Table 2.14: Effect of temperature on beer component transmission and flux.

Conclusion

It appears that increasing the filtration temperature provides an increase in filtrate flux, therefore producing savings through both increased throughput and decreased cooling costs. The potential downside is the increased transmission of haze forming components or the increased leaching of unwanted components from yeast-laden feeds. This should not present a significant problem, as the effective pore sizes of membranes used are likely to be tighter than those provided by kieselguhr.

2.2.6 Feed type

Hug *et al.*(1989) filtered samples of yeast-laden fermentation product, storage beer and rest beer. The filtration characteristics are shown in Table 2.15.

Material	Average flux over first 6 hours (l m^{-2} h^{-1})
Fermentation product	21
Storage beer	24
Rest beer (+yeast)	28

Table 2.15: Filtration characteristics of different feeds.

Alternatively, samples were centrifuged (10 minutes at 1000 g) and microfiltered. The analyses of both non-volatile and volatile components are compared in Tables 2.16 and 2.17.

		Fermentation beer				Storage beer	
		Fresh		1 week old		Fresh	
		Centri	Micro	Centri	Micro	Centri	Micro
Wort	GG%	12 59	10.72	10 78	9.27	10.33	8.50
Alcohol	GG%	4.17	4.07	3.79	3 70	3.34	3 00
Extract	GG%	3 98	2.31	2.93	1 61	3 42	2.43
Colour	EBC	21	6.1	20	6.1	17	5.7
pH		5 15	5.25	6 77	6.45	4.94	5 05
Viscosity	mPa s	1.73	1.42	1.80	1.57	1.98	1 78
Iodine value	ΔE578	0 45	0 03	0 51	0.05	0 49	0 05
β-glucan	mg l^{-1}	215	5	187	3	247	7
Total N	mg l^{-1}	868	545	916	607	828	691
$MgSO_4$ - N	mg l^{-1}	170	29	200	34	201	72
Polyphenol	mg l^{-1}	280	123	270	148	318	228
Anthocyanin	mg l^{-1}	84 3	36 2	75.7	42 3	96.1	63 9
Bitters	BE	36	27	36	27	23	22

Table 2.16: Comparison of non-volatiles and method of separation (microfiltration and centrifugation).

	Unfined tank beer	Fermentation beer				Storage beer	
		Centrifuged		Microfiltered		Centri	Micro
		Fresh	1 week	Fresh	1 week	Fresh	
	Amount in mg l^{-1}						
isobutylacetate	0 042	0 059	0 030	0 053	0 029	0 022	0.019
ethylbutyrate	0 053	0 115	0.094	0.106	0 094	0.057	0 053
isoamylacetate	1.689	3.441	2.771	3.141	2 665	0 889	0.781
ethylcapronate	0 122	0 109	0 077	0 109	0 062	0 059	0.049
hexylacetate	0.007	0 009	0.004	0.007	0 003	0.003	0 003
heptylacetate	0 004	0 011	0.010	0 007	0.007	0 001	0 001
ethylcaprylate	0.098	0 077	0 040	0 057	0 074	0 111	0 042
ethylcaprinate	0 016	0 038	0.077	0 005	0 008	0.113	0 012
2-phenylethyl-acetate	0 431	0 604	0.313	0 496	0 267	0.294	0 252
1-propanol	11.730	17.108	18.326	15.617	17 529	11 383	9 391
isobutanol	10.210	14.635	16.641	13.437	15 867	9.188	7 797
1-butanol	0 063	0.087	0.080	0 081	0.076	0 079	0.067
1-pentanol	0 017	0.020	0 018	0 019	0 018	0.018	0 016
1-hexanol	0 033	0 054	0 048	0 049	0 041	0.041	0 036
1-heptanol	0 012	0 127	0.128	0 108	0.120	0 055	0 045
1-octanol	0 011	0 024	0 048	0 022	0.042	0.016	0 013
isobutyric acid	0 485	0 000	0 000	0 000	0 000	0 428	0 361
butyric acid	0 000	0 000	0.000	0 000	0 000	0 000	0.117
isovaleric acid	0.793	0 000	0 000	0.000	0.000	0.766	0.714
capronic acid	1.205	0 037	0.1	0 016	0 283	1.197	1 078
caprylic acid	2.103	0 018	4.348	0.175	4 566	3.612	3.184
caprinic acid	0.181	0.395	4 359	0 089	2.494	1 580	0.948
9-decanoic acid	0.113	0 103	1.247	0.036	0 808	1.124	0 824
methionol acetate	0 114	0 019	0 014	0.016	0 009	0.007	0 006
furfurylalcohol	1.450	1.278	1 189	1.238	1 167	1 070	0 932
methionol	1 284	1.397	1.341	1 260	1.317	0.862	0.760

Table 2.17: Comparison of -volatiles and method of separation (microfiltration and centrifugation).

This suggests that there is a loss of non-volatiles during microfiltration (see also Section 2.2.1). In the case of volatiles, however, there appears to be a gain in

concentration during centrifugation but a loss during microfiltration, although this appears to be age dependant (see methionol for example, in Table 2.17).

Unsurprisingly, as shown by Walla (1994) an increase in yeast concentration causes a drop in the amount of beer that may be recovered, as it is difficult/uneconomical to run at a solids content above 20-25%. The compositional changes of fermentation tank bottoms filtered through a 0.45 μm polysulphone membrane at different concentrations have been demonstrated by Ryder *et al.* (1988) in Table 2.18. This is echoed by Siebel *et al.* (1988).

Parameter	Control	Permeate @ yeast solids (dry wt. %)				
		11.2	14.0	16.6	18.9	22.1
O.G. (°Pl)	13.30	12.3	12.3	12.4	12.6	12.8
% alcohol (wt.)	4.12	4.33	4.42	4.43	4.53	4.55
% RDA	61.50	69.6	71.1	70.8	71.2	70.4
% App. extract	3.48	1.93	1.70	1.83	1.74	1.89
% Real extract	5.34	3.90	3.71	3.85	3.80	3.95
Bitterness (EBU)	23.8	30.7	34.5	39.0	38.4	39.0
pH	4 00	4.35	4.50	4.65	4.70	4.75
Free amino N	66.90	80.10	93.40	102.30	109.10	111.50
Haze - initial	-	45	54	56	52	50
After forcing	-	115	120	118	110	115

Table 2.18: Beer analysis data for increasing yeast concentrations.

The most noticeable features of this data are an increase in alcohol, bitterness, free amino nitrogen and pH, along with a decrease in real extract. The increase in free amino nitrogen may be explained by its probable leakage from the yeast. This would also explain the pH change. The decrease in real extract may be the result of a loss of long chain carbohydrates. On tasting, the increase in bitterness was not detected but there was an increase in alcoholic taste.

Burrell *et al.* (1994a, b) showed the effects of beer type on filtration by taking two beers, one with a large number of fine particles (beer A) and the other with the main particle size close to that of the membrane pore size (beer B). Both were filtered using a 0.5 μm ceramic membrane at 1.3 bar and 2.2 m s^{-1}. The flux of beer A dropped from 53 l m^{-2} h^{-1} after 5 hours to 22 l m^{-2} h^{-1} after 20 hours whilst beer B dropped from 10 l m^{-2} h^{-1} after 5 hours to 7 l m^{-2} h^{-1} after 20 hours. This clearly shows that the particle size is very important in determining flux, probably due to pore sized particles becoming trapped within pores, rendering them completely blocked.

A similar trend has been shown by Bühler *et al.* (1993). Two beers were taken, one with a much finer haze (beer B) than the other (beer A). Both were filtered using a 0.5 μm alumina membrane. Beer A showed a slow flux decline to approximately 20 l m^{-2} h^{-1} after 20 hours, whilst beer B showed a rapid flux decline over the first 5 hours to about 6 l m^{-2} h^{-1} after 20 hours.

Pilot scale studies by Burrell *et al.* (1994a, b) clearly demonstrated the effect of solids loading when the size distributions were taken into account. A higher solids loading caused a decrease in flux, although the effects of a change in particle size distribution may be overridden by this. Le (1987) also showed a decrease in flux with feed solids. The flux was found to be somewhat more dependent on concentration at lower concentrations. This was shown to be due to a decline in the mass transfer coefficient caused by an increase in feed stream viscosity. Finnigan *et al.* (1989) reported that an increase in solids may lead to a reduction in haze. Burrell and Reed (1994a) attributed the improvement in clarity to a secondary membrane type effect, whereby the fouling layer prevents the passage of haze materials.

Three conditioned beers were filtered through a 0.22 μm polysulphone membrane by Ryder *et al.* (1988). The compositional analysis for each is given both before and after filtration in Table 2.19. The authors state that the results are the same within experimental error and no taste differences were detected. It does however appear that there is a slight reduction in viscosity and polyphenols. A loss in β-glucans could result in a viscosity reduction. The control analyses do show that these beers are all quite similar. However, close inspection of the data does suggest that they do behave

differently. Taking the values for colour as an example, beer A decreases after filtration, beer B remains the same and beer C appears to rise, although this could indeed be due to experimental error.

Parameter	Run A		Run B		Run C	
	Control	Test	Control	Test	Control	Test
Bitterness (EBU)	9.5	9.5	10.0	10.0	10.0	9.0
pH	4.15	4.18	4.18	4.17	4.17	4.14
Foam Σ	112.0	114.0	126.0	118.0	123.0	122.0
Colour (EBC)	2.8	2.5	2.6	2.6	2.7	2.9
Viscosity	1.51	1.49	1.51	1.48	1.48	1.40
% App. extract	2.30	2.21	2.30	2.26	2.26	2.27
% Real extract	4.03	3.96	4.03	3.97	3.98	3.99
% Alcohol (wt.)	3.78	3 81	3.78	3.72	3.75	3.75
% Orig. extract	11.39	11.37	11.39	11.22	11.28	11.29
% RDA	66.0	66.5	66.0	66.0	66.1	66 1
% Reducing sugars	1.14	1.07	1.07	1.11	1.05	1.10
% Dextrin	1.80	1.87	1.85	1.86	1.85	1.79
% Protein	0.35	0.35	0 37	0.35	0.35	0.35
Chloride (ppm)	286	284	282	285	284	283
Polyphenols (ppm)	252	248	257	251	258	248
Haze - fresh	54	53	54	56	52	46
After forcing	48	63	41	55	51	51
24 hour	118	77	109	76	86	68

Table 2.19: Analyses of different beer types.

Nielsen (1989) highlights the influence of the feed on the process. The filtration fluxes for storage tank bottoms are in the range 8-10 l m^{-2} h^{-1}, as they contain small sized particles such as protein-tannin complexes. Fermentation tank bottoms have higher capacities of the order of 15-20 l m^{-2} h^{-1}.

It is possible that the age of beer may also be of importance. Xu *et al.* (1995) filtered fresh and 10 day old beer through a series of two 0.8 μm poly (difluorure vinylidene) membranes. Fresh beer caused a similar pressure drop through both membranes, whilst the stored beer produced a larger pressure drop across the first and a much lower pressure drop across the second. The authors attributed this to a formation of aggregates on storage, that blocked the pores of the first membrane. However, this may have also been due to microbial spoilage with time.

Conclusion

With yeast-laden material, extra components may be leached from the cells during filtration. As the solids loading becomes higher there is less of an effect on flux. With different beer types, the particle size appears most important, with lower fluxes achieved when particle size and pore size are similar.

2.2.7 Membrane material

The effect of membrane material (all 0.2 μm, one assumes) has been studied by Müller (1992). Polysulfone gave an 80% recovery of O.G. and bitter substances and a near 100% recovery of alcohol. It was however found to be temperature and pH sensitive. Polypropylene gave an 80 - 100% recovery of alcohol and O.G., a maximum of 35% recovery of bitter substances and produce a beer with a soapy off flavour. α-alumina gave a 92 - 100% recovery of O G., alcohol and bitter substances

The effect of membrane material has been studied by Xu *et al.* (1995, 1996). Beer with a mean particle size of 0.8 μm was filtered through a range of 0.4 μm rated membranes made of polyvinylidenefluoride (PVDF), PVDF+polyethylene imine (PEI) and PVDF+polyvinylic alcohol (PVA). The experiments were carried out at constant pressure, maintained by controlling the CO_2 in the system, under constant recycle. It was found that with no precirculation of feed, the PEI showed a lesser flux than the other two membranes, which were equivalent. However, after a 5 minute precirculation of feed the PEI and PVA fluxes were greater than the PVDF flux. This

may be explained by looking at the beer-membrane interactions. From a knowledge of the membrane properties and the zeta potential of the beer particles (-ve), a table of interactions may be drawn (Table 2.20).

Membrane	Beer/membrane interactions		
	Electrostatic	Hydrophobicity	Overall
PVDF	repulsive	attractive	competition
PEI	attractive	repulsive	competition
PVA	neutral	repulsive	repulsive

Table 2.20: Beer/membrane interactions.

As PVA repels the beer particles, it may well explain its better flux in both experiments. Without precirculation, fouling may be mainly due to internal pore plugging, hence electrostatic forces would predominate and explain the better flux for PVDF than PEI. With precirculation, a deposit may well be formed, hence the hydrophobic forces would predominate and explain the better flux for PEI than PVDF. Experiments carried out to investigate the effect of membrane material on turbidity (without pre-circulation) revealed PEI to give the lowest value and PVA to give the highest. This suggests that PEI has a higher affinity for the substances in beer giving a higher retention, whilst PVA shows a low protein adsorption capacity and hence a lower retention.

Frieling (1990) has presented work comparing sheet filtered Kieselguhr filtrate with its crossflow filtered equivalent. 0.45 - 2.0 μm polysulfone and fluropolymer membranes were used at 0-5°C, 3.5-5.0 m s^{-1} and 1.0-1.8 bar. The results are compared in Table 2.21, below. Taste analyses of the samples were similar and the experimental values are within the error limits. The flux declines for each membrane are given in Figure 2.3.

	Sheet filter	Polysulfone		Fluropolymer
		2.0 µm	0.45 µm	1.0 µm
App. extract %	1.61	1.72	1.75	1.63
Real extract %	3.41	3.50	3.51	3 43
Alcohol wt.%	3.95	3.93	3.89	3.96
Alcohol vol.%	5.03	5.00	4.94	5.03
Orig. extract %	11.11	11.15	11.08	11.14
App. atten. %	85.52	84.60	84.28	85.35
Colour EBC	5.24	5.31	5.33	5.24
pH	4.26	4.26	4.28	4.30
Bitterness EBU	25 05	25.30	24.27	25.41
FAN ppm	122.46	125.90	128.45	125.37

Table 2.21: Effect of membrane type on beer quality - Kieselguhr filtrate.

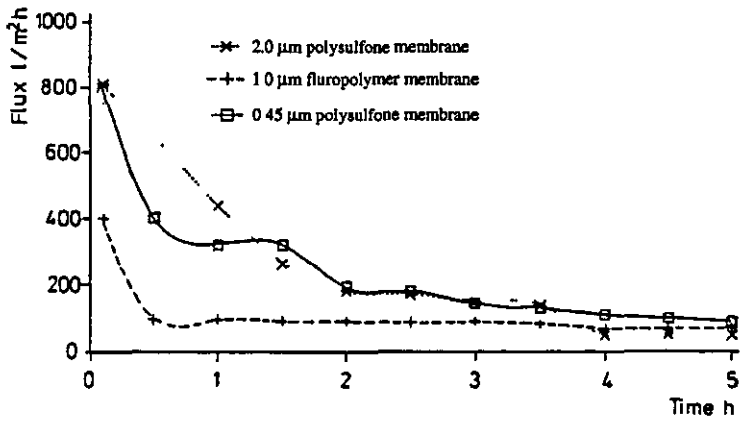

Figure 2.3: Effect of membrane type on filtrate flux - Kieselguhr filtrate.

Frieling (1990) also compared the performances of a sheet filter and polymeric membranes for the filtration of cellar beers. Experiments carried out with a 2.0 µm membrane were stopped, as the membrane became totally clogged during the first run. The flux decline for each membrane used is shown in Figure 2.4.

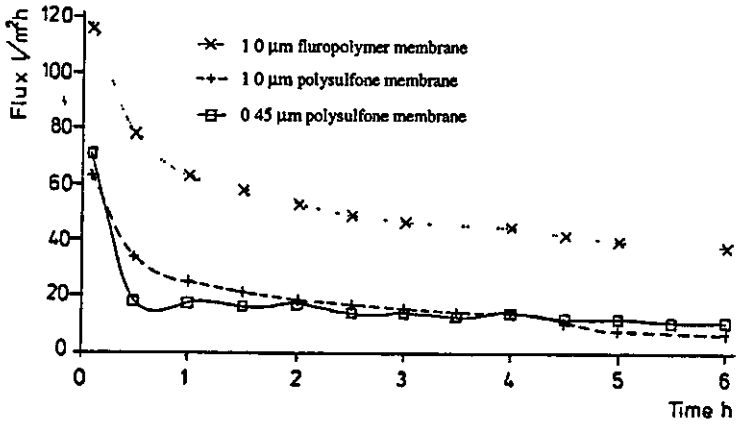

Figure 2.4: Effect on membrane type on filtrate flux - cellar beer.

In these experiments beer components were lost. This was found to be irrespective of the membrane type, and it is therefore assumed a secondary membrane is responsible. The analyses of the beers are given in Table 2.22.

	Sheet filter	Polysulfone		Fluropolymer	
		2.0 µm	1.0 µm	0.45 µm	1.0 µm
App. extract %	1.61	1.08	0.98	1.07	1.18
Real extract %	3.41	2.94	2.79	2.94	3.02
Alcohol wt.%	3.95	4.05	3.94	4.08	4.04
Alcohol vol.%	5.03	5.14	5.00	5.13	5.13
Orig. extract %	11.11	10.84	10.48	10.88	10.89
App. atten. %	85.52	90.02	90.72	90.21	89.23
Colour EBC	5.24	4.35	4.02	4.34	4.93
pH	4.26	4.22	4.27	4.31	4.22
Bitterness EBU	25.05	26.95	23.07	25.73	23.93
FAN ppm	122.46	117.86	103.43	120.29	122.32

Table 2.22: Effect of membrane type on beer quality - cellar beer.

Conclusion

This suggests that, depending on the feed type, the membrane may have more or less of an influence on the resultant filtrate. The optimum membrane type does, of course, depend on other factors such as cost and ease of cleaning.

2.2.8 Pore size

Le (1987) investigated the effect of pore size on the crossflow microfiltration of two beer streams, namely fermentation vessel bottoms (10-15 g solid l^{-1}) and maturation vessel bottoms (40-50 g solid l^{-1}). Higher overall fluxes were achieved using a 0.45 μm membrane compared with a 0.8 μm membrane.

A conditioned beer was filtered through 0.22, 0.45, 0.65 and 3.0 μm polysulfone membranes by Ryder *et al.*(1988). The analyses are given in Table 2.23. This data suggests a decrease in alcohol, protein and bitterness, with the greatest decreases occurring with the 0.22 μm membrane.

Parameter		Pore size (μm)			
	Control	0.22	0.45	0.65	3 0
App. extract (°Pl)	2.86	2.65	3.04	2.80	3.15
Real extract (°Pl)	4 66	4.38	4.76	4.53	4.88
% Alcohol (wt.)	3 94	3.78	3.77	3.77	3.79
O.G. (°Pl)	12.30	11.73	12.08	11.85	12.23
pH	4.60	4.61	4.61	4.61	4.62
% Reducing sugars	1.48	1.56	1.56	1.58	1.60
% Protein	0.72	0.59	0.67	0.62	0.70
Colour (°L)	-	3.2	3.7	3.4	4 6
Bitterness (EBU)	15.1	13.5	14.4	13.8	14.1

Table 2.23. Beer analyses with pore size.

Using a beer of constant solids loading and distribution, Burrell *et al.* (1994a, b) showed that an increase in membrane pore size from 0.5-1.3 μm produced an increase in flux (at 1.3 bar, 2.2 m s^{-1}) at the laboratory scale. This may be due to the fact that larger pores have a greater porosity. Finer pores, however, tend to be associated with a gel layer on the membrane surface. This gel may remove fine particles and lower its permeability whereas the larger pores will simply allow the fines to pass through. Also, with larger pores, there are fewer particles large enough to block the pores. The potential gel layer formed on finer membranes may also be used to explain an increase in haze at larger pore sizes. At the pilot scale these effects are not seen but the opposite appears to occur. It is stated that this cannot reasonably be explained by differences in beer solids, although a different beer type is used. It is suggested that a pore blocking mechanism is present in the coarser membrane, with particles becoming trapped within the pores, whilst the particles remain on the surface of the finer membrane.

In later work, Burrell *et al.* (1994c) also filtered a rough beer through ceramic membranes with pore sizes 0.2, 0.35, 0.5 and 0.8 μm. The beer used was known to cause problems using kieselguhr. The major cause for poor performance has been attributed to the presence of particles below 0.5 μm. The 0.8 μm membrane produced high initial fluxes, but these fell below the fluxes for the membranes with pore sizes ≤0.5 μm. The concept that fine material plugs the pores deep within the membrane explains this poor flux behaviour. These larger pore sized membranes displayed little/no loss of components. The 0.2 and 0.35 μm membranes produced greater fluxes, but they suffered a loss of head retention value and present gravity. The loss of head retention was due to a reduction in the level of head forming proteins. Molecular interactions in the gel layer are believed to be responsible for these losses.

Conditioned beer filtered by Gan *et al.* (1997) through ceramic membranes showed that a reduction in pore size led to a higher flux (suggesting pore plugging). However, when comparing the head retention value (and similarly density) of 0.2 and 0.5 μm filtered beer, it was seen that the larger pore size would transmit proteins responsible

for head formation. The 0.2 μm membrane rejected these proteins to a greater extent as it fouled.

Work comparing membrane material and pore size conducted by Frieling (1990) and Czech (1995) may be found in Section 2.2.7.

Conclusion

Pore size is almost certainly not a factor to be studied alone, but a combination of pore size and particle size appears to be important (as stated in Section 2.2.6).

2.2.9 Reduction of fouling

It can be seen from the sections above that fouling can be reduced by choosing optimal operating parameters such as temperature, crossflow velocity, transmembrane pressure, membrane pore size and membrane material. Other methods have been proposed, at least for solid-liquid systems, such as baffling, backflushing, oscillating flow and a form of vortex type flow. Of these, the method that appears to have received the most attention for the crossflow microfiltration of beer is backflushing.

Backflushing involves the passage of a fluid, often permeate, through the membrane from the permeate side back to the feed side. This removes some, if not all, of the fouling layer and hence restores flux. Czech (1995) states that backflushing results in an increase in filtrate flux, although the precise conditions are omitted. They also report an increase in filtrate flux with flow reversal. Atkinson *et al.* (1985) collected filtrate in a reservoir to which pressure pulses were applied by CO_2. Laboratory scale results using cold conditioned beer and a 0.2 μm polypropylene membrane with a backwash pulse for 1 second a minute, showed only a small drop in flux over a 4 hour period. Reed and Leeder (1986) and Reed (1986) also point to the advantage of short backflush pulses of typically 1 second per minute.

The periodic backflushing process has been optimised by Walla (1994). A yeast-laden beer was filtered at 1.5 bar, with a backflush cycle repeated every 3 minutes, at varying pressures and for varying durations. The data (Table 2.24) suggests an optimal procedure as lasting for 10-20 seconds at a pressure of 0.5-1.0 bar. The specific fluxes for a 1.5 bar backflush are lower, because although there is a better removal of the fouling layer, the loss of backflushed beer is greater.

Backflush duration	Backflush pressure	Specific flux
(s)	(bar)	($l\ m^{-2}\ h^{-1}$)
5	0.5	33.9
5	1.0	35.4
5	1.5	34.7
10	0.5	37.1
10	1.0	37.3
10	1.5	32.7
20	0.5	35.7
20	1.0	36.6
20	1.5	32.7
No backflush		32.8

Figure 2.24: Optimisation of the backflushing process.

Gan *et al.* (1997) performed backflushing, shown in Figure 2.5, using a combination of permeate and CO_2. The backflush frequency was 1 pulse every five minutes, with a pulse duration of 0.5 seconds and a backpressure of 2.0 bar. It is pointed out that the base flux level is 100% higher than without backflush and the peak flux drops with run time and also declines more rapidly with run time. This increasing decline suggests that backflushing does not completely reverse fouling. They went on to optimise the backflush parameters to minimise the flux decline with runtime. The modified parameters are shown in Table 2.25. They resulted in a 400% increase in the ten-hour average flux.

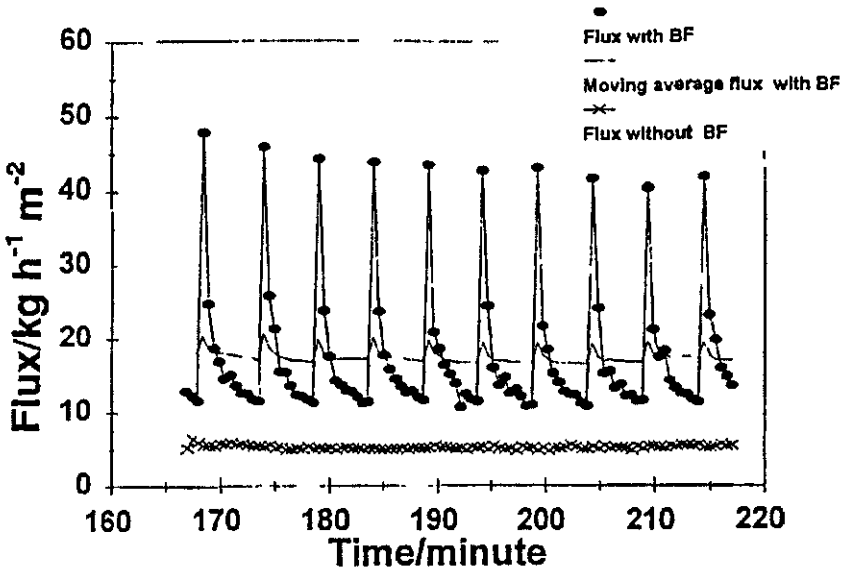

Figure 2.5: Effect of backflush.

Stage	Frequency	Length	TMP	Backpressure
(hr)	(minute^{-1})	(s)	(bar)	(bar)
1	1	0.5	0.8	2.5
2	2	0.3	1.3	2.5
3	4	0.2	1.7	4 0
4	8	0.1	2.0	5.0

Table 2.25: Optimised multi stage backflushing

Backflushing has been shown to affect the transmission of larger molecular species involved in bitterness and present gravity by Reed *et al.* (1989a) and Reed (1989b), as shown if Figure 2.6. Filtering tank bottoms through a 0.2 μm polypropylene tubular membrane on both the laboratory and pilot scale, backflushing promoted the immediate transmission of total soluble nitrogen and present gravity to feed values, whilst head retention and bitterness values reached equilibrium sooner, albeit after two hours of operation.

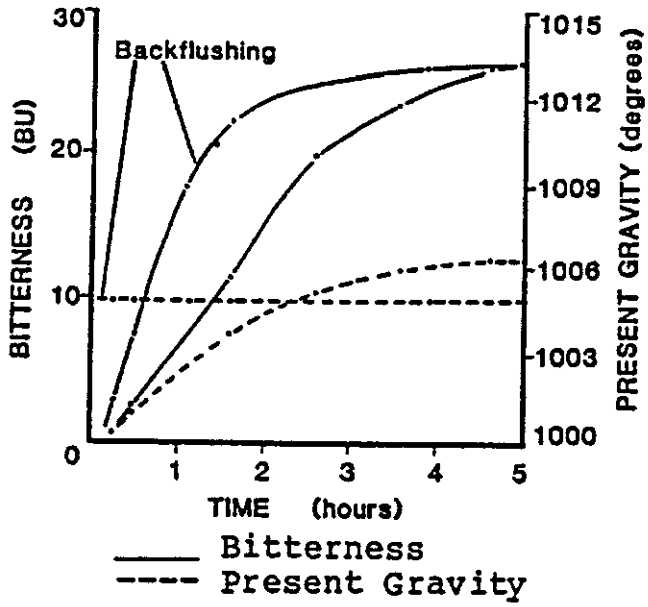

Figure 2.6: Effect of backflush on bitterness and present gravity (pilot scale).

Czech (1995) comments that the reversal of flow can lead to an increase in flux of 30-50%. This is a general observation made for the filtration of beer through membranes in a range of materials and pore sizes.

Of the other methods of fouling reduction, the use of oscillating or pulsatile flow (Gan *et al.* (1997)) has been shown to improve flux, although not significantly in commercial terms, when filtering a rough beer and comparing results of experiments with the same net volumetric flow of feed. On the laboratory scale, Reed *et al.* (1989a) showed the benefit of turbulence promoters by comparing a tubular and sheet 0.2 μm polypropylene module for the filtration of unfined beer. The sheet module contained turbulence promoters and gave a steady state flux of 60 l m^{-2} h^{-1} (and did not require backflushing compared) to 30 l m^{-2} h^{-1} for the tubular module.

Conclusion

Backflushing, oscillatory flow and turbulence promoters are all of use in reducing fouling. It is clear, however, that the parameters used for backwashing need to be tailored for the system in question.

2.2.10 The "gel" layer and fouling mechanisms

A major problem with crossflow filtration is the formation of a fouling layer on the membrane surface, although fouling may also occur within the membrane structure. The flow of feed tangentially to the membrane tends to limit the thickness of the layer but it does not entirely remove it. In particulate systems the fouling layer is comprised of particles held in place by inter-particle forces. Molecular systems tend to form gel layers of deposited particles. Molecules absorb to the membrane surface with other molecules subsequently binding through strong inter-molecular forces, such as van der Waals, hydrogen, electrostatic, etc.

Letters (1995) has investigated the composition of carbohydrate gels that could be formed during filtration. Hazes and gels were isolated from beer by centrifugation and were then analysed for carbohydrate components. α-glucans, β-glucans, glycogen and mannan fractions were all identified as gel forming. Of the factors affecting gel formation, two are relevant to crossflow microfiltration. Firstly, increases in amylose and high molecular weight β-glucan concentration resulted in more rapid gel formation. Secondly, shear plays an important role. High shear forces acting on β-glucans, mainly from pumping, accelerated gel formation. The mechanical shearing of yeast may cause the cells to fracture, resulting in the release of gel-forming mannan fragments.

Stirred cell (0.2 μm) fouling studies have been performed by Burrell *et al.* (1994c). Enzymes were added to commercial beer samples in order to degrade molecules believed to be foulants. This study showed that β-glucans and to a lesser extent α-glucans were largely responsible for membrane fouling. Similar studies, with

similar findings, have been carried out by Gan *et al.* (1997). They acknowledge that the addition of a quantity of enzyme may in turn lead to membrane fouling. The main findings were that carbohydrates such as β-glucans and starch molecules/particulates caused fouling, but proteins appeared to have little effect. Crossflow experiments (0.5 μm) confirmed this work and also showed pentosans to have an effect. Calcium and copper ions were found to be present on the membrane surface. These ions may be responsible for forming large molecular aggregates of carbohydrates and proteins. Siebel *et al.* (1988) agree and, in addition, found fouling due to hemicelluloses, with full flux restored by treating with exo- and endo-β-glucanases and side activities of β-glucosidase, cellobiase, pentosanase, xylanase, pectinase and protease.

Lenoël *et al.* (1993, 1994) have proposed the model shown in Figure 2.7. Stirred cell studies were carried out on a lager beer through a 0.2 μm PET membrane. Their approach was to examine the data in terms of standard blocking equations. The data suggests an initial build up of protein within the membrane until the internal area is saturated, followed by the build up of colloidal matter forming a secondary membrane. Further work by Blanpain and Lalande (1996, 1998) on 0.2 μm PC membranes using both clarified and rough beer demonstrated further that most of the resistance across the membranes came from the reversible layer of macromolecules and that the presence of yeast had little effect.

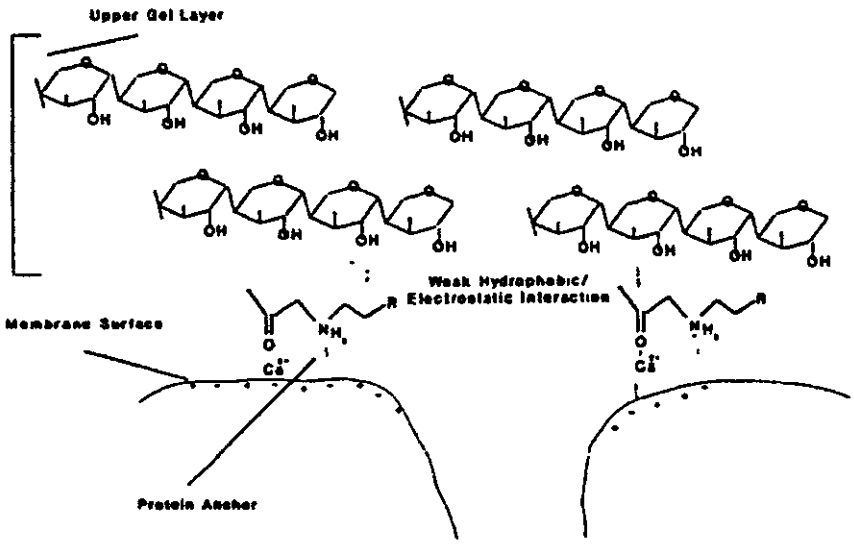

Figure 2.7: Proposed gel layer model of Lenoël *et al.* (1994).

Conclusion

Fouling appears to occur initially by adsorption within the membrane. This is then quickly followed by a layer deposited on the surface of the membrane. This secondary membrane, comprising long chain protein and carbohydrate material, is responsible for the large flux reduction and removal of other molecules from the permeate.

CHAPTER 3
PROTEIN CROSSFLOW FILTRATION

As beer is such a complex feed, it is difficult to ascertain the precise mechanisms responsible for fouling and rejection, as has been seen in the previous chapter. Other well studied feeds such as wine, fruit juice, milk and whey have also been the subject of considerable interest for the application of crossflow filtration, but are also fairly complex. In such systems, proteins have been identified as being major foulants. For this reason much research has been conducted into the area of protein crossflow filtration using streams containing, at most, a few different molecules in the feed.

There are a huge number of publications on the area of protein crossflow filtration. This review is intended to briefly examine the effects of altering process variables, with explanations provided where possible. Many papers do not agree on the effects of changing variables, emphasising the complex nature of systems and showing that individual systems behave in their own way. The adsorption of proteins onto materials such as membranes is a subject in its own right, and has not been covered here in detail, but is briefly mentioned were essential to the discussion.

3.1 PROTEIN CONCENTRATION

Clark *et al.* (1991), Grund *et al.* (1992) and Kelly and Zydney (1995) have shown that the filtrate flux of protein solutions decreases with protein concentration. An increase in concentration resulted in a more rapid flux decline, reaching steady state sooner, but attaining a similar final flux according to Kelly and Zydney (1995). Work by Bowen *et al.* (1995) and Prádanos *et al.* (1996) also showed a greater rate of flux decline at higher concentrations, although they found that initial fluxes were similar, with the steady state flux lower at higher concentrations. Clark *et al.* (1991) also reported rejection to be concentration dependent for concentrations above 1 g l^{-1} in their system.

Ingham *et al.* (1980), filtering albumin through a PM-30 ultrafiltration membrane, showed that steady state flux was dependant on concentration with three distinct effects observed over different concentration bands. Over the concentration range 0.001-0.01 mg ml^{-1}, there was a sharp decrease in flux, as increasing the concentration caused more protein to adsorb to the membrane. For concentrations in the range 0.01-0.1 mg ml^{-1}, the concentration had little effect on steady state flux. At higher concentrations up to 100mg ml^{-1} the steady state flux was, again, seen to decrease with concentration due to concentration polarisation.

However, when filtering a protein precipitate at constant feed concentration, Taylor *et al.* (1994) showed that an increase in feed concentration actually resulted in an increase in flux (Figure 3.1). In this case the system comprises protein aggregates as well as soluble material. A possible explanation for this increase in flux is a scouring effect of the high velocity particulates disrupting the polarised layer. Alternatively the increase in concentration may increase the viscosity of the stream, increasing the wall shear stress, leading to an increase in mass transfer away from the wall

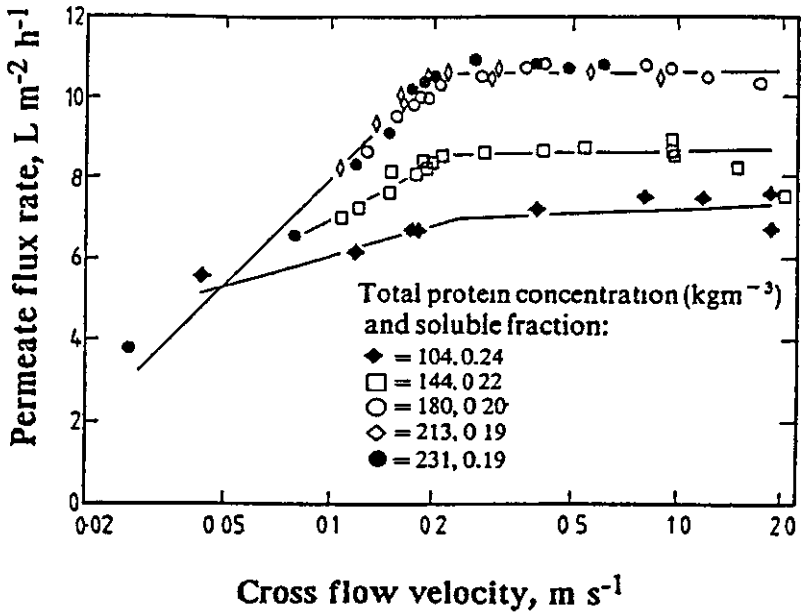

Figure 3.1: The effect of protein precipitate concentration on permeate flux. (Taylor *et al.* (1994))

3.2 PROTEIN TYPE

The effect that different protein types have depends on several factors. Generally, as expected, larger proteins are more likely to be retained than smaller ones. However, as can be seen in sections 3.8 and 3.9, the iso-electric point (IEP) of the protein is also very important. Palacek and Zydney (1994) suggested that the magnitude of the protein charge could be of importance. They showed an increase in the time taken for the protein layer to compress and rearrange to a new steady state with pressure, as the protein charge increased.

A range of proteins filtered by Prádanos *et al.* (1996) showed that the differences in size between membrane pores and proteins were important. They filtered pepsin (36 kDa), BSA (67 kDa), invertase (270 kDa), lipase (80 kDa) and γ-globulin (150 kDa) through a 0.02 μm membrane. The three latter proteins were found to cause steep flux decline, whilst the first two were gradual. Pepsin and BSA showed low retention, with lipase, γ-globulin and invertase showing retentions of 20%, 60% and 100% respectively. Flux decline was explained in terms of the number of pores of each size, and the influence each pore size would have on flux. The size of invertase meant that it could not penetrate pores, but was capable of blocking pores. The size of lipase and γ-globulin, compared to the pores, meant they had the ability to block pores with a high flux capacity, whilst BSA and pepsin were capable of blocking pores that had little effect on flux.

Other factors may also be important. For example, Grund *et al.* (1992) filtered solutions of both BSA and fatty acid poor BSA. They showed that in the absence of fatty acids, the filtrate flux was increased and the irreversible compressibility of the cake layer was decreased. It was assumed that the standard BSA was present as dimers and trimers, whilst the fatty acid poor version existed as single molecules. The problem of aggregates has also been identified by Kelly and Zydney (1995). Whilst filtering BSA through a 0.2 μm PVDF membrane, a BSA solution was found to foul severely, whilst a solution prefiltered through a 100 kDa filter, removing aggregates, was found to virtually eliminate the fouling. The aggregate fouling was found to be

irreversible. The importance of molecular groups within the protein are also of importance as demonstrated by the same workers. Solutions of prefiltered BSA and s-cysteinyl-BSA were filtered through membranes fouled by aggregates. The filtrate flux was found to further decline in the presence of the BSA solution, whilst the s-cysteinyl-BSA showed little decline. This indicates that, in this system, the free thiol group (-SH) is vital in the attachment of native protein to deposited aggregates.

3.3 MEMBRANE PORE SIZE AND STRUCTURE

As would be expected from simple fluid mechanics, smaller pores generally result in lower permeate fluxes and an increase in rejection as reported by Le Berre *et al.* (1994), Tracey and Davis (1994) and Sayed Rosauri *et al.* (1996). Clark *et al.* (1991) showed that the limiting flux occurred at lower pressures for smaller pore sizes and at higher concentrations, rejection was independent of pore size, probably due to the effects of a secondary membrane. As shown by Grund *et al.* (1992), when comparing the filtration of standard BSA with a fatty acid poor version, smaller pores resulted in a greater flux, probably due to a decrease in fouling in this case. As identified in the previous section by Prádanos *et al.* (1996) the differences/similarities in membrane pore size and protein dimensions may be important.

Pore size and structure also appear to be responsible for the type of fouling layer formed. Kim *et al.* (1992 and 1993) showed that high initial fluxes, as expected from a porous membrane with large pores, resulted in the formation of aggregates, formed due to rapid supersaturation of the solution at the membrane surface. Lower initial fluxes produced sheet like protein layers. These findings were confirmed by Sayed Rosauri *et al.* (1996), who found that the fouling layer was thicker on a 100,000 MWCO than a 50,000 MWCO membrane.

3.4 MEMBRANE MATERIAL

Membrane material has been shown to have a varied effect on crossflow filtration. It is well known that proteins adsorb easily onto surfaces because the protein side groups interact with other side groups or surface groups, due to interactive forces. Examples of such forces are electrostatic interaction, hydrophobic interactions and hydrogen bonding. A membrane surface with opposite charge to the protein, or a hydrophobic surface are likely to cause an increase in adsorption. Bowen and Gan (1992) showed that a PVDF Durapore membrane adsorbed less of an enzyme than a similar ceramic anopore membrane. Iordanskii *et al.* (1996) reported a greater steady state adsorption of protein onto polysulfoneamide membranes than polysulfone. A protein-amide interaction was suggested as the cause because the reversibility (= reversible adsorption/total adsorption) was found to increase with membrane amide group content.

Studies have also shown that the membrane properties may also be altered by changing the surface groups present. Dumon and Barnier (1992) showed that, for a ZrO_2 membrane, nitrate and hydroxyl groups acted as favourable adsorption sites for protein adsorption between pH 5.2 and 7. Phosphate and citrate sites were unfavourable adsorption sites at pH 6.8-7.8. The use of phosphate sites was further investigated by Randon *et al.* (1995). Using an inorganic membrane, phosphate sites were shown to (1) increase BSA rejection, (2) improve filtrate flux and (3) decrease adsorption. This was partly explained by looking at surface adsorption through two very simple equations;

$$\mathrm{BSA} + \mathrm{site} \rightarrow \mathrm{BSA}_{\mathrm{site}} \qquad\qquad \mathrm{PO}_4 + \mathrm{site} \Leftrightarrow \mathrm{PO}_{4\,\mathrm{site}}$$

So in the case of adsorption, the surface phosphate groups simply took up potential surface sites. Although the surface became highly covered, the phosphate groups were much smaller than BSA. This caused a smaller decrease in effective pore size and enhanced the flux. The rejection could not be explained in quite the same way. In this case, bonded BSA lowered the surface repulsion but the phosphate groups remained highly repelling and hence the rejection was improved. Butyl phosphoric acid groups were shown to improve rejection further, due to their hydrophobic nature.

Further work by Doyen *et al.* (1996) identified the need for caution when comparing membrane materials. Polysulfone, zirconia and a polysulfone/zirconia mix membranes with similar MWCO were used. The polysulfone membrane showed a flux lower than the zirconia membrane, which was in turn a quarter that of the composite. Electron microscopy revealed pore sizes to be of similar size, but the pores were not homogeneously distributed for the polysulfone membrane, unlike the composite which was homogeneous, and the membrane was thinner with a higher surface porosity. For the filtration of cheese whey, although the steady state flux was comparable for all three membranes, the composite exhibited a higher whey permeability coefficient in the pressure dependent filtration regime. The similarity in steady state flux demonstrates that there is minimal interaction between protein and the membrane material.

3.5 TRANSMEMBRANE PRESSURE

Increases in transmembrane pressure have been reported to result in flux increases by Grund *et al.* (1992), Balakrishnan *et al.* (1993), Tandon *et al.* (1994), Tracey and Davis (1994) and Van Oers *et al.* (1995). A typical conclusion stated by Bowen *et al.* (1995) is that increases in transmembrane pressure (2-20 psi), in this case for the filtration of BSA on a 0.2 μm PC membrane, caused higher initial and final fluxes. Bauser *et al.* (1982), Doyen *et al.* (1996) and Fauchille and Gachelin (1996) reported this increase only occurred up to a maximum and then steadied out, with a further increase in pressure having no effect on the flux. This was attributed to the formation of a gel layer on the membrane surface. When the gel was fully formed, i.e. when the

flux reached a maximum, an increase in pressure simply acted to compress the gel, reduced its permeability and thus cancelled out the increased driving force, resulting in no flux change. Van Eijndhoven *et al.* (1995) attributed the limiting flux to osmotic pressure effects.

Grund *et al.* (1992) showed that protein transmission initially decreased with pressure, as the pressure compressed the cake layer which became less permeable and offered a greater resistance to the passage of protein through it. However, a further increase in pressure caused the transmission to increase. Van Oers *et al.* (1995) filtered BSA at different pressures and then challenged the fouling layer with other solutes including polyethylene glycol (PEG). Increases in TMP were found to increase the rejection of the other components due to the compression of the layer. Reporting a similar trend, van Eijndhoven *et al.* (1995) explained this in terms of diffusion. At low pressure, and hence low velocity, diffusion across the membrane was significant and led to similar bulk and filtrate concentrations. As the pressure was increased, the rate of diffusion decreased relative to convection, leading to a reduction in filtrate concentration. At much higher pressures, protein accumulation occurred at the membrane surface, increasing the filtrate concentration.

Increases and decreases in transmission have been observed by Balakrishnan *et al.* (1993). Experiments involving bacitracin and lysozyme at pH 6.8 filtered through a MX-10 and MX-100 rotating unit showed a decrease in transmission with TMP. However, filtering lysozyme at pH 12.5 (where the sign of the protein charge is the opposite to pH 6.8) transmission was found to increase with TMP. Obermeyer *et al.* (1993) simply reported an increase in transmission with TMP.

3.6 CROSSFLOW VELOCITY

When looking at the effects of crossflow velocity on filtration, it is worth remembering that increasing crossflow velocity leads to an increase in wall shear. It is therefore comparable to the effect of stirring speed in dead end filtration and rotational speed when a revolving membrane is used. Hence this section assumes the effect of crossflow velocity to be the same as that of wall shear.

In general, an increase in wall shear results in an increase in permeate flux. Such results have been shown by Bauser *et al.* (1982), Clark *et al.* (1991), Obermeyer *et al.* (1993), Doyen *et al.* (1996) and Iritani *et al.* (1996), amongst others. A possible explanation is that higher wall shear may act so as to remove macromolecules from any gel layer present, reducing its thickness and hence its resistance. However, in some cases the flux has been shown to be independent of wall shear. For example, Tandon *et al.* (1994) and Balakrishnan *et al.* (1993) reported no significant effect for the filtration of a range of proteins through 10,000 (0-30 psi) and 100,000 (0-10 psi) MWCO PAN membranes. Fauchille and Gachelin (1996) reported no increase in flux for a dilute human albumin feed, but showed an increase in permeate flux for more concentrated feeds, suggesting that the concentration of the stream influenced the effect of shear.

Considering the overall fouling to be comprised of reversible and irreversible (adsorption) fouling, Ingham *et al.* (1980) showed that shear had little influence on the irreversible fouling encountered when filtering albumin solutions through hollow fibre modules, but the reversible fouling was decreased at higher shears, suggesting that gel polarisation was occurring, in agreement with previous comments.

The feed pH is also an important factor and the following work may be explained by taking into account comments made in Section 3.8. Solutions of lysozyme studied by Balikrishnan *et al.* (1993) showed no flux dependency on crossflow velocity at pH 6.8, but then displayed a dependency at pH 12.5 when filtered through a 100,000 MWCO PAN membrane. Prádanos *et al.* (1996) filtered solutions of γ-globulin, lipase and BSA at the same pH. In this case only the BSA showed any noticeable flux dependency with crossflow velocity. The initial flux decay increased and steady state was reached earlier with a decrease in velocity.

Taylor *et al.* (1994) showed that the effects of velocity and wall shear fell into two distinct regions. For the pilot scale filtration of soya protein through a PM50 membrane, crossflow velocities over about 0.2 m s^{-1} (dependant on transmembrane pressure) had little effect but flux was found to vary linearly with velocity, on a log scale, below this value, as seen in Figure 3.2. Wall shear rate had no effect during

pressure dependant filtration, but increased flux in the pressure independent filtration regime. This may be explained by considering the film model, whereby a thin polarised layer forms on the membrane surface. At steady state the flux and layer thickness remain constant, as the convection of solute towards the membrane is matched by the diffusion away.

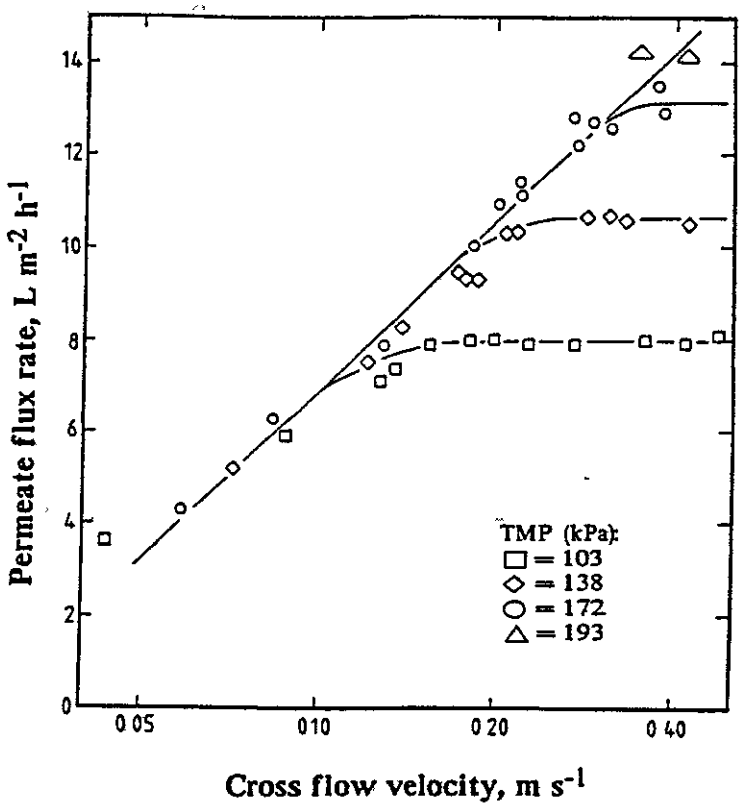

Figure 3.2: The effect crossflow velocity on permeate flux. (Taylor *et al.* (1994)).

Increases in wall shear rate have been shown to cause decreases in protein transmission by Clark *et al.* (1991) and Iritani *et al.* (1996). Balikrishnan *et al.* (1993) reported a dependency of transmission on crossflow velocity for lysozyme and bacitracin at pH 12 with no effect at pH 6.8. However, Obermeyer *et al.* (1993) showed an increase in transmission with an increase in crossflow velocity for the filtration of whey protein at pH 6.5 through a ZrO_2 50 nm pore diameter membrane. The effect was lessened for a pre-adsorbed membrane.

Shear may also have been responsible for causing molecular deformation. Aggregation of proteins at high shear rates, that caused proteins to unfold, have been observed by Kim *et al.* (1993). The denaturation of proteins by shearing forces have also been demonstrated by Jonsson *et al.* (1996). This caused an increase in molecule-molecule interactions to produce aggregates and more adherent cakes. Bowen and Gan (1992) reported a loss of enzyme activity due to shear induced deformation. These changes were possibly permanent.

3.7 TEMPERATURE

The effect of temperature on filtration is two fold. An increase in temperature generally causes a decrease in viscosity but may also cause proteins to aggregate (Xu *et al.* (1995)). When separating a β-casein solution on a ZrO_2 ultrafiltration membrane, Le Berre and Daufin (1994) found that a decrease in temperature caused a reduction in the permeate flux. They explained this in terms of a reduction in diffusivity according to equation 2.1 below. Here, D is the diffusivity, k is the mass transfer coefficient, T is the temperature, μ is the viscosity and a is the solute diameter.

$$D=\frac{kT}{3\pi\mu a} \tag{2.1}$$

3.8 pH

The effect of changing pH may vary depending on the system being studied. These effects are highly influenced by factors such as ionic strength, protein type and membrane type. Generally, as shown by Heinemann *et al.* (1988), steady state protein transmission was highest at the protein IEP, as the protein carried no net charge causing less electrostatic interaction with the membrane. Below this pH, the protein was repelled by the electrical field within the pores which caused a drop in transmission but enhanced the flux, as pore blockage was less likely. Above the IEP

the membrane and protein had opposite charges and were thus attracted to each other, causing pore blockage, resulting in reduced transmission and flux.

Both Palacek and Zydney (1994) and Clark *et al.* (1991) revealed a minimum in steady state flux around the IEP due to protein charge changes altering the intermolecular forces and the packing density. Certainly, static adsorption studies (Iritani *et al.* (1996), Bowen and Gan (1992)) have revealed maximum adsorption, and hence irreversible fouling, around the protein IEP. Clark *et al.* (1991) also showed a maximum in adsorption around the IEP, that decreased at pH values above or below. This was initially attributed to either an increasing tendency for the protein to come out of solution when its net charge is zero, or electrostatic membrane-protein interactions. However, closer inspection of the respective charges revealed a maximum in adsorption would be expected around a pH of 7, whereas it occurs at pH 4.9. This suggested that changes in solubility were quite important. Pouliot *et al.* (1994) also explained an increase in irreversible fouling around the IEP in terms of decreased protein solubility. Protein aggregation around the IEP increased irreversible fouling as the aggregates blocked pores, resulting in a lower flux.

Bowen and Hall (1995) have shown the variation in diameter of a buffered enzyme solution with changes in pH. At pH 7.5 the enzyme was at its smallest and showed its narrowest distribution. Above and below this value both the mean and distribution increased. A more compact structure at the IEP has been reported by van Oers *et al* (1995) and Pincet *et al.* (1995) due to the absence of electrostatic repulsion within the protein structure.

3.9 IONIC STRENGTH

The ionic strength of feed solutions tends to alter the membrane-protein and protein-protein electrostatic interactions. The effect that this may have on the filtration is dependent on several factors, the most important being the protein charge and solution pH. For example, by the measurement of streaming potentials, Konturri and Vuoristo (1996) stated that the presence of ions in solution did change the electrostatic interactions and suggested that they caused the IEP of the proteins to shift. Indeed the

electrostatic interactions became non limiting. Grund *et al.* (1992), Clark *et al.* (1991) and Pouliot *et al.* (1994) showed that this resulted in a decrease in flux with increasing salt concentration. Along with Iritani *et al.* (1995) they attributed this decrease to a compression of the double layer and charge shielding on the proteins. This shielding then resulted in the macromolecules being able to pack more closely, decreasing the permeability and hence reducing the flux. The results of charge shielding have also been seen by Heinemann *et al.* (1988) and Ricq *et al.* (1996). They showed that the filtration became pH independent in the presence of a suitable buffer concentration and Clark *et al.* (1991) showed a decrease in adsorption with increasing salt concentration. The adsorption peak around the IEP was almost eliminated.

Palacek and Zydney (1994) also observed a steady state flux decrease, but this was accompanied by an initial increase in flux. The increase was stated as being due to a decrease in electro-osmotic counterflow, due to a reduction in the Debye length of the protein in a salt solution. In agreement, when filtering a haemoglobin-BSA mixture, van Eijndhoven *et al.* (1995) observed a decrease in flux with decreasing ionic strength. This was also assumed to be due to an electro-osmotic counterflow. The solvent flow caused an unequal flux of ions due to different partitioning at the charged pores. This induced a streaming potential preventing any current flowing across the membrane and reducing the solvent flux due to electrostatic forces acting on the ions. The magnitude of the counterflow increased at low salt concentrations as the thickness of the electric double layer increased.

Grund *et al.* (1992) reported a decrease in transmission in the presence of a buffer, as the charge shielding, again, allowed a more closely packed cake. Van Eijndhoven *et al.* (1995) reported the same effect for BSA, although haemoglobin showed very little change in transmission. However, Heinemann *et al.* (1988) showed an increase in transmission with buffering at pH values away from the IEP.

A study by Millesime *et al.* (1995) revealed four effects of ionic strength depending on the proteins and membranes used; (i) At low ionic strength, with hydrophilic membranes, irrespective of either membrane or protein net charge or with hydrophobic membranes with an identical charge to the protein retention was much

higher than the expected size retention. This is because the free protein acted as a co-ion due to electrostatics. (ii) At low ionic strength, the retention was close to the expected size retention for membranes with a negative charge and proteins with a positive charge. (iii) In the absence of fouling, the retention of hydrophilic membranes reached the expected size retention with increasing ionic strength. (iv) If the ionic strength induced salt promoted interactions with the membrane surface, then the retentions displayed a minima with ionic strength.

Randon *et al.* (1995) explained the enhanced rejection and flux due to the presence of a phosphate buffer as being due to the reversible adsorption of phosphate groups onto the surface, basically taking up potential BSA adsorption sites (full explanation given in Section 3.4).

3.10 MECHANISMS

Many of the mechanisms involved in the fouling of membranes have been mentioned in the previous sections. It is clear that fouling depends on membrane-protein and protein-protein interactions. These interactions may in turn be influenced by pH, ionic strength, concentration and TMP, etc. This section provides an outline of the mechanisms for flux reduction that have been suggested.

There is little doubt that protein adsorption plays a major part in fouling by aggregate free solutions (Chimiel *et al.* (1991), Persson *et al.* (1993), Ko *et al.* (1993), Mochizuki and Zydney (1992), amongst others). Adsorption is influenced by differences in protein and surface properties. Proteins may be captured by a range of mechanisms including electrostatic interactions, hydrogen bonding, van der Waals forces and hydrophobic forces. A good review on the subject is given by Norde (1986). Generally, adsorption must be accepted as an inevitable process occurring on contact between polymeric surfaces and biomolecules. The mechanisms of adsorption will not be covered here.

Several authors (Ingham *et al.* (1980), Grund *et al.* (1992)) have reported that the total fouling resistance produced during filtration of protein solutions is a result of both reversible and irreversible fouling. Irreversible fouling tends to indicate that the proteins are held by strong forces, as in the case of adsorption. By its very nature, reversible fouling suggests that proteins are held by weak forces or merely deposited.

A popular explanation (Bowen *et al.* (1995), Prádanos *et al.* (1996), Jonsson *et al.* (1996)) of the mechanisms at work during the crossflow filtration of protein solutions is to use the complete blocking, standard blocking, intermediate blocking and cake filtration models. The complete blocking model assumes that each particle arriving at the membrane surface blocks a pore/pores without superimposing another particle. The standard blocking model assumes the membrane pores are equal cylinders and that deposition occurs within a pore, decreasing its volume. The intermediate blocking model assumes that particles reaching the membrane surface either settle on other particles or directly block the pores. Finally, the cake filtration model assumes that the membrane can no longer be directly blocked, but particles deposit on top of an existing cake layer. Bowen *et al.* (1995) have proposed a general equation to cover all four models (3.2) with the equations for the constants given in Table 3.1.

$$\frac{d^2t}{dV^2} = \alpha\left(\frac{dt}{dV}\right)^{\beta} \tag{3.2}$$

where t is time, V is total permeate volume and α and β are constants. In Table 3.1, K_A is the blocked surface area of membrane per unit permeate volume, K_B is the decrease in cross section area of pores per unit permeate volume, K_C is the area of cake per unit permeate volume, A_0 is the membrane area, v_0 is the initial flow velocity normal to the membrane and R_r is the ratio of cake resistance over the clean membrane resistance.

Model	α	β
Complete blocking	$K_A v_0$	2
Standard blocking	$\left(2K_B / A_0^{\frac{1}{2}} \right) v_0^{\frac{1}{2}}$	3/2
Intermediate blocking	K_A / A_0	1
Cake filtration	$\left(R_r K_c / A_0^{\frac{1}{2}} \right) v_0^{-1}$	0

Table 3.1: Constants for the generalised blocking model.

Any linearity displayed when plotting the data on the appropriate axes is then indicative of the model being obeyed. The axes are; Q (flow rate) against V for the complete blocking model, t/V against t for standard blocking, $1/Q$ against t for intermediate blocking, t/V against V for cake filtration.

Generally, more than one mechanism of blocking may occur at one time, due to wide variations in pore size distribution and protein/aggregate size. When there is a significant retention of protein by the membrane, Prádanos *et al.* (1996) and Jonsson *et al.* (1996) have shown that the first step in flux decline during ultrafiltration may be described by the intermediate pore blocking model. The slower second step was then dependant on the membrane/molecule size. When the proteins are much larger than the pores, a cake is formed on the membrane, whereas for proteins smaller than the pores, unblocked pores become covered with adsorbed protein and hence flux decay follows a standard blocking model. Concentration may also modify the mechanism. Filtering an enzyme through a microfiltration membrane, Bowen and Hall (1995) showed that in-pore blocking occurred at low concentration, whilst deposits formed at higher concentrations. This was confirmed by atomic force microscopy. Tracey and Davis (1994), during protein microfiltration, also observed internal fouling at low concentrations, following the standard and complete blocking model. At higher concentration, aggregates formed resulting in a build up of cake type deposit.

Kelly and Zydney (1995) found that the early fouling observed when filtering BSA through a 0.2 μm PVDF membrane could not be explained by pore blockage, constriction or cake formation. Instead they proposed two steps. Firstly, the convective deposition of aggregates on the membrane. These aggregates then acted as nucleation sites for the attachment of native protein by disulphide linkage. The filtration of aggregate free BSA showed that the membrane was inert to the direct attachment of native protein.

The presence of two different fouling deposit types have been observed for the ultrafiltration of albumin by Kim *et al.* (1992) whilst little/no internal adsorption was observed on micrographs. Membranes displaying lower initial fluxes formed cakes on their surfaces that were seen to grow and blind the surface. High flux membranes formed aggregates at the mouths of pores, formed by rapid supersaturation (also Kim *et al.* (1993)). This has also been observed by Sayed Razavi *et al.* (1996) for the ultrafiltration of the aqueous extract of soy flour, who add that cakes are thinner than aggregates.

The magnitude of the permeate flux and the thickness of the fouling layer have been shown to be due to a balance in the forces around the membrane. Palecek and Zydney (1994a,b) and Pujar and Zydney (1994) have shown that the fouling layer ceases to grow when hydrodynamic drag forces, caused by the filtrate flow through the layer, and the intermolecular repulsive forces between the fouling layer and the bulk solution are equal. The layer can only grow whilst the drag forces are greater. Changes in pH (charge) and pressure may lead to a more or less open structure in the deposit. The electrostatic interactions may be modified at different salt concentrations, due to changes in the electro-osmotic forces. The charged protein deposit is surrounded by counter-ions. The flow of solvent (permeate) through the deposit provides a greater flow of counter-ions away from the deposit. So as to maintain a net flow of charge, a streaming potential is created, which causes counter-ions to flow in the opposite direction and this causes a reduction in the permeate flux. At increasing salt concentrations the thickness of the protein double layer is decreased and hence the magnitude of the streaming potential is decreased, causing the flux to increase.

Generally, this is counteracted as filtration proceeds due to charge shielding in the deposit causing a tighter packing, reduced permeability and reduced flux.

CHAPTER 4

EXPERIMENTAL MATERIALS AND METHODS

This work is based on the filtration of a model beer solution. Several beer analyses were obtained, from which the key components were selected. The components used are given below, along with the criteria for their selection. The methods for the final feed preparation and experimentation are also detailed.

4.1 CHOICE OF MATERIALS

4.1.1 Beer composition

In this section the detailed composition of beer is reviewed. Three tables of beer components are presented from reviews by Hough *et al.* (1982a, 1982b), Moll (1991) and René and Maingonnat (1993). The review by Moll (1991) is particularly detailed, with only the more major components reported here. It may be seen that beer contains thousands of individual components spanning a wide range of molecular weights and chemistries. Concentrations range from the g l^{-1} range down to $\mu g\ l^{-1}$. It is quite likely that there are other components yet to be discovered.

Generally, the three references agree on component concentrations. The concentration of pentosans given by and René and Maingonnat (1993) are somewhat higher than those given by Moll (1991) (less than 1000 mg l^{-1}). However, there is a larger discrepancy in the protein concentration which ranges from a trace to 5 g l^{-1}. This is probably due to the analyses being carried out on different beers and possibly due to differences in definition of the dividing line between polypeptides and proteins.

	Typical amount		Typical amount
Original wort density	11.80 g/100 g	**Nitrogen compounds**	
Alcohol	3.93 g/100 g	Proteins	5.0 g l^{-1}
Real extract	4.15 g/100 g	Low MW nit. cmpds.	185 mg l^{-1}
Maltose	1430 mg l^{-1}	Proline	357 mg l^{-1}
Maltotriose	1930 mg l^{-1}	Alanine	103 mg l^{-1}
Maltotetraose	3360 mg l^{-1}	**Organic acids**	
Maltopentaose	1330 mg l^{-1}	Citrate	190 mg l^{-1}
Maltohexaose	1150 mg l^{-1}	Acetate	129 mg l^{-1}
Maltoheptaose	1090 mg l^{-1}	Malate	85 mg l^{-1}
Maltooctaose	1220 mg l^{-1}	**Phenolic compounds**	
Maltononaose	1590 mg l^{-1}	Anthocyanogens	46 mg l^{-1}
Maltodecaose	1750 mg l^{-1}	Catechin	5-55 mg l^{-1}
Maltotetradecanose	1020 mg l^{-1}	Quercetin	5-125 mg l^{-1}
Maltooctadecanose	1130 mg l^{-1}	**Inorganic elements**	
Higher dextrins	5490 mg l^{-1}	Potassium	493 mg l^{-1}
Water	919 g l^{-1}	Magnesium	107 mg l^{-1}
Soluble CO_2	5 g l^{-1}	Total phosphorus	308 mg l^{-1}
Secondary products		Sulphate	176 mg l^{-1}
Glycerol	1417 mg l^{-1}	Chloride	179 mg l^{-1}

Table 4.1: Beer composition given Hough *et al.* (1982a, 1982b).

		Conc. ($g\ l^{-1}$)	MW (Da)
Minerals	Ca, K, Mg, Na, P, ...	0.5 - 2	<100
Sugars	Mono and oligosaccharides	7 - 13	200 - 600
	α-glucans (dextrins)	25 - 35	50,000 - 200,000
	β-glucans	0.07 - 0.5	50,000 - 200,000
	pentosans	1.5 - 3.5	50,000 - 200,000
	Total	33 -44	
Organic N	proteins	traces	>150,000
	polypeptides	0.06 - 0.2	5000 - 70,000
	peptides	0.1 - 0.5	1500 - 5000
	amino acids	0.02 0.1	<5000
	Total	0.3 - 1	
Phenolics	monophenols	0.02 - 0.06	<200
	polyphenols (monomers)	0.07 - 0.1	200 - 500
	polyphenols (polymers)	0.02 - 0.06	1000 - 5000
	Total	0.15 - 0.35	
Glycerol		1 - 3	92
Non-volatile acids	Citric, malic, gluconic	0.2 - 1	193, 134, 218

Table 4.2: Basic beer composition given by René and Maingonnat (1993).

	Typical amount (mg l^{-1})	Flavour threshold (mg l^{-1})
Alcohols: (>50 mg l^{-1})		
Ethanol	25000 - 50000	14000
Glycerol	1300 - 2000	
2,3-butanediol	50 - 150	4500
3-methyl-1-butanol	30 - 70	70
Polyphenols: (>5 mg l^{-1})		
Leucocyanidins	4 - 80	
Leucodelphinidin	1 - 10	
Catechin	0.5 - 13	
Carbohydrates: (>1000 mg l^{-1})		
Glucose	40 - 1100	
Maltose	700 - 3000	
Sucrose	0 - 3300	2600
Maltotriulose	400 - 3400	
α-glucans DP 4-10	5360 - 21300	
α-glucans DP 11-35	11000 - 14000	
α-glucans DP 35-250	1700 - 3500	
α-glucans DP >250	1000 - 2000	
Acids: (>100 mg l^{-1})		
Carbon dioxide	3000 - 5500	1000
Acetic	30 - 200	180
Succinic	16 - 140	
Pyruvic	15 - 150	50 - 400
Malic	30 - 150	350
Citric	60 - 210	
Esters: (>5 mg l^{-1})		
Methyl acetate	0.6 - 12	550
Ethyl acetate	8 - 42	25

Table 4.3: Typical composition of a Pilsen beer given by Moll (1991) (cont.)

	Typical amount (mg l^{-1})	Flavour threshold (mg l^{-1})
Aldehydes: (>5 mg l^{-1})		
Acetaldehyde	2 - 20	25
Protocatechualdehyde	1 - 10	
Ketones: (>5 mg l^{-1})		
Hydroxyacetone	15 - 30	70
3-hydroxy-2-butanone	1 - 10	17
Maltol	8	
5-hydroxy-5,6-dihydromaltol	23	
Nitrogen compounds: (>200 mg l^{-1})		
Proline	100 - 400	>1350
N compounds <2600 MW	1200 - 4000	
N compounds 2600 - 4000 MW	400 - 800	
N compounds 4600 - 12000 MW	250 - 560	
True proteins	200	
Inorganics: (>100 mg l^{-1})		
Calcium	20 - 160	
Chloride	150 - 400	700
Magnesium	60 - 140	1400
Phosphorus, inorganic	280 - 720	
Phosphorus, organic	90 - 280	
Potassium	200 - 500	
Sodium	20 - 110	2000
Sulphate	60 - 300	2000

Table 4.3 (cont.): Typical composition of a Pilsen beer given by Moll (1991).

The main component in beer is water contributing over 900 g l^{-1}. The other components chosen for study in this work are listed in the following sections. They have been selected to cover a range of chemistries. Section 4.1.11 details their structures.

4.1.2 Ethanol

The main alcoholic constituent of beer is ethanol, but there are a range of other alcohols which are formed during fermentation. The composition of the alcohols depends on several factors but chiefly the yeast type is most important. Therefore, the use of ethanol in the model solution needs little explanation as, after water, it is the second most concentrated component present. Its typical concentration has been taken as 40 g l^{-1}.

4.1.3 Glycerol

Outside the sugar compounds, glycerol is one of the more concentrated low molecular weight components present in beer. Glycerol (1,2,3-propanetriol) is known to modify flavour, probably due to interactions with other compounds, as it is present at a level below the flavour threshold (at which point it provides a sweet taste). It may also modify viscosity. It is primarily derived from yeast metabolism, but small amounts may be found in cereals. Its typical concentration has been taken as 1500 mg l^{-1}.

4.1.4 Maltose

The sugars provide a large proportion of the material in beer, ranging in size from monosaccharides, such as glucose, to oligosaccharides up to large sugar chains, polysaccharides. The short chain saccharides are produced by the enzymatic degradation of polysaccharides found in the raw materials. These sugars are thought to be responsible for the sweetness in beer but appear to have no other function.

Ideally an oligosaccharide of intermediate molecular weight would have been used, but the cost of maltose oligomers was prohibitive. Therefore maltose was chosen as a typical short chain sugar. Its typical concentration has been taken as 1500 mg l^{-1}.

4.1.5 Citric acid

Beer contains a wide range of non-volatile organic acids including citric, fumaric, lactic, pyruvic, succinic, gluconic acids, etc. They are derived from malt and fermentation products. The concentration of acids depends on the method of malt production and the fermentation conditions. In order to set the pH of the feed solution to 4.2, an acid was required. Citric acid was used as it is the most abundant acid present in beer. Citric acid (2-hydroxy-1,2,3-propanetricarboxylic acid) is a tricarboxylic acid and has similar properties to most organic acids.

4.1.6 Starch

There are three principle types of long chain carbohydrate that have been identified in beer. They are dextrins (α-glucans), β-glucans and pentosans. Dextrins are higher molecular weight carbohydrates, produced during mashing. Although they don't contribute any special flavour, they are thought to give fullness or body, they may act as flavour carriers and may lead to haze, due to their association with polyphenols and proteins. It is uncertain whether they affect head retention. A suitable model for the dextrins is starch as it represents an α-linked polysaccharide.

The β-glucans are derived from the cereal grains and affect the viscosity of both the wort and the beer. They contribute to palate fullness, foam retention and the formation of precipitates and hazes, which are known to lead to the blocking of filters. A representative model for the β-glucans is β-glucan, a 1,4 and 1,3 linked glucose polymer.

The pentosans are non-starchy polysaccharides, derived from the barley endosperm where, together with β-glucans, they act as a binding material. Pentosans do not themselves improve head retention, but they are believed to act with proteins and dextrins to aid head retention and have been found to be present in high concentrations in beer hazes.

Starch has been used in the solution as a model for the long chain α-glucan fraction of polysaccharides present in beer. It is this α-glucan fraction that forms the bulk of the polysaccharides present. The chain length of starch is probably a little too long to be present in beer, but it is cheap, readily available and displays a similar chemistry to the α-glucans. As they are known to cause filtration problems, β-glucans would have been of interest, but their cost in pure form inhibited their use here.

Starch is a polysaccharide derived from cereals, constructed of polymeric chains of α-1→4-glucopyranose units. It consists of a mixture of linear amylose and branched amylopectin. These branches are α-1→6-glucosidic links. The typical concentration of starch was taken as 1500 mg l^{-1}.

4.1.7 Casein

The proteins are derived from barley and to a lesser extent hops and yeast cells. Generally they have molecular weights ranging from 5,000 to 100,000 (although higher values have been reported). During malting and mashing some proteins are broken down by enzymes into smaller fractions i.e. peptides. The higher molecular weight material is known to be important for head retention.

Studies have been carried out using a variety of methods in order to determine the proteins present in beer. Electrophoretic and immunological studies have been carried out on beer proteins by Curioni *et al.*(1995). They found that the only well characterised proteinaceous component found in beer was Antigen 1 (MW~

40 kDa, 20-170 mg l^{-1}), which may be seen as a relatively unmodified protein, although it is in fact a polypeptide.

According to Williams *et al.* (1995) barley albumins and globulins (MW 10,000-40,000) are released into the wort and appear in small amounts (20-600 mg l^{-1}) in the finished product. A study by Dale and Young (1992) carried out by fast protein liquid chromatography, found nitrogenous fractions of high molecular weight (MW) 300,000-500,000, intermediate MW 40,000-60,000 and low MW 5,000-20,000. They also showed that, at least in the case of the intermediate MW compounds, the composition of material depended on the method of brewing and raw materials used.

In this case casein has been used to model the longer chain polypeptides and proteins. As with starch, the chain length may be somewhat larger than that found in beer due to the breakdown of cereal proteins during production. The structures of some beer proteins, as stated above, have been identified but are not commercially available. Amylase may have caused problems in the chosen system due to its ability to enzymatically degrade starch.

Whole casein is composed of three fractions; α, β and γ. Each fraction has a slightly different amino acid composition (Kirk and Othmer, 1979c), as seen in Table 4.4. Also shown in the table are the protein compositions found by Dale and Young (1992) for two British ales. It may be seen that the amino acid composition varies somewhat between whole casein and its fractions. The compositions of the two beer proteins also vary, although it should be noted that the beers in question are not Pilsen type beers on which the model solution is based. Generally, the concentration of most amino acids is comparable between casein and the beer proteins, although casein contains somewhat less alanine, glycine and serine yet more lysine and leucine.

The typical concentration of protein was taken as 150 mg l^{-1}.

Component	whole	α-	β-	γ-	beer A	beer B
	composition, g/100 g					
alanine	3.0	3.7	1.7	2.3	12.30	7.30
arginine	4.1	4.3	3.4	1.9	1.60	1.50
aspartic acid	7.1	8.4	4.9	4.0	9.20	5.10
cysteine	0.34	0.43	0.0-0.1	0.0	0 00	0.70
glutamic acid	22.4	22.5	23.2	22.9	12.90	27.10
glycine	2.7	2.8	2.4	1.5	7.70	6.20
histidine	3.1	2.9	3.1	3.7	4.10	1.80
isoleucine	6.1	6.4	5.5	4.4	3.70	3.50
leucine	9.2	7.9	11.6	12.0	6.50	6.00
lysine	8.2	8.9	6.5	6.2	1.40	2.50
methionine	2.8	2.5	3.4	4.1	0.00	0.30
phenylalanine	5.0	4.6	5.8	5.8	2.70	3.30
proline	11.3	8 2	16.0	17.0	6.60	12.90
serine	6.3	6.3	6.8	5.5	14.60	9.50
threonine	4.9	4.9	5.1	4.4	7.40	4.70
tryptophan	1.7	2.2	0.83	1.2		
tyrosine	6.3	8.1	3.2	3.7	2.20	1.90
valine	7.2	6.3	10.2	10.5	6.80	5.50

Table 4.4: Amino acid composition of casein and two beer proteins.

4.1.8 Calcium sulphate

Beer contains a wide range of inorganics which are mainly derived from the raw materials such as the brewing water and grain. Most potassium, magnesium, sodium, oxalate and phosphate ions are derived from grain, whilst the brewing water supplies most calcium, sulphate, chloride and nitrate ions. The composition of the raw water is often altered by the brewer.

The presence of metal ions in solution can affect the shape and conformation of longer chain molecules. Hence, a metal salt was added to the system. Calcium was chosen as it is a common constituent of brewing water and also a known membrane foulant. Of the inorganic cations present the most common are phosphate, chloride and sulphate. Calcium sulphate is suitably soluble, especially under acidic conditions. Its typical concentration has been taken as 100 mg l^{-1} (of Ca^{2+}).

4.1.9 Catechin

The phenolic content of beer consists of a wide range of phenolic compounds, from monophenols through monomeric and oligomeric polyphenols to long chain polymeric polyphenols. The monophenols consist of phenolic acids, phenolic alcohols, phenolic amines and phenolic amino acids. The monomeric polyphenols consist of the flavan-3-ols (catechins), the flavan-3,4-diols (anthocyanogens) and the flavanols (quercetin, isoquercetin, etc.). They are also major components in colour and taste. It is the intermediate molecular weight (≈1000) compounds that are responsible for colour through a browning reaction. Proteins and polyphenols, along with small quantities of sugars and metal ions, are involved in the formation of insoluble complexes known as haze. Of the polyphenols found in beer, those containing 15 carbon atoms have been identified as being the more concentrated. This group includes several leucocyanidins, leucodelphinidin and catechin. Catechin was used to model this group and was added at a typical concentration of 50 mg l^{-1}, somewhat higher than its actual concentration found in beer.

4.1.10 Ethyl acetate

Ethyl acetate was chosen as a volatile flavour component. It is the most concentrated of the esters present and may potentially be present in a concentration above its flavour threshold. It was used at a typical concentration of 50 mg l^{-1}.

4.1.11 Structures of the components

The structures of all the components used in this study are given in Table 4.5.

	Type	Model for	MW	Structure
Ethanol	Alcohol	Ethanol	46	
Glycerol	Alcohol	Glycerol	92	
Citric acid	Acid	Acids/ setting pH	192	
Acetic acid	Acid	Citric acid substitute	60	
Succinic acid	Acid	Citric acid substitute	118	
Maltose	Carbohydrate	Short chain carbohydrate	342	
Lactose	Carbohydrate	Maltose substitute	342	
Sucrose	Carbohydrate	Maltose substitute	342	
Glucose	Carbohydrate	Maltose substitute	180	

Table 4.5: Organic components in model feed stream: Their role and structure (cont.).

	Type	Model for	MW	Structure
Fructose	Carbohydrate	Maltose substitute	180	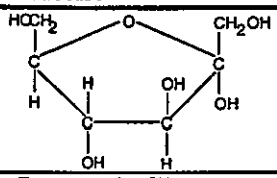
Starch	Poly-saccharide	Long chain carbohydrate	10^6	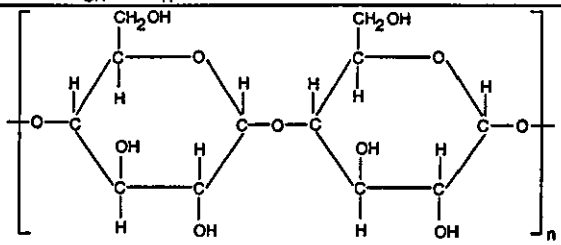 * also branched forms of this unit.
Casein	Protein	Polypeptides/ proteins	$5*10^4$	Amino acid chain
Ethyl acetate	Ester	Major volatiles	88	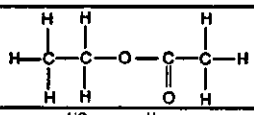
Catechin	Polyphenol	Polyphenol monomers	290	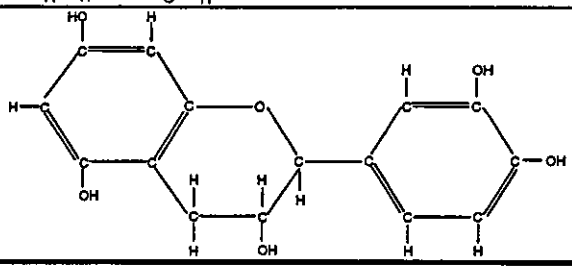

Table 4.5 (cont.): Organic components in model feed stream: Their role and structure.

4.2 EXPERIMENTAL MATERIALS

4.2.1 Chemicals

The following components were used in the production of the model beer solution (in order of decreasing concentration); deionised (DI) water, ethanol, maltose, glycerol, starch, casein, calcium sulphate, ethyl acetate, citric acid and catechin. In certain experiments, maltose was replaced by either lactose, sucrose, glucose or fructose and citric acid was replaced by acetic acid or succinic acid. Materials were of high purity, allowing the effect of single components to be examined.

Component	Supplier	Catlog. no.	Purity
Ethanol	Fluka	02880	>99% v/v
Maltose	Sigma	M-2250	90-95%
Lactose	Fisons	L-0250	Analytical reagent
Sucrose	Tate and Lyle	-	≈ 100%
Glucose	Sigma	G-8270	99.5%
Fructose	BDH	28433	Gen. purpose reagent
Glycerol	Lancaster	14233	99+%
Starch	Sigma	S-9765	ACS
Casein	Sigma	C-7078	Technical grade
Calcium sulphate	Fisons	c/2440/53	Bench reagent
Ethyl acetate	Aldrich	27,052-0	99.8%
Citric acid	Lancaster	4238	99+%
Acetic acid	Aldrich	24,285-3	99+%
Succinc acid	Aldrich	23,968-2	99+%
Catechin	Sigma	C-1251	98%

Table 4.6: Beer component suppliers and purity.

DI water was supplied from a Millipore Milli-RX 20 unit and was of grade II quality with a conductivity of 15 MΩ cm. This water was essentially free of inorganic material and contained organic material at very low concentrations that did not interfere with analytical methods. The supplier, catalogue number and purity of the other components are given in Table 4.6.

4.2.2 Membranes

Polymeric membranes were used in this work. For most work a 0.2 μm cellulose nitrate membrane was used, although other membranes were used in later work. 0.2 μm membranes were chosen as they are sterilising grade membranes, in other words their permeate is bacteria free, although 0.45 μm membranes are regarded

as sufficient in the brewing industry. Membrane materials, suppliers and pore sizes are given in Table 4.7, with their structures given in Table 4.8.

Material	Supplier	Pore size (μm)
Cellulose nitrate	Sartorius	0.2
Polycarbonate	Poretics	0.2
Polyamide	Sartorius	0.2
Polyethersulphone	Gelman	0.2

Table 4.7: Membrane materials and pore sizes.

Membrane		Structure
Cellulose nitrate	CN	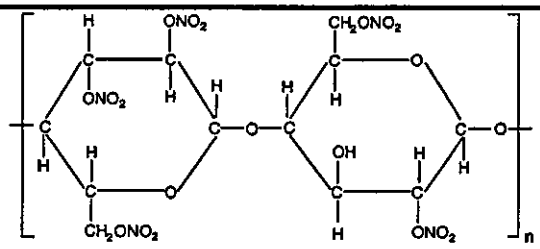
Polyethersulphone	PES	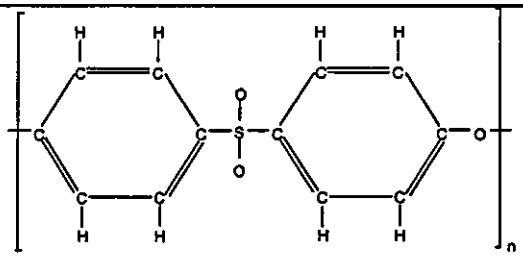
Polycarbonate	PC	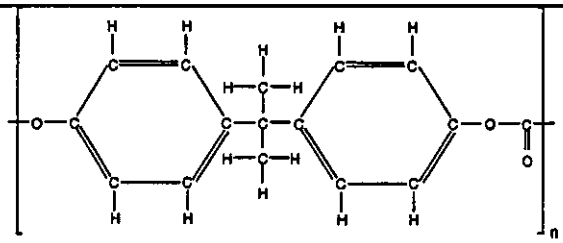
Polyamide	PA	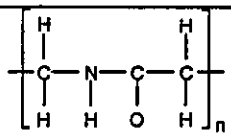

Table 4.8: Chemical structures of membrane materials.

4.3 EXPERIMENTAL APPARATUS

4.3.1 Description

A schematic of the rig may be seen in Figure 4.1, whilst Figure 4.2 shows a photograph of the apparatus. It had a capacity of 7.5 litres and was constructed entirely of stainless steel except for the permeate recycle line, which was plastic. Line pressure, differential pressure across the membrane and the feed flow rate were measured by means of transducers and displayed on a computer, whilst feed temperature was displayed externally on the cooler. Throughout an experimental run, the output signals from the flow and pressure transducers were recorded by the computer and stored on its hard disk.

Cooling was achieved by passing coolant (Synthoil 60 (Fisons)) through a lagged concentric tube type heat exchanger, which also acted as the feed tank. The coolant was cooled/heated by a Kanke cryostat on which coolant temperatures could be set. Experiments were carried out at 20°C ± 1°C.

Pumping was provided by a variable speed positive displacement gear pump. This type of pump is typical of those used in the processing of beverages as it minimises shear on the process fluid, thus reducing the risk of protein denaturation.

The membrane was housed in a flat membrane module, shown in Figures 4.3 and 4.4. Process fluid entered the module and was redistributed over the width of the rectangular flow channel by the central module plate. The backing plates were bolted to the central plate by 6 bolts. This module was designed to hold two membranes, although one side was blanked off throughout this study. Membranes were supported by a porous sintered stainless steel plate, providing an active filtration area of 0.0059 m^2. Flat membrane sheets were cut so as to overlap the support up to the bolt holes. Leaks were prevented by placing a flat rubber gasket between the mating steel surfaces.

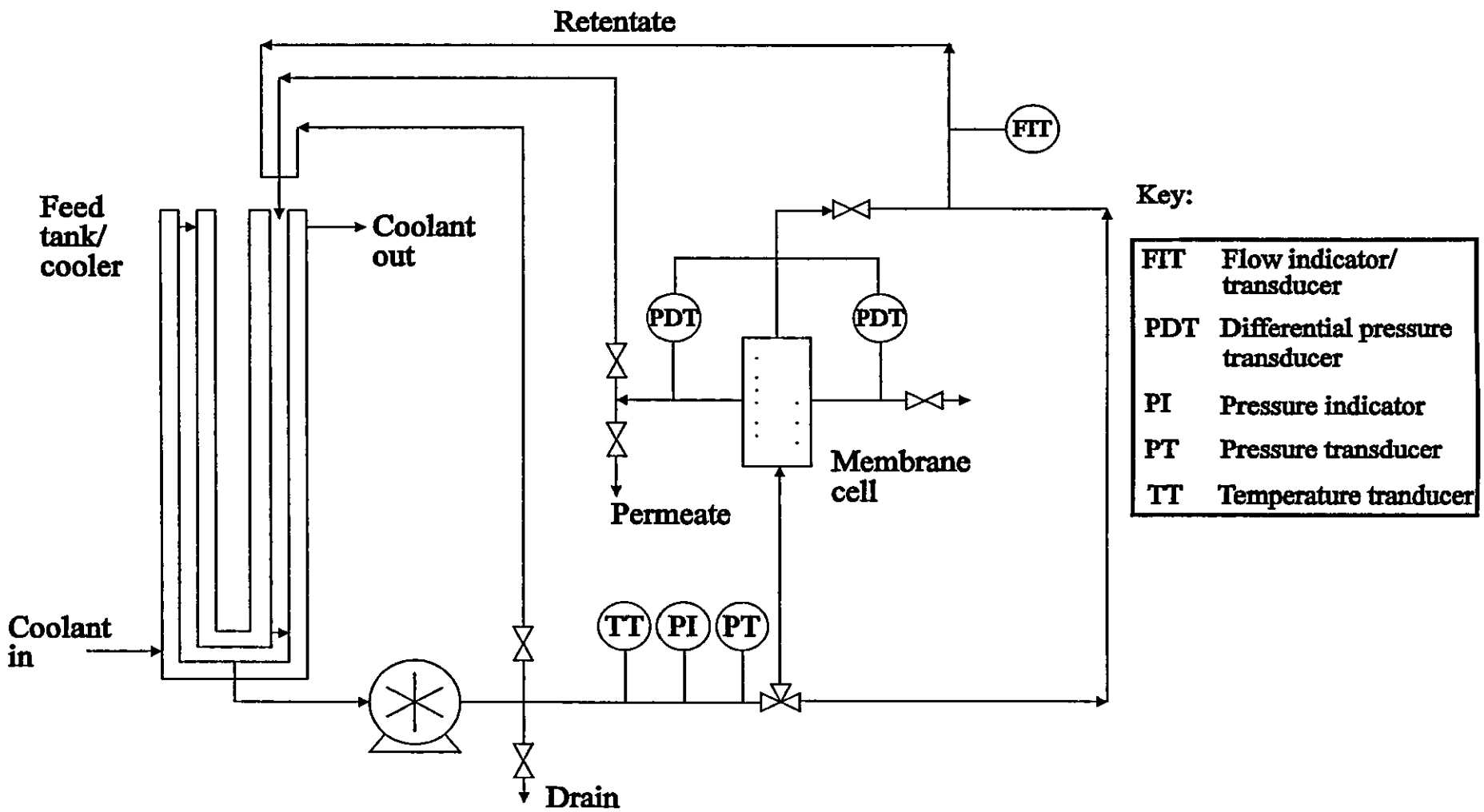

Figure 4.1: Schematic of experimental rig.

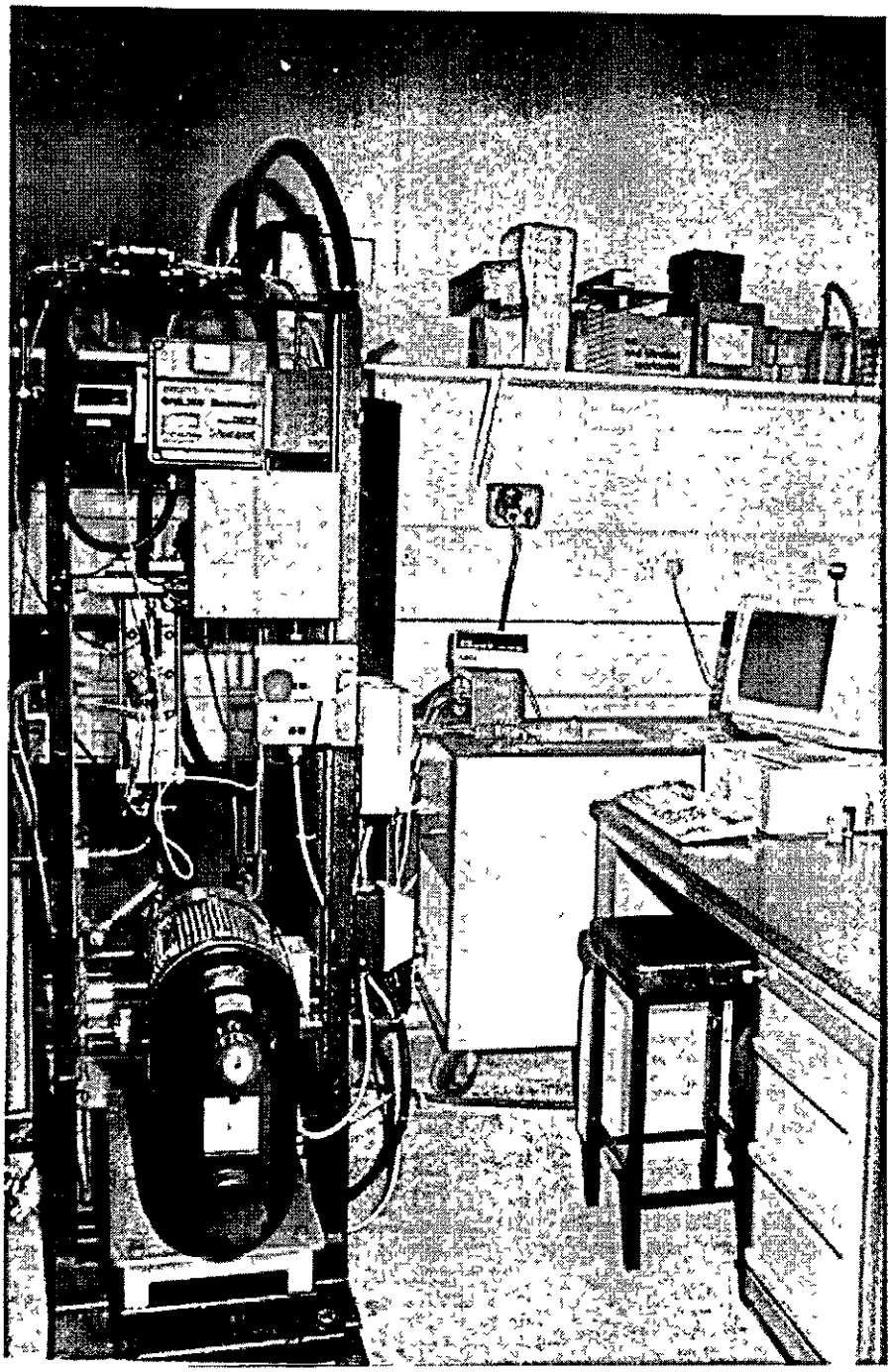

Figure 4.2: Photograph of the apparatus.

Once the rig was running, the crossflow velocity and transmembrane pressure were altered by varying the pump speed and adjusting the valve on the outlet side of the membrane module. Crossflow velocities could be varied over the range 1.1-2.8 m s^{-1} and transmembrane pressures from 1.9 to 4.5 bar. The feed stream could be made to flow either through the membrane module or around the recycle loop by changing the position of the two-way valve. For all experiments both the feed and permeate were continually recycled.

4.3.2 Calibration

There are four types of sensor that need calibrating, namely the magnetic flowmeter, line pressure transducer, differential pressure transducers and temperature probe. The flowmeter was calibrated by means of a bucket and stopwatch. This was done by starting the pump, removing the recycle loop from the feed tank and thus diverting the flow into a bucket. The bucket and contents were then weighed and the mass of water deduced. This was repeated at several pump speeds. These values were then entered into the calibration program on the computer, so that the computer recorded the flow rate in m s^{-1}.

The differential pressure transducers and the line pressure transducer were calibrated by applying a range of known pressures, read by means of a pressure gauge. Again, these values were then entered into the calibration program on the computer, so that the computer recorded the pressure in bar.

The temperature probe was calibrated by running the rig over a range of temperatures, sampling the feed and measuring the temperature with a mercury-in-glass thermometer. These values were then compared to those given externally by the cryostat, given in °C.

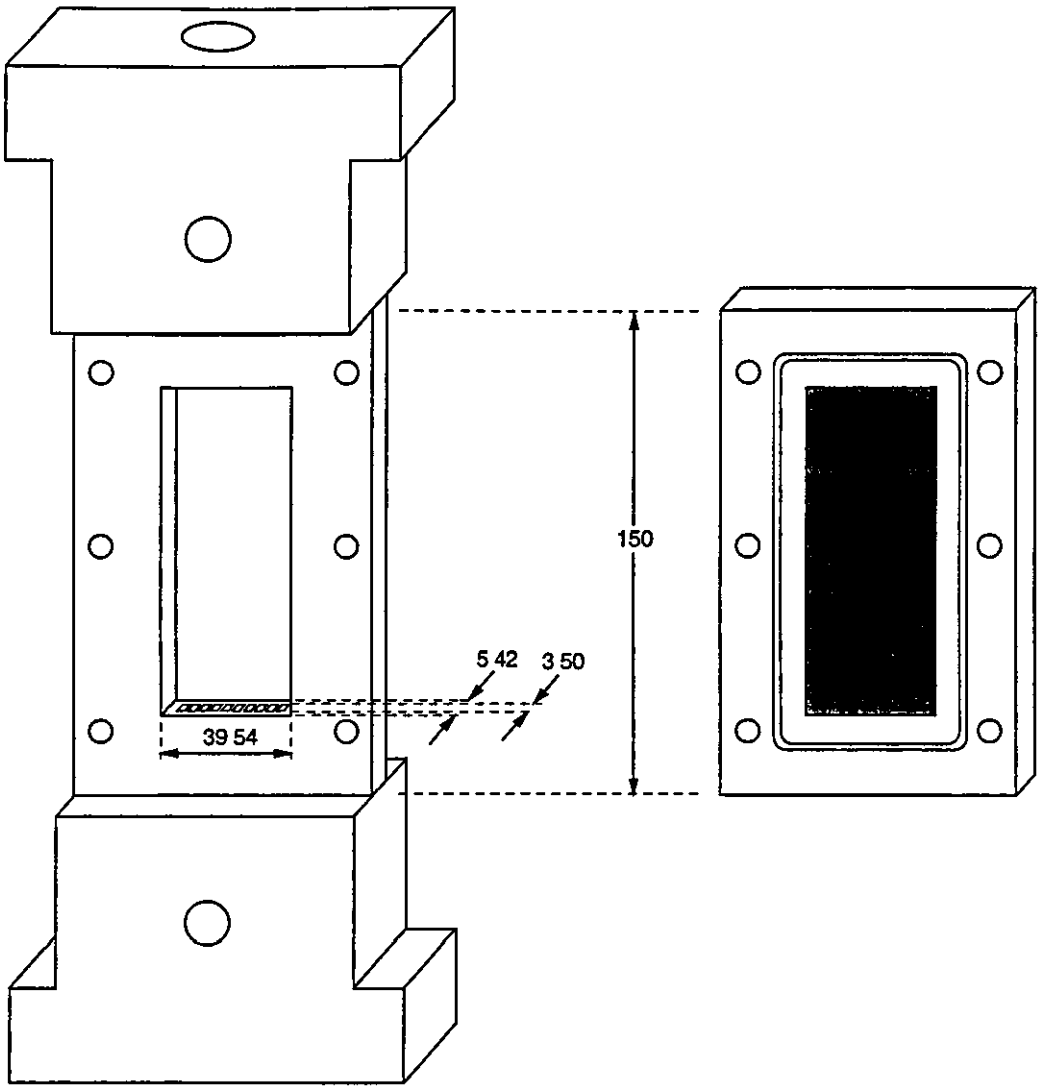

* All dimensions are in mm

Figure 4.3: Diagram of membrane cell and dimensions.

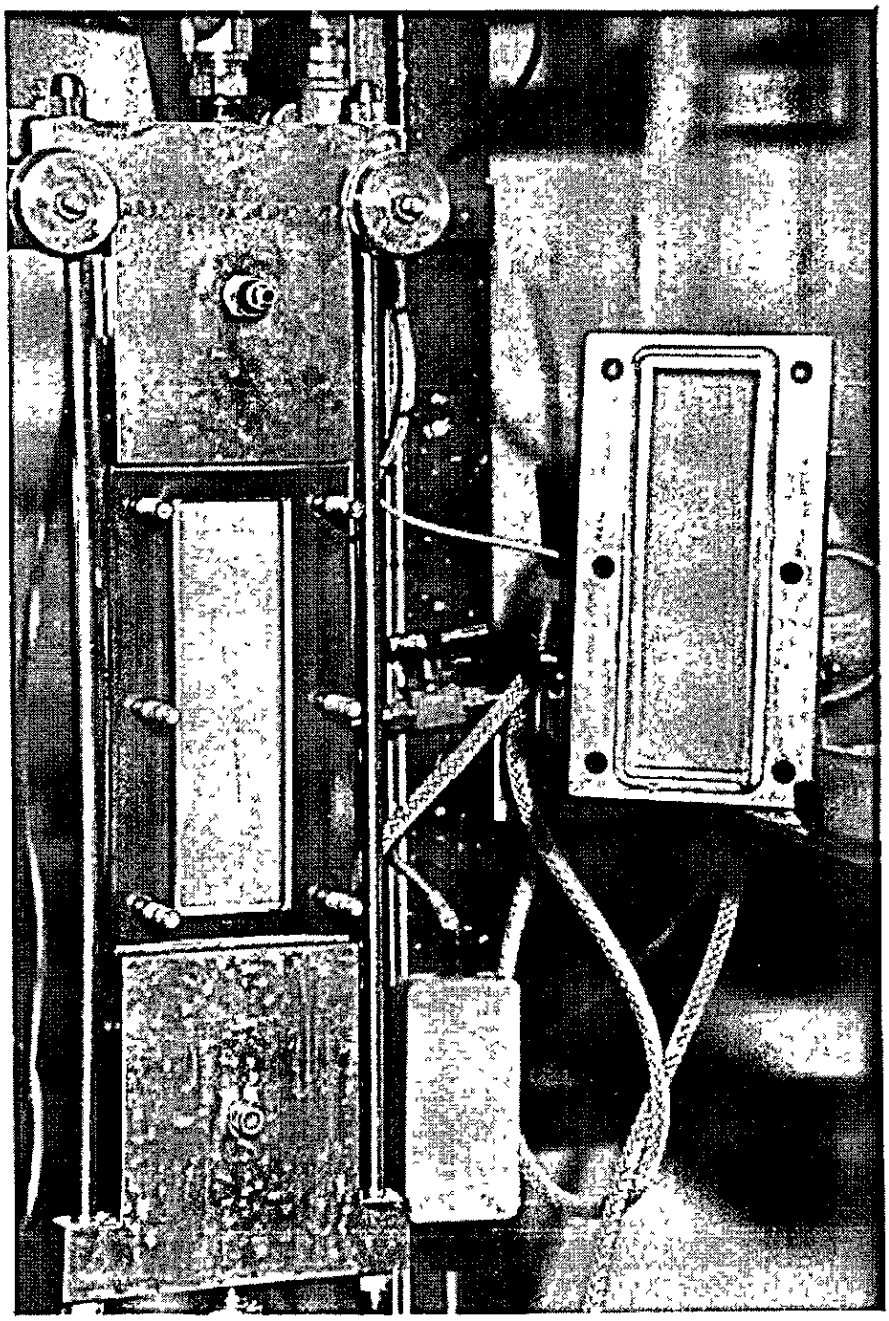

Figure 4.4: Photograph of the filtration cell.

4.4 FEED PREPARATION

4.4.1 Starch

Starch was prepared as a concentrated solution. 6.0 g of starch powder was accurately weighed into a 50 ml glass beaker and 9.0 g DI water added. The contents of the beaker were then stirred to give a thick paste. 450 g of DI water was poured into a weighed 500 ml glass beaker containing a 1 inch magnetic flea. The beaker was placed on a magnetic stirrer/hotplate and heated until it boiled. The beaker was then transferred to a cold magnetic stirrer, stirred rapidly, the thick starch paste added and the small beaker was reweighed. The stirring speed was adjusted to ensure satisfactory mixing as the resulting solution cooled. When cool, the large beaker and contents were weighed, the paste transferred to a 500 ml screwtop glass jar and refrigerated overnight.

The concentration of the solution was then calculated as follows:

$$\text{mass of starch in solution} = \text{mass of starch in small beaker} \times \frac{\text{mass of clean beaker}}{\text{mass of empty beaker}}$$

$$\text{starch concentration in solution} = \frac{\text{mass of starch in solution}}{\text{mass of large beaker and contents} - \text{mass of empty beaker}}$$

4.4.2 Casein

Casein was prepared as a concentrated solution. 2.00 g of casein was accurately weighed into a 100 ml screwtop glass jar. 30 ml of 0.1 M NaOH was added to the jar, by means of a pipette, along with 50 ml of DI water and a 2 cm magnetic flea. The jar was then placed on a magnetic stirrer and stirred rapidly for an hour or until the casein was seen to have fully dissolved. The concentrated solution was then refrigerated overnight.

4.4.3 Calcium sulphate

Calcium sulphate was prepared as a dilute acidic solution due to solubility problems under neutral conditions. The mass of calcium sulphate required in the experimental feed was accurately weighed into a 5 l glass conical flask. 0.9 g of 33% w/w citric acid, 4 l of DI water and a 1 inch magnetic flea were added. The conical was sealed with a rubber bung and placed on magnetic stirrer/hotplate and stirred/heated at 40°C for 1 hour or until the calcium sulphate was seen to have fully dissolved. The resulting solution was left at room temperature overnight.

4.4.4 Catechin

Catechin was prepared as a dilute solution. 0.35 g of catechin were accurately weighed onto a square of aluminium foil. The catechin was then washed off the foil into a 5 l glass conical flask using DI water and made up to 4 l with DI water. The conical was sealed with a rubber bung, placed into a Fritsch laborette type 17.002 ultrasonic bath for 10 minutes, agitated and replaced in the ultrasonic bath for a further 10 minutes.

If used in conjunction with calcium sulphate, the calcium solution was prepared as stated. The catechin preparation was then performed using the calcium sulphate solution in place of DI water.

4.4.5 Feed composition

The feed solution was prepared so that the ratios of components were the same as in the beer solution, rather than replacing missing components with water. An example is given below (Table 4.9). The concentrations in beer are summed to give a total concentration per litre. The density of the solution was assumed to be 1000 g l^{-1}, as there should only be a small deviation from this value in any case. The concentration of each component was then multiplied by a factor of 1000/total concentration of components to give the concentration in the experimental feed. Finally the experimental concentrations were then multiplied by 6 to give their mass required in the final solution.

Component	Conc. in beer	Expt'l conc.	Mass required
	g l^{-1}	g l^{-1}	g
Water	919	955.30	5731.80
Ethanol	40	41.58	249.48
Glycerol	1.5	1.56	9.36
Maltose	1.5	1.56	9.36
Total	962	1000	
(factor)	(1.0395)		

Table 4.9: Example of feed composition calculation.

4.4.6 Experimental feed

A fresh feed solution was prepared prior to each run. This ensured concentrations were exact and there was no build up of contaminants in the system or breakdown of components. Initially 4 litres of DI water were poured into the feed tank. Calcium sulphate and/or catechin were included in this volume when used. The remainder of the feed solutions were prepared in a 5 litre glass conical flask. Firstly powdered components were weighed into the tared flask, followed by the

required amount of DI water, remembering to allow for water in the casein and starch solutions. The flask was then sealed and agitated until the powder was seen to be fully dissolved. Further components were individually weighed into the flask, agitating the flask between each component to ensure it was dissolved. Casein was added last with a pipette and the flask only gently agitated. This was done to avoid the formation of a large foam in the flask. The resultant solution was then poured in the feed tank immediately prior to a run.

4.5 EXPERIMENTAL PROCEDURE

4.5.1 Preparation

Prior to filtration, it was necessary to mix the feed solution, set its pH and allow it to attain the experimental temperature. Therefore the solution was circulated around the rig via the recycle loop (i.e. not over the membrane surface) for half an hour. During this time a concentrated citric acid solution was added to the feed by a dropper until the pH reached 4.2, measured using a Griffin model 80 pH meter.

4.5.2 Filtration

At the onset of filtration, the two way valve (situated below the membrane cell in Figure 4.1) was positioned to allow the feed to flow over the membrane and the permeate sampling valve was closed. The computer logging was then started along with the pump. The desired crossflow velocity and transmembrane pressures were achieved by adjusting the pump speed and control valve. The feed temperature, crossflow velocity and system pressures were monitored throughout and adjusted as necessary.

Permeate flux was measured using a measuring cylinder and stop watch. Firstly the permeate line was drained into a beaker for 30 seconds prior to flux measurement. The flux was then recorded. Sufficient sample was collected to ensure a sampling time of over 30 seconds. The interval between samples

depended on the rate of flux decline with shorter intervals at the start of filtration when the greatest declines were observed.

Permeate samples were taken by draining the permeate line into a 100 ml screwtop glass jar. As with the flux sampling interval, permeate sampling intervals were shorter at the start of filtration. Samples were also taken of the feed and retentate streams and these were likewise stored in glass jars. All samples were refrigerated prior to analysis.

Each experiment was run for at least 2 hours.

4.5.3 Cleaning

At the end of the experiment, the pump was stopped and the drain valve opened. A Decon 90 solution was then poured into the rig and pumped around the filtration and recycle loops at 40°C for an hour. This cleaning solution was then replaced with tap water and the rig was rinsed several times. Finally, the rig was rinsed with DI water until the conductivity fell to 15 MΩ cm.

CHAPTER 5
ANALYTICAL TECHNIQUES

In order to obtain data on the rejection of feed stream components, the concentrations of each component in the feed, permeate and retentate streams had to be obtained. This was achieved using a variety of methods, mainly high pressure chromatography (HPLC) and UV/visible spectroscopy, which are detailed in this chapter.

5.1 HIGH PRESSURE LIQUID CHROMATOGRAPHY (HPLC)

There are five key modules to any HPLC system. They are a pump, an injector, a column, a column heater and a detector. By far the most important is the column, as this is the module that separates the components. HPLC columns provide separation through a number of mechanisms. They are given below:

Ion exclusion chromatography is a separation process whereby mobile ions have a similar charge as the fixed ionic charge group on the copolymer. The charge repulsion then prevents such ions from penetrating the resin. Hence highly charged species are excluded from the intraparticle volume and elute sooner. However, if elution requires more than one column volume, another separation mechanism must accompany ion exclusion.

Ion exchange chromatography works on a similar but opposite principle to ion exclusion chromatography. In this case the fixed ionic charge group on the copolymer is used to separate ions of opposite charge, as the copolymer exhibits varying degrees of selectivity. The selectivity may be altered by changing the composition of ions in the solution.

Ligand exchange chromatography is a mechanism in which a counterion, bound to a cation exchange resin, is used to bind ligands through co-ordination complexes. The ligands are then separated depending upon the strength of the co-ordination complexes and their degree of solubility in the mobile phase.

Size exclusion chromatography relies on the physical exclusion of large molecules. Molecules too large to penetrate the effective pore structure of the resin are excluded

from the intraparticle volume. Smaller molecules can, however, penetrate the pore structure and are thus retained for longer.

Normal phase partition chromatography works on the principle of distributing the sample between the intraparticle bound water and the less polar mobile phase. The compounds then separate according to their preference for polar over less polar solvents.

Reversed phase partition chromatography is similar to normal phase partition except that the sample is distributed between a polar mobile phase and a non-polar resin backbone. The more hydrophobic molecules elute later than the less hydrophobic ones.

Once a suitable column has been selected, then the detector should be chosen from a knowledge of the physical or chemical properties of the separated components. For example, organic acids show under UV light and thus a UV detector would be ideal, whilst sugars may be detected using a refractive index (RI) detector. The signal from the detector is then passed to a chart recorder or integrator.

Finally, the operating conditions have to be chosen to give the optimum separation. Elution times of components may be changed by altering the column temperature, eluent strength and eluent flow rate. Sample loop volume may be changed to detect very dilute components or to avoid saturation of the detector by concentrated components.

5.1.1 Apparatus

The HPLC system used in this study consisted of the following modules; a Kontron HPLC pump (model 420) fitted with a 0.05 - 10 ml min^{-1} pump head; a Waters temperature controlled column oven and a Kontron programmable integrator (model I-459) with plotter. The column and detector are described in more detail below. A schematic of the system is shown in Figure 5.1.

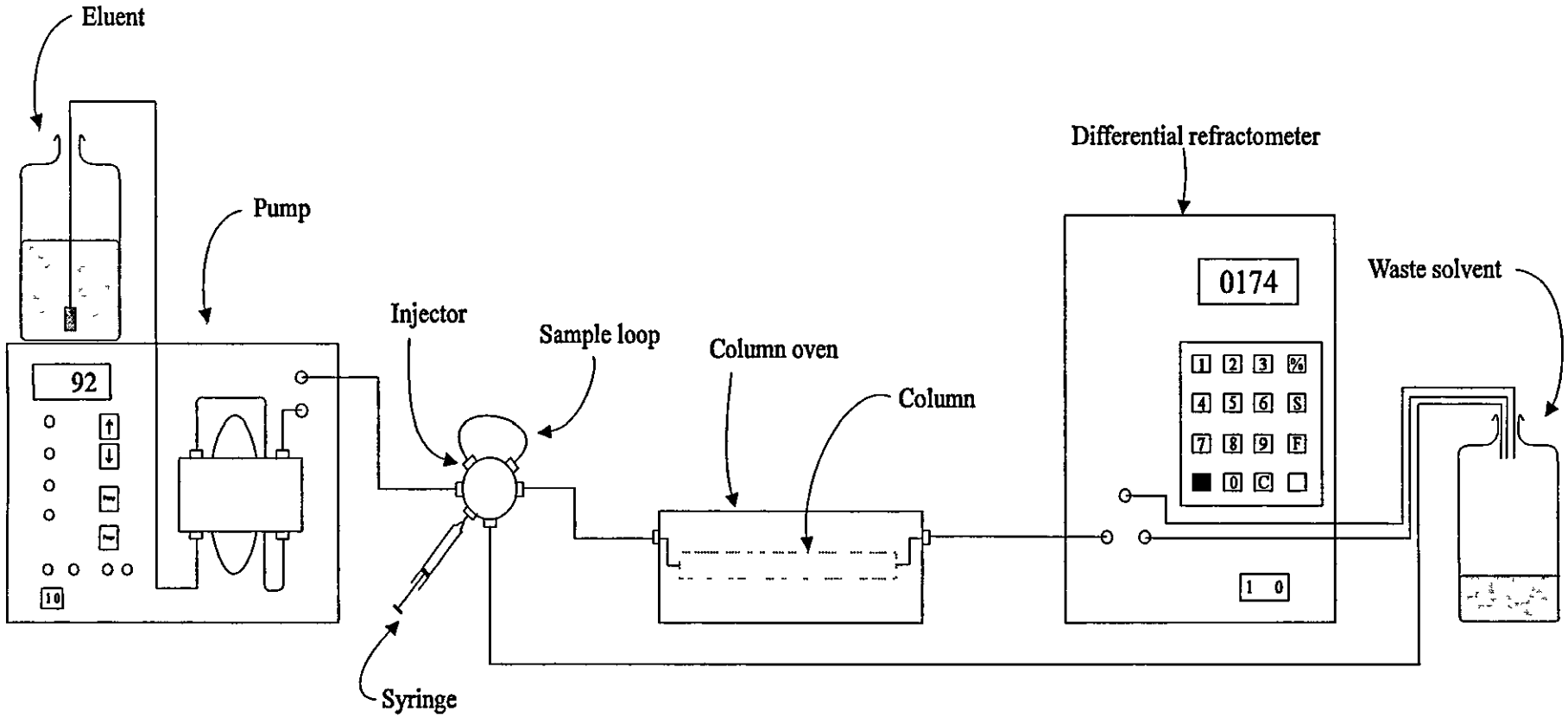

Figure 5.1: Schematic of HPLC apparatus.

5.1.1.1 Column

In order to separate the smaller components, such as alcohols, acids and sugars, an Aminex HPX-87H HPLC column (Bio-rad, model 125-0140) was selected and was protected from damage with a H^+ cation guard column (Bio-rad, model 125-0129). The column consists of a polystyrene-divinylbenzene resin support matrix, with functional hydrogen ion groups attached to it. According to the literature (Bio-rad bulletin 1833, 1928 (1995)) the column separates components by a variety of the mechanisms mentioned above.

5.1.1.2 Detector

The detector used throughout was a Waters refractive index detector (model 410). Refractive index detection is ideal for sugars, ethanol and glycerol, but organic acids are more suited to UV detection. However, the use of RI detection was found to be suitable for all components.

5.1.2 Eluent preparation

The eluent used in all experiments was 0.004M H_2SO_4. A stock solution of 2% w/w H_2SO_4 was prepared in a 2.5 litre winchester from analytical grade sulphuric acid (Aldrich 43,321-7, 97.5+%) and DI water. Eluent was prepared in 2.5 litre batches by diluting the stock solution with DI water and was stored in screwtop tinted winchesters. Care was taken to ensure that the eluent remained particulate free. The eluent had to be degassed by sparging with helium at 2 bar for at least 5 minutes prior to every use. This minimised the possibility of gas bubbles coming out of solution during HPLC.

5.1.3 Sample preparation

Instructions supplied with the Aminex column state the sample should be filtered through a 0.45 μm filter prior to injection to remove particulates. This was guaranteed with permeate samples as they had passed through a 0.2 μm membrane during experimentation. Rather than filter the feed and retentate samples, risking the interaction and potential loss of components in doing so, they were instead centrifuged at 13000 rpm (micro centaur) for 5 minutes to remove particulates.

With samples containing sucrose, it was necessary to hydrolyse the sucrose into fructose and glucose, as it otherwise reacts on the column. 10 ml of sample was pipetted into a boiling tube. 0.5 ml 1.5M sulphuric acid was added and the tubes boiled for 25 minutes. On cooling, 0.6 ml 10% w/w sodium hydroxide were added and the sample made up to 20 ml with DI water. The samples were then analysed for glucose as normal, with the sucrose concentration determined by multiplying the glucose concentration by 4 to account for the dilution and the formation of fructose. The method of checking for complete hydrolysis is given in Appendix 1.

5.1.4 Acid/alcohol/carbohydrate analysis

The general operating procedures used during analysis are given below. The exact details of integrator settings are given in Appendix 1 . In all cases the eluent was pumped at 0.2 ml min^{-1} until equilibrium was reached before increasing the flow rate to the required level.

5.1.4.1 Without maltose

In cases where the samples did not contain maltose, the operating parameters in Table 5.1 were used, as they separated the components in as short a time as possible. Each sample was injected 3 times in 100 μl aliquots to ensure that the sample loop had been adequately flushed.

Module	Parameter	Setting
Pump	Flow rate	0.6 ml min^{-1}
	Max. pressure	80 bar
Injector	Sample loop	20 µl
RI detector	Sensitivity	32
	Scale factor	20
	Temperature	35°C
Column	Temperature	50°C

Table 5.1. HPLC operating parameters for acid/alcohol/carbohydrate analysis without maltose.

5.1.4.2 With maltose

When maltose was present in the samples, the operating parameters had to be changed in order to separate maltose, citric acid and glucose (an impurity in the maltose) satisfactorily. The eluent flow rate and column temperature were reduced to a level whereby separation was achieved in as short a time as possible. The operating parameters used are given in Table 5.2. Each sample was injected 3 times in 100 µl aliquots to ensure that the sample loop had been adequately flushed.

Module	Parameter	Setting
Pump	Flow rate	0 43 ml min^{-1}
	Max. pressure	70 bar
Injector	Sample loop	20 µl
RI detector	Sensitivity	32
	Scale factor	20
	Temperature	35°C
Column	Temperature	30°C

Table 5.2. HPLC operating parameters for acid/alcohol/carbohydrate analysis in the presence of maltose.

A typical chromatogram is shown in Figure 5.2.

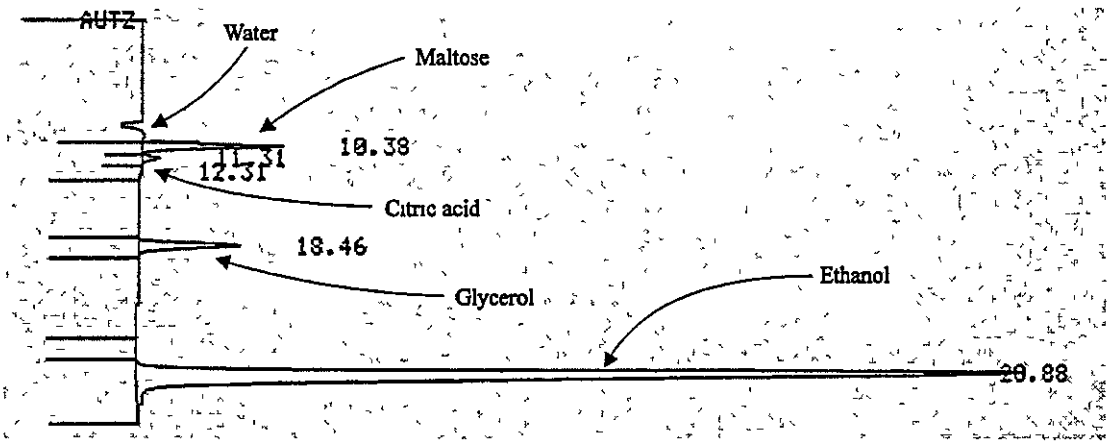

Figure 5.2: A typical chromatogram.

5.1.5 Ethyl acetate analysis

Ethyl acetate analysis was performed by HPLC using the same apparatus as above. The development of the method and integrator settings are given in Appendix 1. The operating parameters are summarised in Table 5.3. A larger sample loop was used due to the low concentration. The flow rate was governed by the maximum allowable pressure drop across the column. An increase in column temperature decreased the pressure drop and thus the flow rate could be increased. However, elevated temperatures appeared to cause the ethyl acetate to break down on the column. Each sample was injected 4 times in 100 µl aliquots to ensure that the sample loop had been adequately flushed.

Module	Parameter	Setting
Pump	Flow rate	0.65 ml min^{-1}
	Max. pressure	100 bar
Injector	Sample loop	100 µl
RI detector	Sensitivity	64
	Scale factor	20
	Temperature	35°C
Column	Temperature	30°C

Table 5.3. HPLC operating parameters for ethyl acetate analysis.

A typical chromatogram is shown in Figure 5.3.

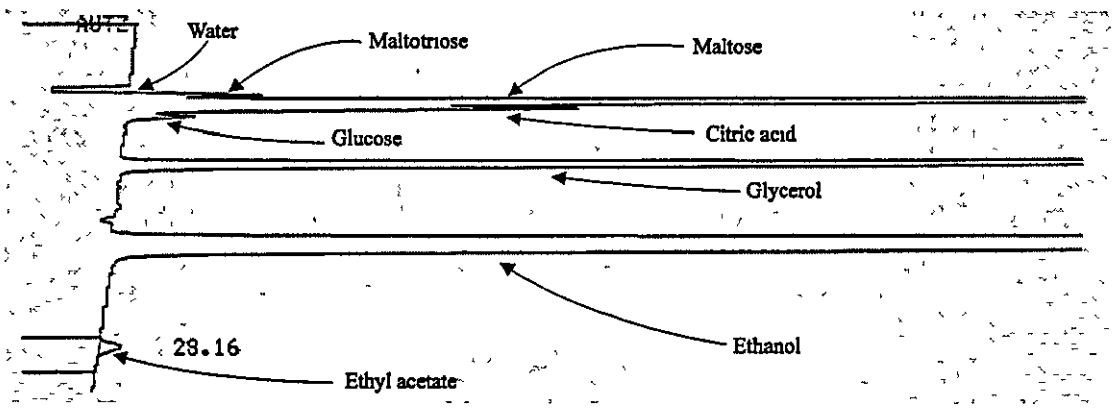

Figure 5.3: A typical chromatogram.

5.1.6 Calibration

Prior to calibration, the elution time of each component was deduced by running the required method and injecting each sample individually. A sample containing all components at known concentrations was run and the integrator method file was then edited. The times and concentrations of the peaks were entered and the integrator calibrated.

5.2 STARCH ANALYSIS

5.2.1 Enzymatic hydrolysis

Initially, starch analysis was carried out using a starch assay kit supplied by Sigma. Starch was enzymatically broken down to glucose producing an equal amount of NADH in doing so. NADH showed under UV light, and thus concentrations could be deduced by measuring the absorbance at 340 nm on a spectrophotometer. The reactions and conditions required are:

$$\text{Starch} + (n-1)H_2O \xrightarrow[60^\circ C, 15\ \text{minutes}]{\text{Amyloglucosidase}} n\ \text{glucose}$$

$$\text{Glucose} + \text{ATP} \xrightarrow[30^\circ C, 15\ \text{minutes}]{\text{Hexokinase}} \text{Glucose} - 6 - \text{phosphate} + \text{ADP}$$

$$\text{Glucose} - 6 - \text{phosphate} + \text{NAD} \xrightarrow[30^\circ C, 15\ \text{minutes}]{\text{Glucose-6-phosphatedehydrogenase}} 6 - \text{Phosphogluconate} + \text{NADH}$$

where ATP is adenosine triphosphate, ADP is adenosine diphosphate, NAD is nicotinamide dinucleotide and NADH is nicotinamide dinucloetide dehydrogenase.

1.0 ml of sample was mixed with 1.0 ml of starch assay reagent in a clean test tube. The tubes were then incubated in a shaking water bath for 15 minutes at 60°C. The tubes were then removed and allowed to cool to room temperature. 100 µl aliquots of the cool hydrolysed samples were then transferred to a series of test tubes containing 1.0 ml of glucose assay reagent, mixed and left to stand at room temperature for 15 minutes. The absorbance at 340 nm was then measured on a Perkin Elmer lambda 2 spectrophotometer.

This method was later replaced due to its relatively high cost.

5.2.2 Iodine binding method

An obvious cheap alternative to enzymatic hydrolysis was thought to be the classical starch-iodine binding reaction. However, it was unknown if other components in the sample would interfere with the reaction. Another problem is that amylose and amylopectin, the two main constituents of starch, stain different colours from blue to red. Therefore a study was carried out on this method, and its development may be seen in Appendix 1. The results of the study suggested that the method may be of some use, although results should be treated with care.

A stock solution of iodine in potassium iodide was prepared by weighing 30 g of analytical grade potassium iodide (Fisher, P/5880/48) into a 1 litre glass beaker. 750 g of DI water and a magnetic flea were added and the beaker placed on a magnetic stirrer. Once fully dissolved, 13 g of analytical grade iodine (Fisher, I/0500/48) was added and the solution stirred for some time until the iodine was seen to be fully dissolved. The solution was then made up to 1 litre. A test solution was prepared from the stock solution by diluting an aliquot with DI water to give a 0.001M iodine solution.

For analysis, 250 µl of sample were placed in a test tube and diluted with 2750 µl of DI water. 1ml of the 0.001M iodine test solution was added and each tube was agitated. Absorbance was then measured over the range 400 nm to 1000 nm in quartz cuvettes using a Perkin Elmer lambda 2 spectrophotometer. The starch concentration was then deduced from the absorbance at 600 nm. The absorbance was scanned over a large range in order to check for differences in the profile of the absorbance-wavelength plot that may have indicated changes in the composition or molecular weight of the starch.

The calibration data is shown in Figure 5.4.

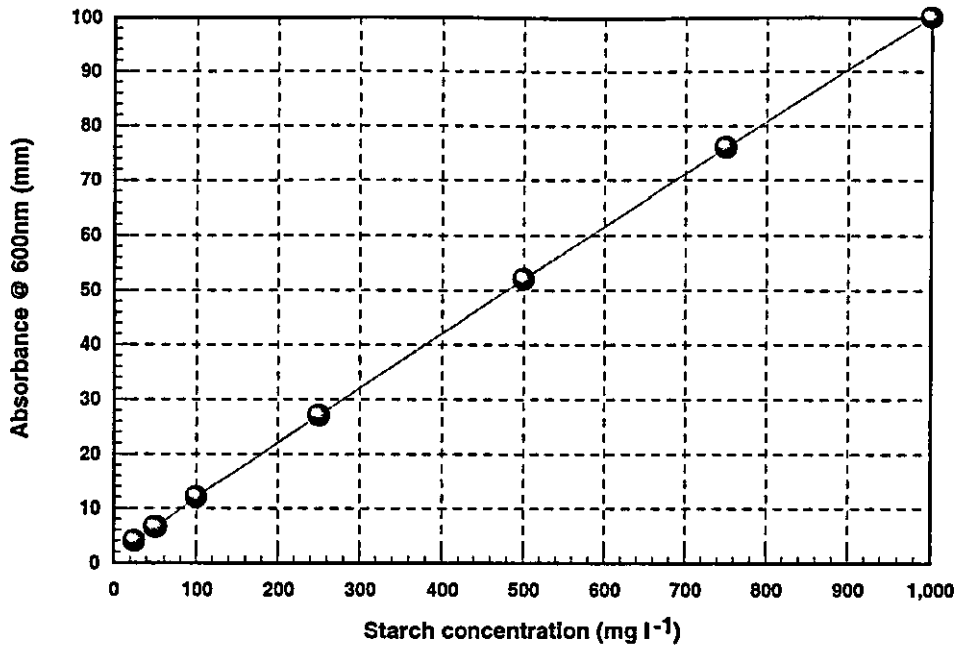

Figure 5.4: Starch analysis calibration data.

5.3 CALCIUM ANALYSIS

Calcium analysis could be performed in a number of ways such as wet chemistry, ion exchange chromatography or atomic adsorption spectrophotometry (AAS). Chemical methods were potentially problematic due to the interference of other components. Ion exchange chromatography and AAS generally overcome this problem. Of these two methods, AAS was chosen mainly as it is far quicker and also because it requires very small sample volumes.

Calcium concentrations were determined using a Perkin Elmer 3030 atomic adsorption spectrophotometer with a calcium/magnesium lamp. The instrument was used in the absorbance mode rather than emission. The operating parameters are given in Table 5.4.

Parameter	Value
Wavelength	420.9 nm
Lamp current	7 mA
Slit	0.7 nm
Acetylene flow rate	16 ml min^{-1}
Air flow rate	40 ml min^{-1}
Readings per average	10
Autozero	After every sample

Table 5.4: Operating conditions for the atomic adsorption spectrophotometer.

The instrument was fed with DI water and left for approximately half an hour once the flame had been lit, allowing it to reach steady state. A 1 ppm solution of Ca^{2+} ($CaCl_2$) was then run and the sample flow rate adjusted until a maximum in the absorbance reading was reached. Experimental samples were diluted so that the Ca^{2+} ion concentration was within the range of the instrument. Thus, 200 µl aliquots of sample were diluted with 5 ml DI water and stored in screwtop glass jars. Prior to analysing the samples, a series of Ca^{2+} ion standards (1, 2, 4, 6 ppm) were run to calibrate the instrument. This same set of standards were run after sample analysis. The Ca^{2+} ion concentration of each sample was then deduced from the average of the two sets of calibration data. A typical set of calibration data is shown in Figure 5.5.

There was found to be no interference in the measurement from other components in the samples and the method was found to be linear over the range 1-8 ppm Ca^{2+} with a maximum error of 2%. This is shown in Appendix 1.

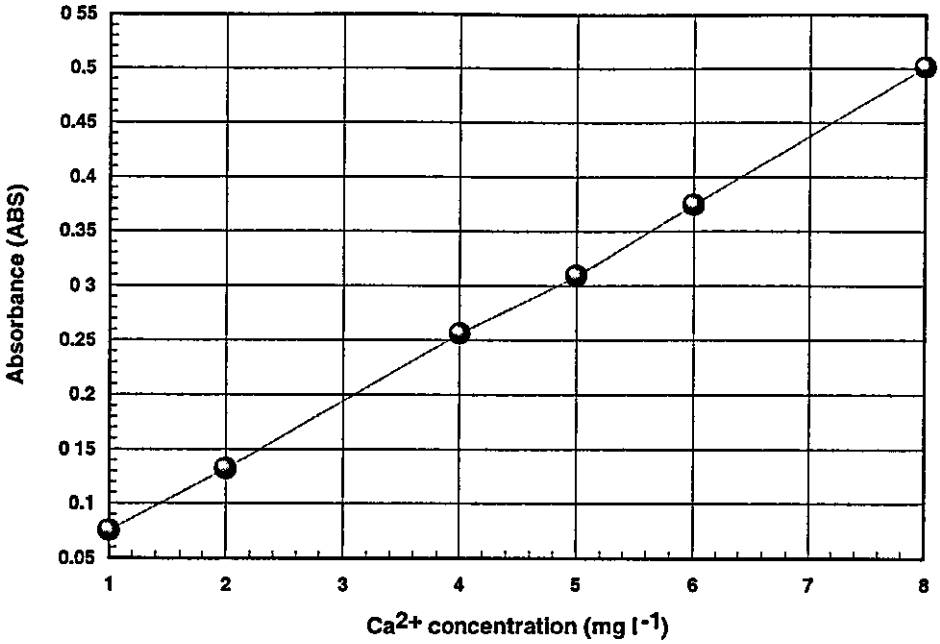

Figure 5.5: AA calibration data.

5.4 PROTEIN ANALYSIS

Methods often used in the determination of protein concentration in solution are given by Pollock (1981) and Williams *et al.* (1995) amongst others. They include UV spectrophotometry, Biuret method (alkaline potassium tartrate tetrahydrate/copper (II) sulphate pentahydrate solution), Folin-Ciocalteau (Lowry) method (alkaline sodium potassium tartrate tetrahydrate/copper (II) sulphate pentahydrate/sodium carbonate solution), Kjeldahl method (boiling with concentrated sulphuric acid and catalyst), BCA assay (bicinchoninic acid/copper (II) sulphate pentahydrate), Bradford assay (dye), PRM assay (pyrogallol red-molybdate solution) or simple nitrogen analysis. UV Spectrophotometry and nitrogen analysis suffer from the interference of other components that adsorb UV or contain nitrogen. The other methods are colour reactions from which concentration may be deduced from the absorbance light at the appropriate wavelength. In this case the PRM assay method was chosen, as work by Williams *et al.* (1995) showed it to be the most suitable.

The microprotein-PR™ reagent (Sigma, 611-2) was a solution containing 0.05 mmol l^{1} pyrogallol red, 0.16 mmol l^{-1} sodium molybdate, buffer, chelating agent, stabiliser, surfactant and preservative. The solution was stored in a fridge (2-8°C). Although the solution is intended for use in the determination of protein in human and animal fluids, it is also suited to this application, as stated by Williams *et al.* (1995). This method measures the change in absorbance at 600 nm when the pyrogallol red-molybdate complex binds basic amino acid groups of the protein.

Prior to analysis, the reagent was warmed to room temperature. 20 µl aliquots of sample were then added to a series of labelled test tubes. 20 µl of DI water and 20 µl of a 200 mg l^{-1} casein standard were added to two additional test tubes. 1ml of reagent solution was pipetted into each tube and gently mixed. The tubes were placed in a water bath at 30°C for 3 minutes. The absorbance at 600 nm was immediately measured on a Perkin Elmer lambda 2 spectrophotometer. The protein concentration was finally read from the calibration graph below (Figure 5.6).

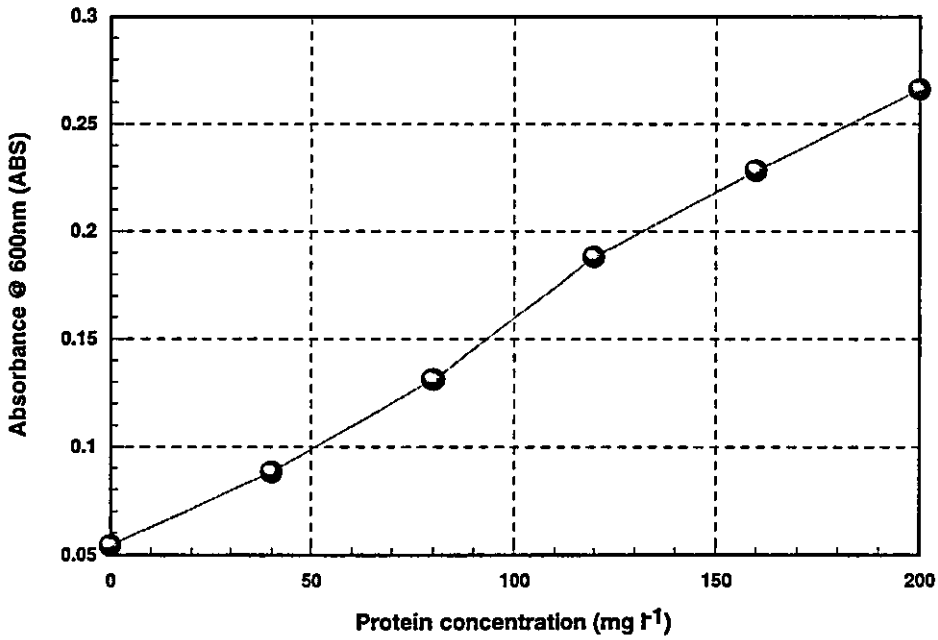

Figure 5.6: Protein analysis calibration data.

5.5 CATECHIN ANALYSIS

Methods of polyphenol (tannin) determination in foodstuffs are given by Joslyn (1970). They include Folin-Denis (phosphotunstomolybdic acid), ferric chloride, vanillin (vanillin/sulphuric acid solution), Harris and Ricketts (nylon 66 treatment then n-butanol/hydrochloric acid solution), Mitchell's (ferrous tartrate), cinchonine-tannate (cinchonine sulphate), Stainsky's (hydrochloric acid/formaldehyde), copper acetate and Löwenthal (acid permanganate solution). The first five methods rely on the absorbance of light by the resulting solutions, with the other methods being gravimetric. UV spectroscopy may be used but the polyphenol must first be isolated from the sample. HPLC is another alternative but would have required a different column to that already mentioned.

It was decided to use the ferric chloride method, as the solution is relatively simple, interferences are minimal and the reagents involved are readily available and cheap. An exact method is given by de Clerck *et al.* (1947). This method was modified and details are given in Appendix 1. 3 ml aliquots of sample were pipetted into a series of test tubes. 20 µl of 0.25M sodium carbonate solution and 500 µl 0.15M iron (II) chloride solution were added to each tube 3 minutes prior to measuring the absorbance at 600 nm using a Perkin Elmer lambda 2 spectrometer. The calibration data is shown in Figure 5.7. It should be noted that the feed concentration was determined by sampling the feed prior to the addition of starch or casein, because the high concentration of these large molecules caused light scattering and resulted in a much higher apparent absorbance.

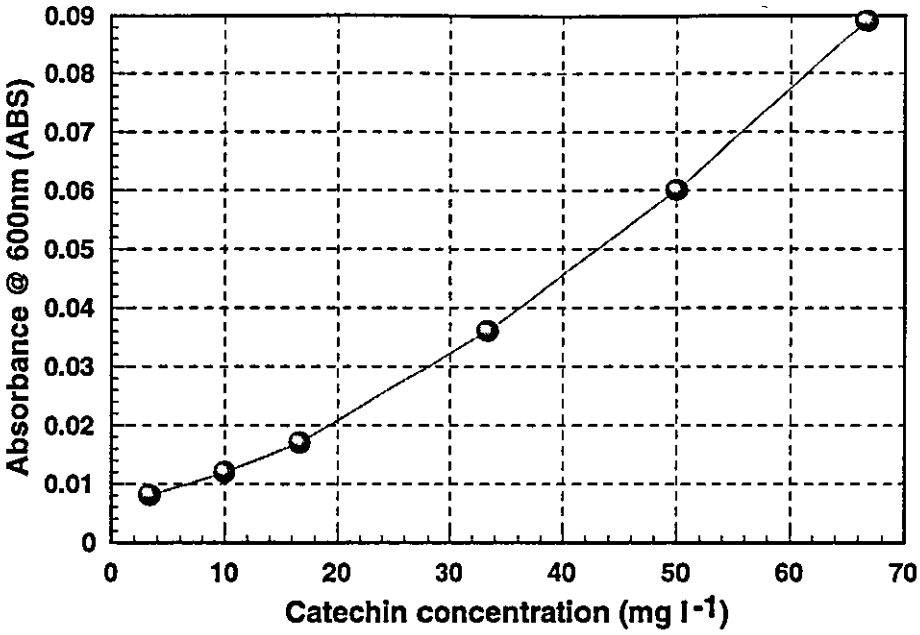

Figure 5.7: Catechin analysis calibration data.

CHAPTER 6

RESULTS AND DISCUSSION

Experiments were initially carried out using a simple base feed containing water, ethanol, glycerol, citric acid and maltose. As experimentation progressed further, components such as starch and casein were added or removed from the feed stream in order to build a model solution The final feeds contained water, ethanol, glycerol, maltose, starch, casein, citric acid, calcium sulphate, catechin and ethyl acetate. Results and discussion are presented here in the order in which the feed solution was compiled Unless otherwise stated, experiments were carried out at a crossflow velocity of 2 m s^{-1}, a transmembrane pressure of 1 9 bar and at 20°C, using a 0.2 μm cellulose nitrate membrane

6.1 FEED SOLUTION

Initially, a simple solution containing water, ethanol, glycerol, maltose and citric acid was filtered through a 0 2 μm cellulose nitrate membrane. The flux decline observed is shown in Figure 6 1. The flux declined from 3300 to 250 l m^{-2} h^{-1} during the course of a 10800 second run. Given that all the components in the feed are many orders of magnitude smaller than the membrane pore size, the magnitude of the decline is somewhat surprising The reason for this is that the rig constitutes a "real" system, in which the pump may supply fouling material, unlike the case of a stirred cell driven by compressed air, which is capable of thorough cleaning.

An interesting property of citric acid is its ability to form complexes with metal ions (*Kirk and Othmer 1979a, b*). Generally, two or more of the one hydroxyl and three acid groups are used to form a ring type structure. The pump may act as donor of metal ions such as chromium This flux decline could therefore be attributed to the adsorption of citric acid or citric acid aggregates onto the membrane surface Assuming the membrane to consist of a series of cylindrical pores and applying the equation for streamline flow in a cylindrical pipe, the drop in flux would indicate a change in pore size from 0 2 μm to 0 044 μm (Appendix 2.3). Citric acid molecules

would have a molecular radius in the region of 0.36 nm, assuming that they are spherical (Appendix 2.3). A citric acid complex, consisting of a ring of citric acid ions surrounding a metal ion, is likely to be around 2 nm in diameter. It is therefore unlikely that citric acid adsorption alone could account for the loss in flux observed here, as a coverage of two layers of molecular aggregates would not reduce the hydraulic radius sufficiently. It is therefore assumed that other particulate matter in the feed water is responsible.

In terms of steady state rejection, there is little/no rejection of glycerol and a slight rejection of ethanol (0.5%) and maltose (1%). Although citric acid is initially transmitted by the membrane, it shows a surprisingly high steady state rejection of about 50% at steady state, as shown in Figure 6.2. This data suggests that there are very slight interactions between both ethanol and maltose and the membrane and strong interactions between citric acid and the membrane. Any molecular aggregates formed by citric acid are unlikely to be large enough to be retained by a 0.2 μm membrane.

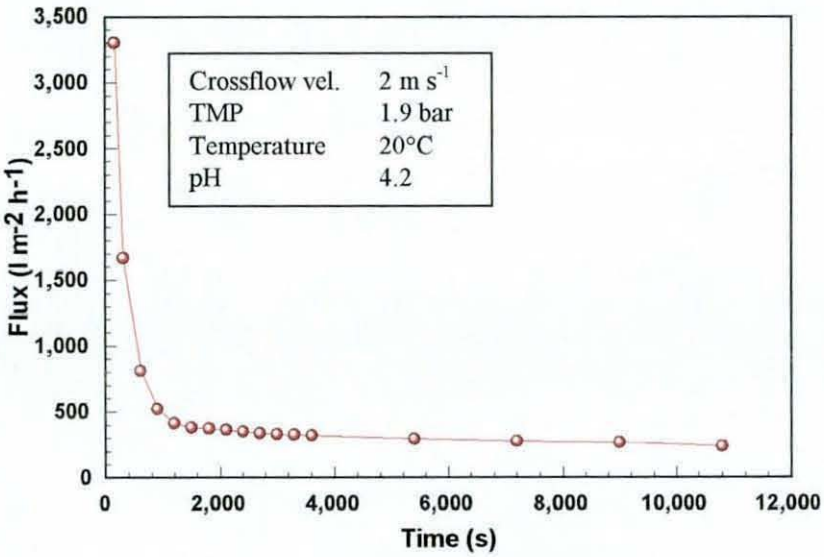

Figure 6.1: Flux decline with base solution.

A more plausible explanation may be provided from a knowledge of the membrane surface charge. Bowen and Cooke (1992) have reported the zeta-potential of cellulose nitrate membranes, of the type used here, to be negative, i.e. they have a negative surface charge. Clearly, any dissociated acid will also carry a negative surface charge.

It therefore seems feasible to attribute this rejection behaviour to electrostatic repulsion.

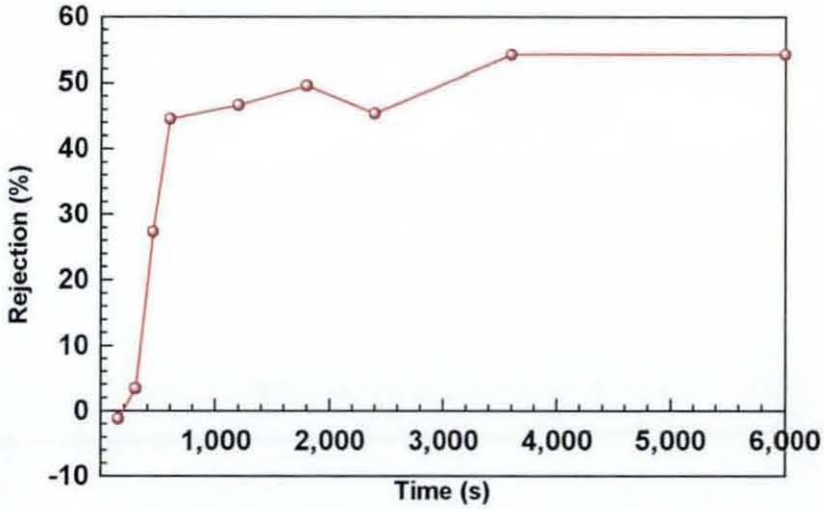

Figure 6.2: Citric acid rejection.

6.2 EFFECT OF ACID TYPE

As stated in the previous section, citric acid is rejected by the CN membrane to an appreciable extent. Therefore experiments were carried out with two other organic acids, namely acetic and succinic. Figure 6.3 shows that these acids were rejected to a lesser extent. At steady state the rejections of acetic and succinic acids were about 5%, which is much less than the 50% steady state rejection observed with citric acid. The rejection of other components was unaffected by the acid used. The initial and steady state flux for citric acid was somewhat lower than for the other acids as shown in Table 6.1, although this appears to be unimportant as the rejections of other components remain similar.

	Citric acid	Acetic acid	Succinic acid
Ethanol (%)	0.2	0.5	0.5
Glycerol (%)	0	0	0
Maltose(%)	1	2.5	2
Acid (%)	50	5	5
Initial flux ($l\ m^{-2}\ h^{-1}$)	4000	5500	5500
Steady state ($l\ m^{-2}\ h^{-1}$)	300	400	450

Table 6.1: Effect of acid type on flux and rejection.

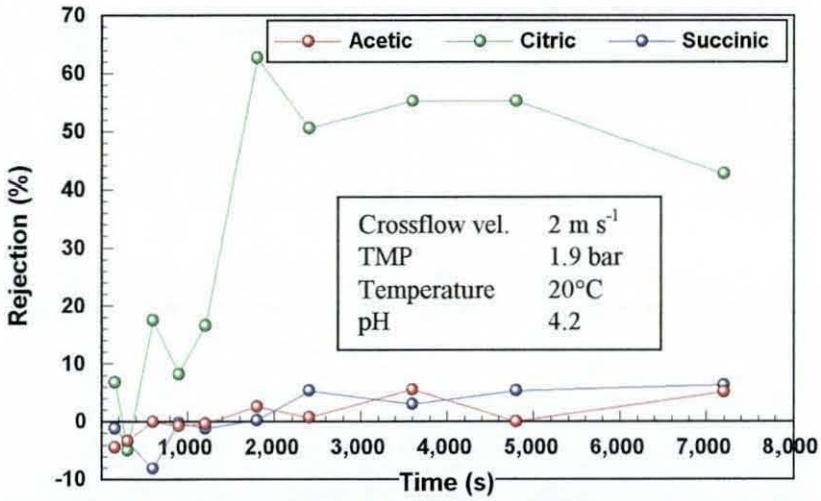

Figure 6.3: Rejection of different acid types.

The rejection behaviour of citric acid compared to the other two acids may again be explained in terms of electrostatic repulsion with the membrane. As stated in Section 6.1, cellulose nitrate membranes have a negative surface charge. From a knowledge of the acid dissociation constants, pK_a, the fraction of each ionic species may be calculated as a function of pH, as detailed in Appendix 2.1. Plots of fraction of species against pH are given in Figure 6.4. An approximate charge density may then be calculated from the molecular weight and density of each acid. These calculations assume that the acid molecules may be approximated by spheres and that charge is

	Fraction (%)	Charge density (C m^{-2})
HAc	78.2	-
Ac^-	21.8	-0.169
H_2Suc	46.8	-
$HSuc^-$	51.2	-0.134
Suc^{2-}	2.0	-0.268
H_3Cit	6.5	-
H_2Cit^-	73.7	-0.121
$HCit^{2-}$	19.6	-0.243
Cit^{3-}	0.2	-0.364

Table 6.2: Fraction and charge density of acid species.

evenly spread over the surface of the sphere. These calculations are detailed in Appendix 2.2. Table 6.2 shows the fraction of each acid species and their charge density at pH 4.2. It should be remembered that this ionisation is a dynamic process.

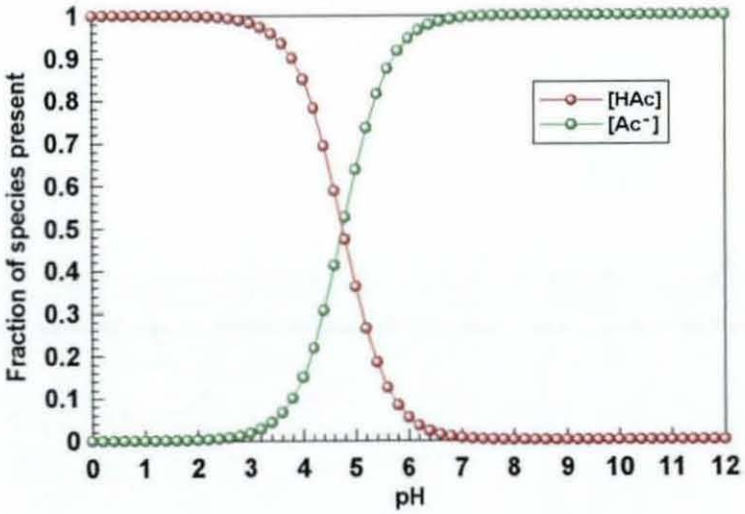

Figure 6.4a: Effect of pH on acetic acid species.

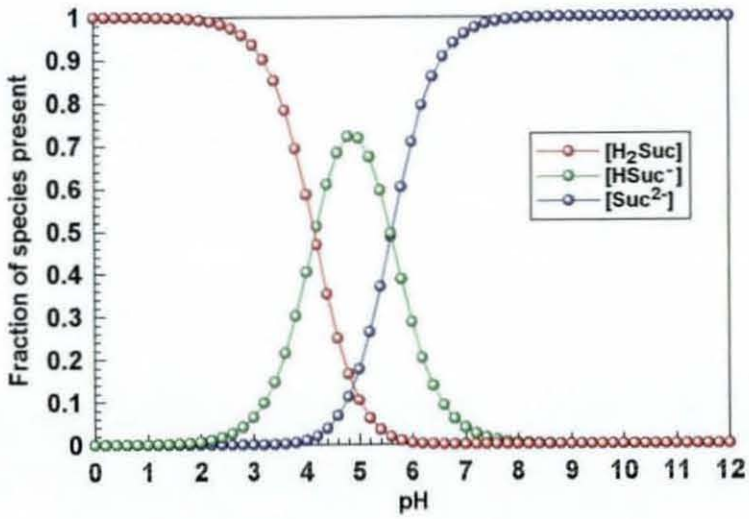

Figure 6.4b: Effect of pH on succinic acid species.

Citric acid is ionised to a much greater extent than the other two acids at pH 4.2, with a 20% fraction showing a surface charge higher than the other two acids. Assuming that a greater negative surface charge density would result in a greater repulsion with a negatively charged surface, this may go some way to explaining its greater rejection. It does somewhat less to explain the similar rejection of the other two acids, although the

less ionised acetic acid does have a greater charge density than the major succinic acid ion.

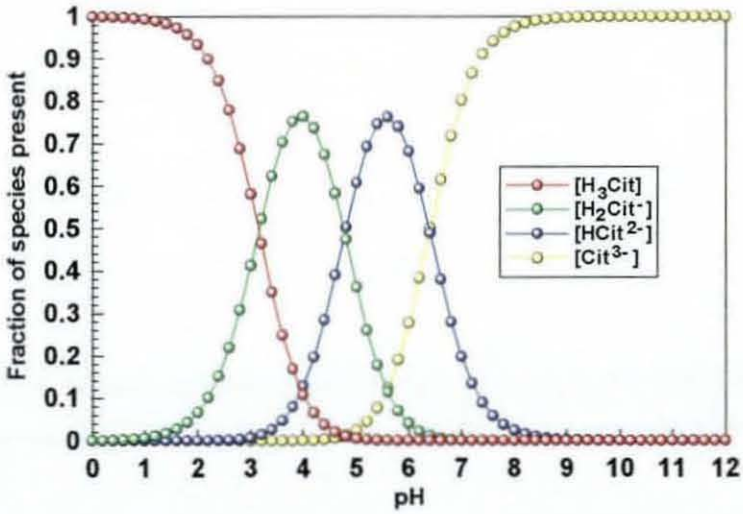

Figure 6.4c: Effect of pH on citric acid species.

6.3 STARCH ADDITION

The addition of 1000 mg l^{-1} starch to a feed solution filtered under the normal conditions resulted in a drastic flux reduction, as shown in Figure 6.5. The initial flux was reduced from 3300 to 55 $l\,m^{-2}\,h^{-1}$ and the steady state flux from 300 to 33 $l\,m^{-2}\,h^{-1}$. The steady state rejections of glycerol and citric acid remained similar, but the rejections of ethanol and maltose increased from 0.5 to 2.0% and 1.0 to 3.0% respectively.

The dramatic fall in flux in the presence of starch in the feed, accompanied with a quite obvious rejection of starch (seen by the loss of turbidity between the feed and permeate) suggests that starch is deposited on the membrane. Indeed, a slightly milky gel-like deposit was observed on the membrane at the end of experimentation. The literature (Lenoël *et al.* (1993, 1994), Burrell *et al.* (1994) and Gan *et al.* (1997) amongst others) suggests that α-glucans, such as starch, are responsible for the formation of a secondary membrane. The mechanisms of fouling are discussed later (Section 6.12).

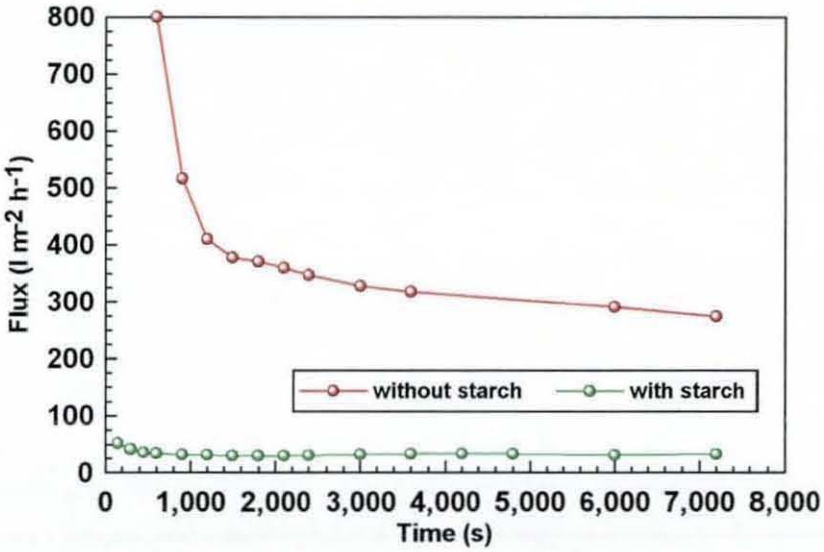

Figure 6.5: Effect of starch addition (1000 mg l^{-1}) on flux.

At pH 4.2, starch has a negative zeta potential (see Section 6.4) of around –10 mV. Using the argument that negative citric acid ions are repelled by the negatively charged membrane surface, it could be argued that starch would be repelled in the same way. However, starch is many orders of magnitude larger than citric acid and thus any back diffusion/repulsion away from the surface is likely to be much slower than for citric acid and probably much slower than the bulk flow towards the surface, leading to it forming a fouling layer.

The continued rejection of citric acid may therefore be explained as previously, being now repelled by a negatively charged membrane coated in a negatively charged deposit. The slightly higher rejections of ethanol and maltose may be due to the large decrease in permeate flux through the membrane (see Section 6.11) as well as the increased potential for intermolecular interactions in the presence of starch. Starch consists of two distinct types of molecules, namely amylose and amylopectin. The latter is a branched molecule that tends to take up a random conformation in solution, whilst the former is linear and is known to form a helical structure held together by hydrogen bonds. It is therefore possible that starch deposited on the membrane is capable of forming hydrogen bonds with other materials, such as maltose.

6.3.1 Effect of starch concentration

The effect of starch concentration was investigated by adding starch to the base solution in the concentration range 100 to 2000 mg l^{-1}. Increasing the starch concentration over this range resulted in decreased initial fluxes from 140 to 42 l m^{-2} h^{-1} and a fall in steady state flux from 75 to 32 l m^{-2} h^{-1}. As may be seen be in Figure 6.6, it took longer to reach steady state at lower starch concentrations. This behaviour is similar to that reported in studies investigating the effect of changes in protein concentration (see Section 3.1). It is also interesting to note that the flux reaches a minimum and then begins to increase slightly after the first 1500 seconds of filtration at starch concentrations of 1000 mg l^{-1} and above.

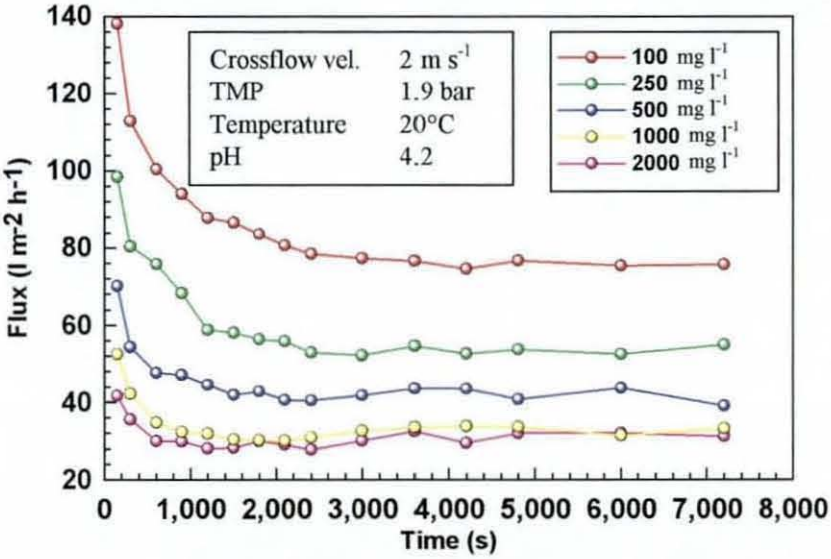

Figure 6.6: Effect of starch concentration on flux.

	100 mg l^{-1}	250 mg l^{-1}	500 mg l^{-1}	1000 mg l^{-1}	2000 mg l^{-1}
Ethanol (%)	2.0	2.0	1.8	1.8	1.8
Glycerol (%)	0	0	0	0	0
Maltose (%)	2.0	1.8	3.3	3.5	3.0
Starch (%)	>90	>90	>90	>90	>90
Citric acid (%)	55	57	55	60	60
Flux (l m^{-2} h^{-1})	75	55	40	33	32

Table 6.3: Effect of starch concentration on steady state rejection.

Palacek (1994) and Palacek and Zydney (1994) allowed deposited protein layers to "relax" overnight, before passing clean water through them Water fluxes were seen to drop with time, indicating a rearrangement in the deposited layer. The increase in flux after 1500 s at higher starch concentrations may therefore be due to changes in the structure of the fouling layer. A fresh starch paste or gel is thermodynamically unstable (Collison (1968)), undergoing retrogradation on ageing, which occurs more quickly for amylose than amylopectin Initially, the helical configuration of the amylose molecule becomes stretched, causing intramolecular bonds to be broken. Bound water is then lost and the molecules re-orientate themselves. Finally hydrogen bonding occurs between adjacent molecules. This results in the layer attaining a more crystalline state. Starch may be deposited on the membrane in a random manner. This layer may then become structured, as explained above, resulting in a reduced hydraulic resistance.

Increasing the concentration of starch appears to have little effect on steady state rejections of the other components as shown in Table 6.3, although there does appear to be slight increases in both maltose and citric acid rejection. This may be due to the subsequent decrease in flux caused by the increase in starch concentration, rather than any direct starch-maltose or starch-citric acid interactions.. This is discussed in Section 6.11.

6.3.2 Effect of crossflow velocity

Starch was added to the base solution at a concentration of 1500 mg l^{-1} and filtered at a transmembrane pressure of 3.3 bar over a range of crossflow velocities from 1.1 to 2 8 m s^{-1}. An increase in crossflow velocity over this range resulted in an increase in initial flux from 52 to 85 l m^{-2} h^{-1} with an increase in steady state flux from 33 to 60 l m^{-2} h^{-1}, as shown in Figure 6 7.

An increase in crossflow velocity appears to have little effect on steady state rejections, although it may slightly decrease ethanol and glycerol rejections (Table 6 4) Once again, this may be due to the increase in permeate flux or a reduction in the thickness of the starch layer.

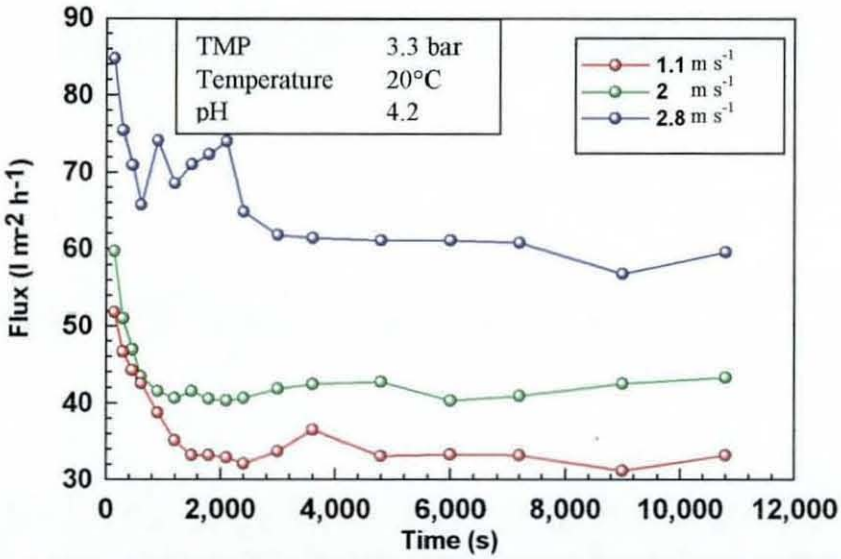

Figure 6.7: Effect of crossflow velocity on flux.

	1.1 m s^{-1}	2.0 m $s^{-1}s^{-1}$	2.8 m s^{-1}
Ethanol (%)	0.7	0.2	0.2
Glycerol (%)	0.8	0	0
Citric acid (%)	40	55	55
Starch (%)	100	100	100
Flux (l m^{-2} h^{-1})	33	42	60

Table 6.4: Effect of crossflow velocity on steady state rejection.

As is widely accepted in the field of crossflow filtration, the increase in flux with crossflow velocity is a result of the increased shear acting on the fouling layer, resulting in a decrease in thickness and, hence, hydraulic resistance. The lower rejections of glycerol and ethanol may result from the increased shear across the membrane causing a thinner fouling layer to form, increasing transmission as reported by Walla (1994). Alternatively, the higher permeate flux may lead to higher shear forces at the membrane pore entrances, resulting in a greater transmission of components (see also Section 6.11).

6.3.3. Effect of transmembrane pressure

Transmembrane pressure experiments were conducted at a starch concentration of 1500 mg l^{-1} in the base solution and at a crossflow velocity of 2.0 m s^{-1}. The resultant steady state flux and rejections may be seen in Table 6 5. The steady state flux and rejections appear similar, irrespective of the TMP This may be due to the fact that the fouling layer is compressed, increasing its hydraulic resistance and counteracting the increase in driving force across it. This behaviour has been observed during protein crossflow microfiltration by Bauser *et al.* (1982), Taylor *et al.* (1993), Doyen *et al.* (1996) and Fauchille and Gachelin (1996). Lenoel *et al.* (1993) and Gan *et al.* (1997) also reported similar steady state fluxes with changes in TMP.

	1 9 bar	3 3 bar	4.5 bar
Ethanol (%)	0 6	0 2	0.7
Glycerol (%)	0	0	0
Citric acid (%)	45	55	40
Starch (%)	100	100	100
Flux (l m^{-2} h^{-1})	52	42	49

Table 6.5: Effect of transmembrane pressure on steady state rejection

6.4 CASEIN ADDITION

Casein was added to the base solution at a concentration of 200 mg l^{-1}. As shown in Figure 6 8 this caused a reduction in initial flux from 3300 to 310 l m^{-2} h^{-1} and a drop in steady state flux from 300 to 28 l m^{-2} h^{-1} from the base solution case As in the case of starch, this reduction in flux may be attributed to a build up of casein on the membrane surface, resulting in a secondary membrane. The permeate flux reduction due to the addition of casein is not surprising given the wealth of literature on protein adsorption to polymeric surfaces and fouling of membranes (Chapter 3). Fouling mechanisms are discussed in Section 6.12.

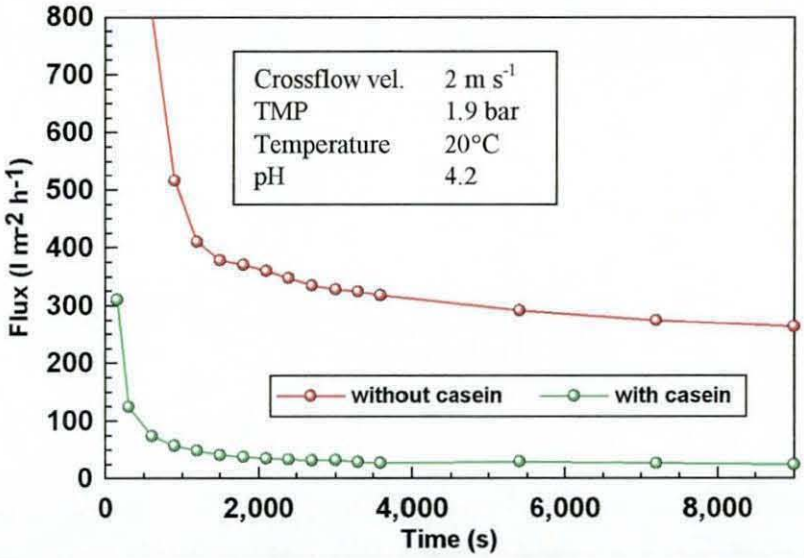

Figure 6.8: Effect of casein addition (200 mg l^{-1}) on flux.

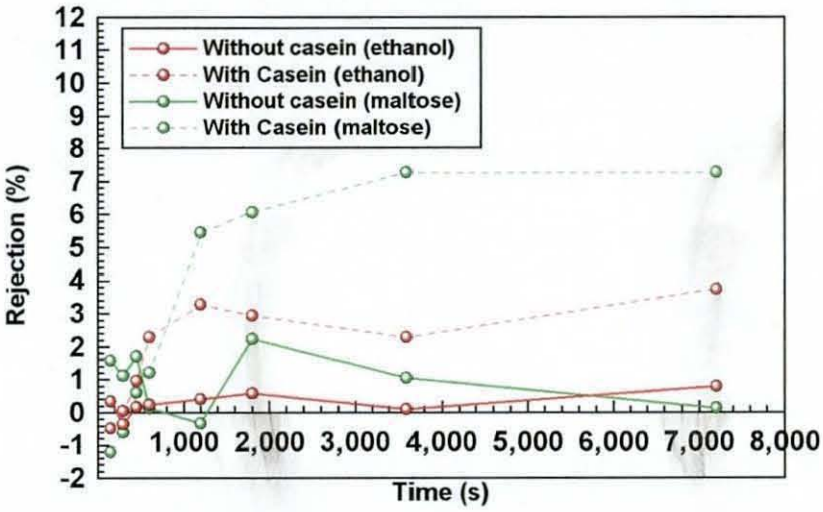

Figure 6.9: Effect of casein addition (200 mg l^{-1}) on ethanol and maltose rejection.

The addition of casein to the system resulted in almost complete rejection of casein, the complete transmission of citric acid, no change in glycerol behaviour and increased rejections of ethanol (0.5 to 3.0%) and maltose (1 to 7%), as shown in Figure 6.9. These increases in rejection are greater than for the addition of starch to the system, especially in the case of maltose. As the steady state fluxes are similar to those achieved with starch, this suggests a specific interaction between casein and maltose. The binding of sugars to proteinaceous materials has been observed previously. Tsapyuk and Mank (1987) have studied the transmission of sucrose through a gelatin layer. They deposited a gelatin layer on ultra- and microfiltration membranes to form a

dynamic membrane. A sucrose solution was then passed through this layer and the rejection measured. A substantial sucrose rejection was observed.

Up to this point, there has been a substantial rejection of citric acid. It should be noted that there is a citric acid concentration of 100 mg l^{-1} in this case, as opposed to 25 mg l^{-1} reported thus far. This is because the casein is introduced with NaOH present. Later work, however, shows that this is not simply a concentration effect because there is no citric acid rejection with a casein concentration of 25 mg l^{-1} and citric acid concentration of 28 mg l^{-1}. The casein, itself, must therefore be responsible for this trend.

Returning to the earlier hypothesis for the rejection of citric acid by the membrane (Section 6.2) and the starch layer (Section 6.3), it should be noted that casein has a positive zeta potential (Figure 6.10) of +11 mV at pH 4.2. Therefore it seems feasible that casein may be electrostatically attracted to the membrane surface and therefore it is of no surprise that it fouls the membrane. Carrying out streaming potential work on membrane surfaces onto which proteins have been adsorbed, Ricq *et al.* (1996) have observed that the new membrane interface displayed similar surface properties, from a charge point of view, to that of the protein. Assuming now that the membrane surface effectively exhibits a positive surface charge, the negatively charged citric acid ions should no longer be electrostatically repelled and the rejection would be expected to decrease, as it does.

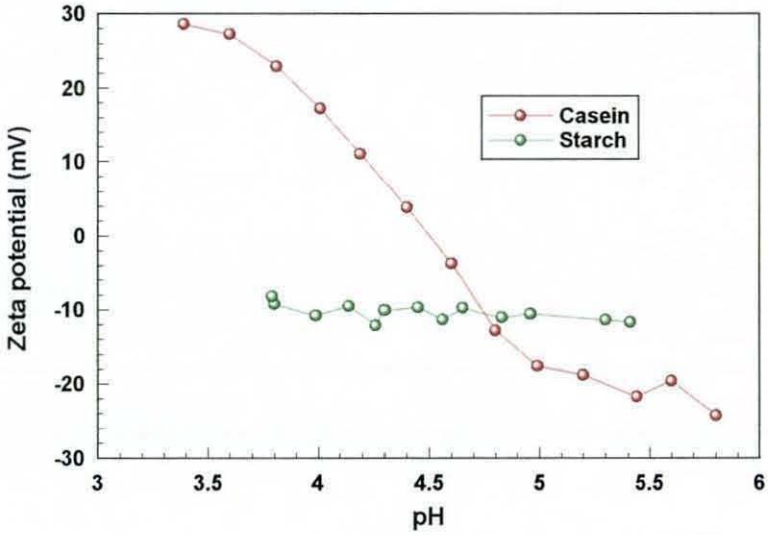

Figure 6.10: Zeta potential vs. pH plot for casein.

Under specific conditions, proteins (or parts of proteins) form helices in solution due to hydrogen bonding between the N-H and C=O groups four amino acid groups along the protein chain. In solution, globular structures are achieved whereby hydrophobic parts of the protein reside towards the central core surrounded by hydrophilic parts at the interface with the solution. However, proteins can change shape with pH or shear for example. As in the case of starch, there is clearly the potential for hydrogen bonding with other molecules. Indeed, the hydrogen bonding of carbohydrates (such as maltose and glucose) to proteins has been studied by Quiocho (1993). Additionally, casein also contains charged amino and acid groups as well as both hydrophilic and hydrophobic regions that may also be responsible for further intermolecular interactions. Amino groups are used in chromatography in the separation of carbohydrates (Schoenmakers 1986), again highlighting the possibility of interaction between the protein and sugar. Therefore hydrogen bonding and other intermolecular interactions may account for the increased rejections of ethanol and maltose. However, for this to occur the protein must change its structure from that in solution to that on the membrane surface, as no maltose/ethanol appears to be "locked up" with the protein in solution.

6.4.1 Effect of casein concentration

The effect of casein concentration on the system was studied by adding casein to the base solution in concentrations ranging from 25 to 200 mg l^{-1}. As was expected from the literature, increasing concentration over this range led to flux reductions. Initial fluxes fell from 580 to 320 l m^{-2} h^{-1}, whilst steady state fluxes dropped from 150 to 27 l m^{-2} h^{-1}, as shown in Figure 6.11. Generally, the time taken to achieve steady state flux increased at lower casein concentrations.

Increases in steady state rejections with increasing casein concentration were observed for ethanol (1 to 3%), maltose (1 to 8%) and casein (90 to 98%), as may be seen in Table 6.6. As with starch, these increases may be due to decreases in permeate flux or fouling layer thickness (Section 6.11).

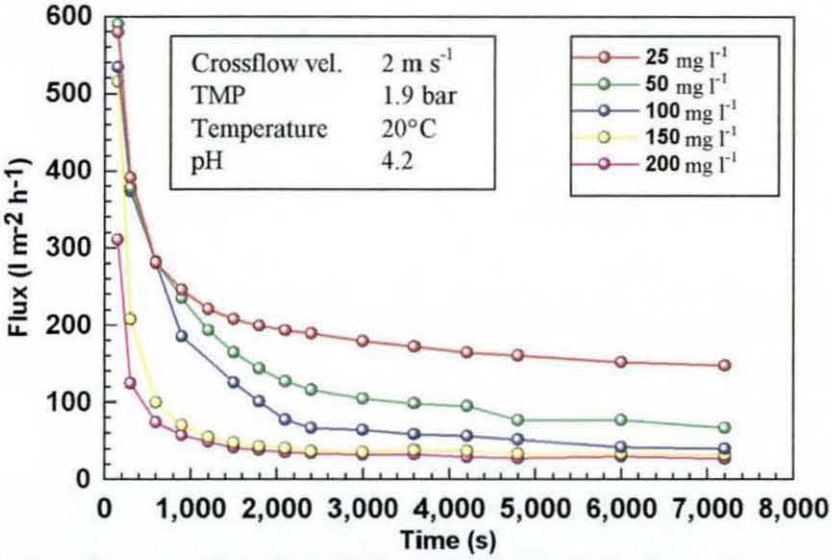

Figure 6.11: Effect of casein concentration on flux.

	25 mg l^{-1}	50 mg l^{-1}	100 mg l^{-1}	150 mg l^{-1}	200 mg l^{-1}
Ethanol (%)	1	1	2.5	2.2	3
Glycerol (%)	0	0	0.7	1	0.7
Maltose (%)	1	1.5	4.5	10	7
Citric acid (%)	0	0	0	0	0
Casein(%)	-	90	95	96	98
Flux (l m^{-2} h^{-1})	150	70	40	33	27

Table 6.6: Effect of casein concentration on steady state rejection.

6.4.2 Effect of crossflow velocity

Casein was added to the base solution at a concentration of 100 mg l^{-1} and filtered at a transmembrane pressure of 3.3 bar at crossflow velocities in the range 1.1 to 2.4 m s^{-1}. As shown in Figure 6.12, increasing the velocity over this range resulted in increased initial flux from 110 to 260 l m^{-2} h^{-1} and a change in steady state flux from 18 to 79 l m^{-2} h^{-1}. The steady state rejection data presented in Table 6.7 is somewhat inconclusive, as increases in crossflow velocity appear to have little effect on rejections, although maltose rejection drops at the highest velocity.

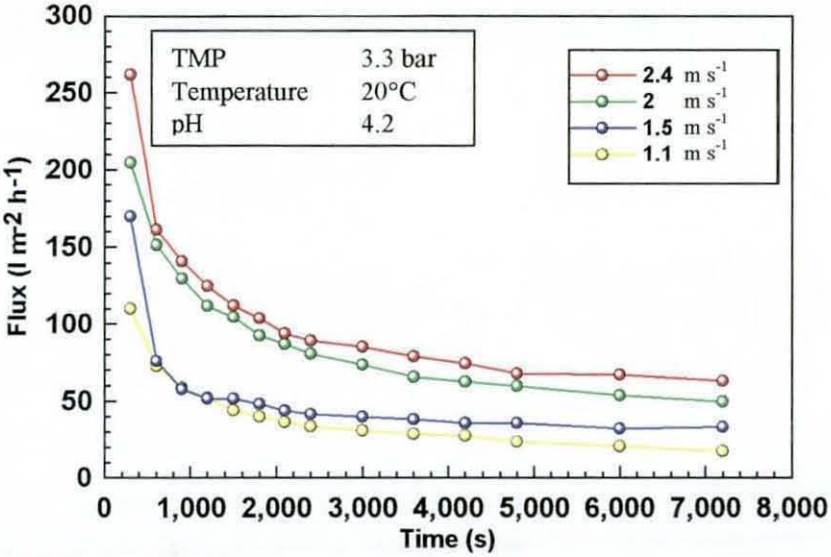

Figure 6.12: Effect of crossflow velocity on flux.

Many authors in the literature have reported permeate flux increases with increases in crossflow velocity, so the flux data is as expected. However, it is surprising that little change in rejection occurs with changes in crossflow velocity, as it would be expected that the fouling layer is thinner resulting in higher fluxes and a greater transmission of beer components, as reported by Walla (1994). In the case of maltose, transmission seems more possible at higher crossflow velocities as the cake becomes thinner.

	1.1 m s^{-1}	1.5 m s^{-1}	2.4 m s^{-1}	2.8 m s^{-1}
Ethanol (%)	2.2	2.0	3	2
Glycerol (%)	1.9	2	1.3	1.2
Maltose (%)	13	10	13	5
Citric acid (%)	0	0	0	0
Casein(%)	100	100	96	99
Flux (l m^{-2} h^{-1})	18	33	65	79

Table 6.7: Effect of crossflow velocity on steady state rejection.

6.4.3. Effect of transmembrane pressure

In this system, increases in transmembrane pressure over the range 1.9 to 4.5 bar, at a crossflow velocity of 2.0 m s^{-1} and a concentration of 100 mg l^{-1}, appear to result in increases in steady state flux, as shown in Figure 6.13. Steady state rejections are decreased, except in the case of casein, as TMP increases (Table 6.8).

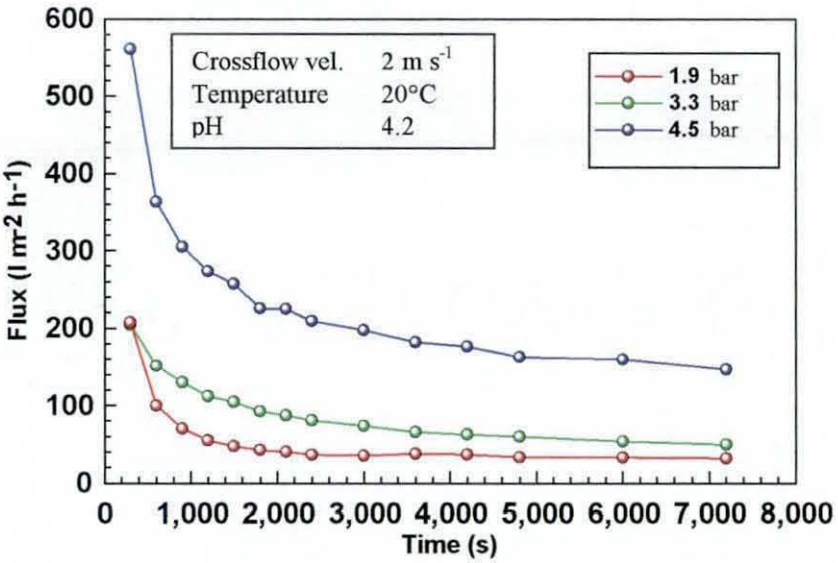

Figure 6.13: Effect of transmembrane pressure on flux.

	1.9 bar	3.3 bar	4.5 bar
Ethanol (%)	2.5	2.0	0
Glycerol (%)	0.7	0.8	0.3
Maltose (%)	4.5	1.2	0
Casein (%)	95	95	96
Flux (l m^{-2} h^{-1})	40	50	150

Table 6.8: Effect of transmembrane pressure on steady state rejection.

The steady state flux data suggests that the fouling layer due to casein is not compressible, unlike starch. Increases in the driving force across the membrane then result in an increase in flux. Again, as discussed in Section 6.11, the increase in component transmission may be a result of the increased flux. The data also suggests that a structural change in the deposit occurs as TMP is increased, as the steady state

flux increases disproportionately with TMP According to Darcy, the flux should be proportional to $\Delta P/l$, the pressure drop and thickness of the bed. The bed is unlikely to become thinner at higher transmembrane pressure, so it would appear that the casein deposit becomes more open

6.5 STARCH AND CASEIN ADDITION

Casein in the concentration range 50 to 150 mg l^{-1} was added to a base solution, already containing 1500 mg l^{-1} starch. The flux decline profiles resembled that of starch laden solutions more than casein laden ones. However, steady state fluxes were slightly lower than in the case of starch alone. A further experiment carried out at a starch concentration of 500 mg l^{-1} and a casein concentration of 150 mg l^{-1} resulted in a similar flux profile, although the steady state flux was about 28 l m^{-2} h^{-1}.

Table 6.9 shows the effect of changing casein concentration on rejection in this system. It appears that maltose rejection increases with increasing casein concentration and citric acid rejection drops The run carried out at starch and casein concentrations of 500 and 150 mg l^{-1} respectively, resulted in similar rejections as the analogous experiment at the higher starch concentration

	50 mg l^{-1}	100 mg l^{-1}	150 mg l^{-1}
Ethanol (%)	2 4	2 8	2.7
Glycerol (%)	0	0.3	0.6
Maltose (%)	2.0	3.9	4.3
Citric acid (%)	28	13	8
Casein (%)	100	100	100
Flux (l m^{-2} h^{-1})	24	24	24

Table 6 9: Effect of casein concentration on steady state rejection in the presence of both starch and casein

It is interesting to compare this data with that for changes in starch and casein concentration only. It appears that the rejection of maltose with casein is somewhat suppressed, as is the rejection of citric acid with starch. This data, along with data for

starch and casein alone, suggests that the presence of starch is largely responsible for flux decline but has less effect on the rejection of components, but the opposite is true for casein Starch is present at tenfold greater concentrations than casein for the data in Table 6.9 and this may account for its dominance in flux decline

The modification of component rejection with casein concentration suggests that it may also be found in the fouling layer. When the chemistries of the two molecules are compared, it is hardly surprising that casein dominates rejection effects. Starch is a polymer built up of glucose units, thus containing only carbon, hydrogen and oxygen atoms and displaying a limited chemistry Casein is a polymer built from a range of amino acids, containing nitrogen and sulphur as well as carbon, hydrogen and oxygen atoms It therefore displays a range of chemistries, contains both basic and acidic moieties, hydrophilic and hydrophobic areas and is likely to take part in hydrogen bonding. In this case it appears that a higher percentage of casein in the feed results in a larger amount being present in the fouling layer, although it appears not to significantly alter the hydraulic properties of the layer as the steady state fluxes remain similar

6.6 EFFECT OF SUGAR TYPE

Having observed a large increase in maltose rejection during the filtration of feeds containing casein (Section 6.4), a series of experiments with other mono/disaccharides was carried out The disaccharides consisted of lactose and sucrose, whilst the monosaccharides used were glucose and fructose All experiments were carried out at starch and casein concentrations of 1500 mg l^{-1} and 150 mg l^{-1} respectively. In these experiments, similar flux decline profiles resulted, although the steady state flux of lactose was lower than for the other sugars. The rejection data is presented in Figure 6 14 and summarised in Table 6.10. The rejection of the monosaccharides appears lower than for the disaccharides (5% compared to 10%). It should be noted that these rejections are on a mass basis. As the monosaccharides have a molecular weight half that of the dissacharides, then it may be seen that both groups of sugars display similar

rejections on a molar basis. The lactose rejection appears slightly greater than for the other sugars but this may be explained by the lower filtration flux in this case.

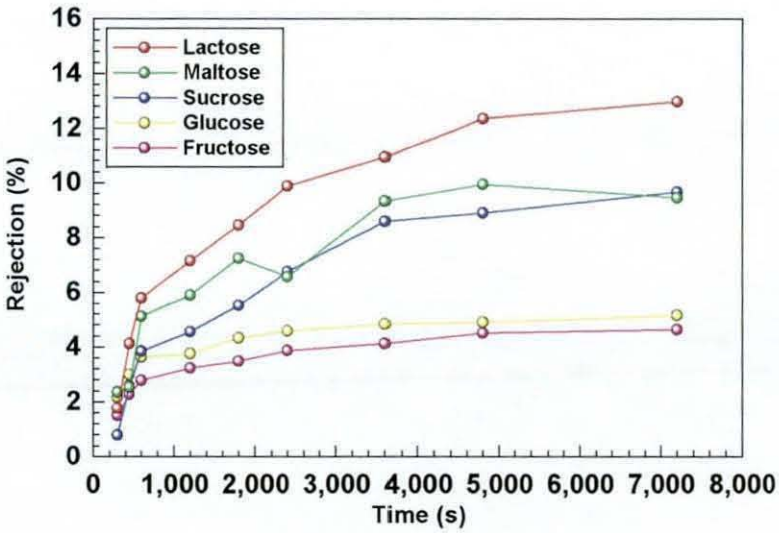

Figure 6.14: Rejections of different sugars.

	Lactose	Maltose	Sucrose	Glucose	Fructose
Rejection (%)	12	9	9	5	5
Flux ($l\ m^{-2}\ h^{-1}$)	23	36	32	34	32

Table 6.10: Steady state rejection/flux for different sugars.

A suggested mechanism for the rejection of sugars with casein in the system is shown in Figure 6.15. If it assumed that the rejection is due to the adsorption of the sugars by the protein, probably through hydrogen bonding, and that a single "sugar ring" adsorbs to a given protein site, then it would explain that twice the mass of disaccharides are rejected compared to the monosaccharides.

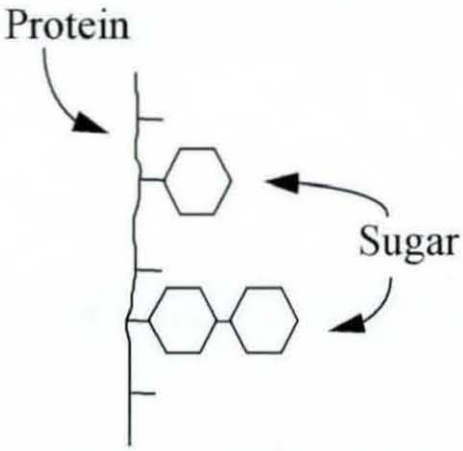

Figure 6.15: Suggested mechanism for sugar rejection with casein.

6.7 CALCIUM ADDITION

Calcium ions were added to the feed stream in the form of calcium sulphate. The effects of their presence were investigated in systems containing starch, casein and a combination of the two, along with the other feed components. Using the methods outlined in Appendix 2.2, the charge density of calcium may be taken as +0.541 C m^{-2}, making it the most densely charged species in this system.

6.7.1 Effect on feed containing starch

Figure 6.16 shows the effect of calcium ion addition to a starch containing feed stream. The presence of these ions resulted in a decrease in both initial and steady state fluxes from 42 to 27 l m^{-2} h^{-1} and 31 to 20 l m^{-2} h^{-1} respectively A change in concentration from 50 mg l^{-1} to 100 mg l^{-1} appears to have had little impact on the flux. The general trends in component rejection with time remained the same as for experiments performed without calcium ions. The steady state rejections of the components are given in Table 6.11. The addition of calcium ions appears to have had little effect on the steady state rejection of the components, although the rejection of ethanol was slightly increased. There was very little, if any, rejection of calcium ions.

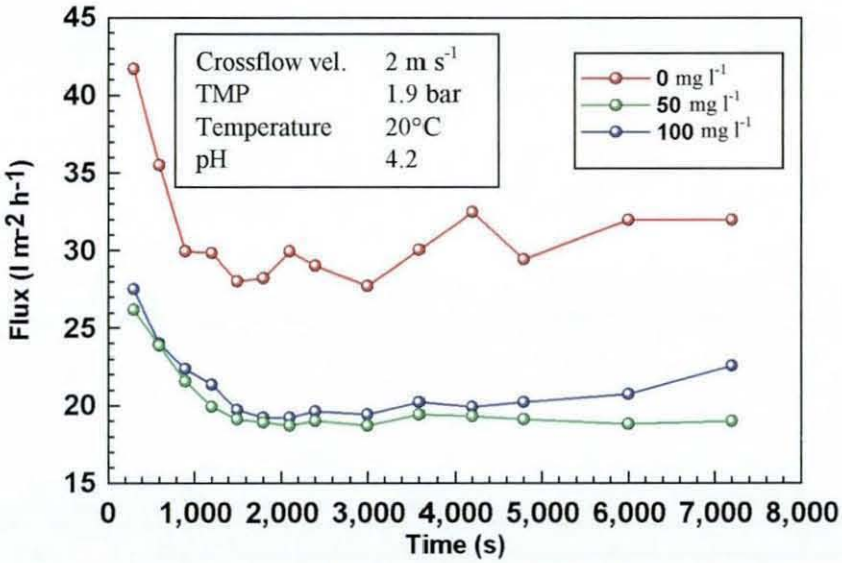

Figure 6.16: Effect of calcium ions on filtrate flux in the presence of starch.

	0 mg l^{-1}	50 mg l^{-1}	100 mg l^{-1}
Ethanol (%)	2	3	3.5
Glycerol (%)	0	0	0
Maltose (%)	2.5	2.5	2.5
Starch (%)	-	99	99
Citric acid (%)	50	>10	>10
Calcium (%)	-	1	0
Flux (l m^{-2} h^{-1})	31	20	20

Table 6.11: Effect of calcium on steady state rejections in the presence of starch.

Changes in flux decline behaviour with ionic strength have been observed during protein microfiltration (Section 3.9). In adding calcium ions to the system the ionic strength is effectively being altered. The decline in flux observed may be due to a compression of the starch double layer and charge shielding, causing it to pack more closely and hence reducing the permeability of the layer. The composition of the layer is therefore largely unaltered and hence component rejections remain unaltered.

6.7.2 Effect on feed containing casein

The addition of calcium to a feed stream containing casein (150 mg l^{-1}) had a dramatic effect on both initial and steady state flux, as may be seen in Figure 6.17. The addition of 50 mg l^{-1} Ca^{2+} resulted in an initial flux increase from 520 to 1200 l m^{-2} h^{-1} and a steady state increase from 30 to 190 l m^{-2} h^{-1}. A further increase in calcium ion concentration to 100 mg l^{-1} resulted in an increase in initial flux but a similar steady state flux. The differences in ethanol rejection with time are shown in Figure 6.18. The high initial fluxes in these experiments allow initial rejection data to be taken as valid. The addition of calcium clearly results in a reduction of ethanol rejection from 2.5 to 0.6% and maltose form 8 to 0%. Figure 6.18 is also representative of the smaller components, such as glycerol and maltose. The steady state rejections are presented in Table 6.12. There appears to be a slight rejection of calcium.

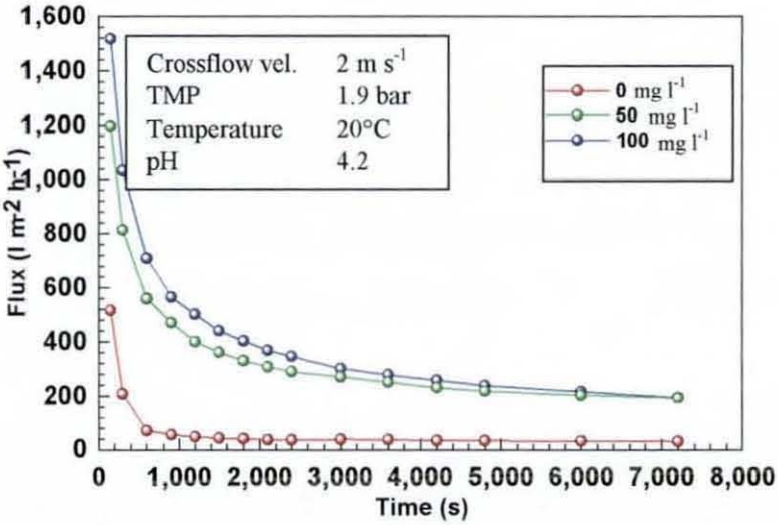

Figure 6.17: Effect of calcium ions on filtrate flux in the presence of casein.

	0 mg l^{-1}	50 mg l^{-1}	100 mg l^{-1}
Ethanol (%)	2.5	0.6	0.6
Glycerol (%)	1	0	0
Maltose (%)	8	0	0
Casein (%)	95	96	95
Citric acid	0	>5	>5
Calcium (%)	-	3	3
Flux (l m^{-2} h^{-1})	30	192	192

Table 6.12: Effect of calcium on steady state rejections in the presence of casein.

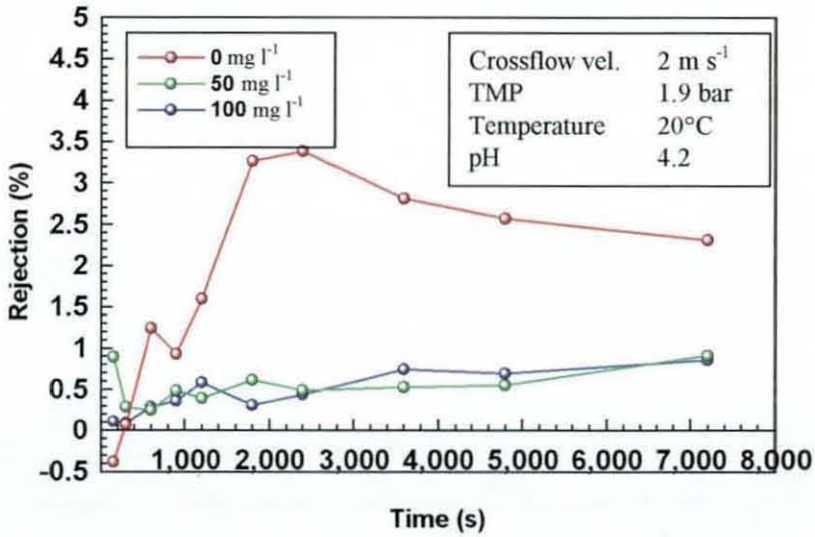

Figure 6.18: Effect of calcium ions on ethanol rejection in the presence of casein.

The small rejection of calcium, in this case, may indicate an interaction with casein. Whole casein contains phosphate groups which are then capable of binding calcium ions, which may explain the rejections observed. As with starch, the addition of calcium ions effectively modifies the ionic strength of the system and it may be expected that this would lead to charge shielding and a more compact fouling layer. However, casein is composed of four casein fractions, namely α s1 casein, α s2 casein, β casein and κ casein. The first two fractions may be precipitated at very low concentrations of calcium. Precipitation of casein would result in large aggregates forming, causing a much coarser (and possibly thinner) fouling layer with a higher permeability. Effectively the protein would no longer be in solution and therefore its hydrogen bonding potential with maltose would be greatly reduced.

6.7.3 Effect on feed containing both starch and casein

Figure 6.19 show the influence of adding calcium ions to a feed solution containing both starch (1500 mg l^{-1}) and casein (150 mg l^{-1}). At a concentration of 50 mg l^{-1}, the presence of calcium ions appeared to slightly increase flux. In the concentration range 100 to 150 mg l^{-1}, both initial and steady state fluxes were reduced slightly from 30 to 28 l m^{-2} h^{-1} and 25 to 20 l m^{-2} h^{-1} respectively. The trends in rejection of the

components generally remained unaltered through calcium ion addition, as shown in Table 6.13, although the steady state rejection of maltose was lowered with increasing concentration.

As mentioned in Section 6.5, flux decline behaviour is dominated by starch and the flux decline observed on the addition of calcium may be assumed to be that for starch alone. Likewise, the increase in maltose transmission with calcium concentration may be explained by an increase in the amount of protein precipitated.

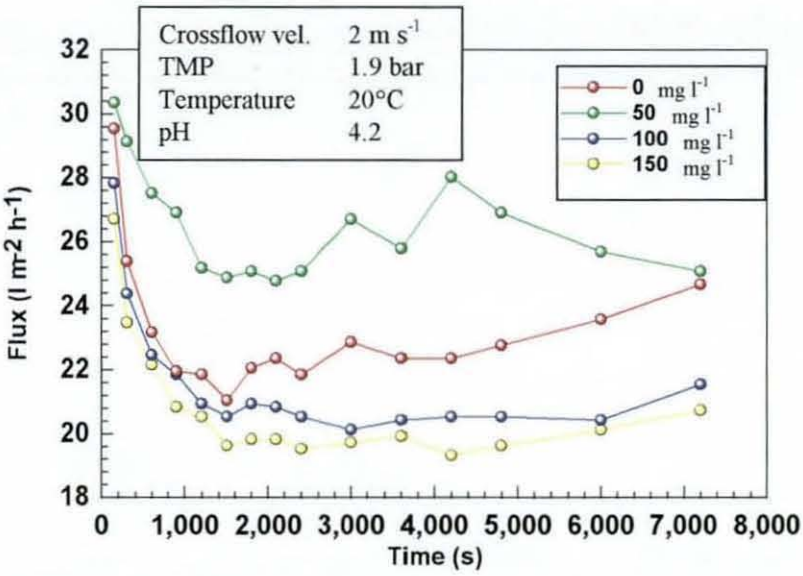

Figure 6.19: Effect of calcium ions on filtrate flux in the presence of starch and casein.

It is also interesting to note that there is a "negative rejection" of calcium, suggesting that calcium was somehow concentrated across the membrane. These values were reproducible and outside the errors of the method of analysis. There are two potential explanations. The calcium concentration in the boundary layer may increase due to its interaction with casein. This increased concentration may permit calcium ions to diffuse into the permeate stream passing through the boundary layer and the deposit, increasing its concentration and leading to what appears to be a concentration of calcium across the membrane. However, this would then be expected to happen when only casein is present, which it does not. An alternative explanation may be due to an electrostatic/electroosmotic effect, but this seems unlikely as it did not occur with starch or casein alone.

	0 mg l^{-1}	50 mg l^{-1}	100 mg l^{-1}	150 mg l^{-1}
Ethanol (%)	2.5	3	3.5	2 5
Glycerol (%)	0	0	0	0
Maltose (%)	4.5	4	2.5	2
Casein (%)	100	100	100	100
Starch (%)	-	98	98.5	98
Citric acid	0	0	0	0
Calcium (%)	-	-3	-8	-5
Flux (l m^{-2} h^{-1})	25	25	20 5	20

Table 6.13: Effect of calcium on steady state rejections in the presence of both starch and casein)

6.8 CATECHIN ADDITION

The effect of catechin addition to the base solution is shown in Table 6.14 It should be noted that the catechin appeared to "soak up" hydrogen ions and thus three times the amount of citric acid was added to set the pH. This is somewhat surprising from its structure, as the hydroxyl group of phenol is slightly acidic This type of polyphenolic substance is known to be responsible for colour formation. When in solution browning may occur enzymatically (i e polyphenol oxidase) or non-enzymatically (often catalysed by metal ions) to form a range of larger complexes

	0 mg l^{-1}	50 mg l^{-1}
Ethanol (%)	0 2	0
Glycerol (%)	0	0 2
Maltose (%)	1	0
Citric acid (%)	50	5
Catechin (%)	-	3
Flux (l m^{-2} h^{-1})	320	380

Table 6.14: Effect of catechin on steady state rejection using the base solution only.

The addition of catechin to the base solution appears to have little effect on the steady state characteristics of the system, with catechin displaying a small rejection (3%), suggesting a possible interaction with the membrane, as it is unlikely that any complexes would be large enough to be sieved out by the membrane However, the

rejection of citric acid may be seen to decrease significantly from 50% to 5% This may be due to the much higher concentration of citric acid (75 mg l^{-1}) in this experiment compared to the analogous case without catechin (25 mg l^{-1})

6.8.1 Effect on feed containing starch

The effect of catechin addition to a solution containing starch (1500 mg l^{-1}) is given in Table 6 15 It has little effect on the steady state rejections Again, the amount of citric acid added was greater than expected but comparable to that added to the base solution above. In this case, although the citric acid rejection appeared to be reduced, the magnitude was not as drastic as in the absence of starch The catechin rejection with starch (9%) is higher than in the base solution (3%), although the steady state flux is somewhat lower (23 rather than 380 l m^{-2} h^{-1}). It may be that the catechin interacts with the starch or the lower flux may cause a more pronounced interaction with the membrane (see Section 6.11).

	0 mg l^{-1}	50 mg l^{-1}
Ethanol (%)	2	3
Glycerol (%)	0	0
Maltose (%)	3	3
Citric acid (%)	60	40
Starch (%)		98
Catechin (%)	-	9
Flux (l m^{-2} h^{-1})	33	23

Table 6.15· Effect of catechin on steady state rejections in the presence of starch

6.8.2 Effect on feed containing casein

From the data in Table 6 16, it appears that catechin may interact with casein (150 mg l^{-1}) as the permeate flux and catechin rejection increase significantly. It should also be noted that the polyphenol rejection is greater in this system than with starch, even though the steady state flux with starch is lower. This is not entirely surprising as polyphenols and proteins are known to interact, often leading to haze in beer and wine

Catechin may combine with casein to form an insoluble complex that cannot pass through the membrane, accounting for the increase in catechin (and casein) rejection. However, the change in flux is relatively small compared to that seen on calcium addition (Section 6 7 2) This suggests that there is less insoluble material present The fact that there is no change in maltose rejection would support this assumption.

	0 mg l^{-1}	50 mg l^{-1}
Ethanol (%)	2.5	3
Glycerol (%)	0.5	0 3
Maltose (%)	8	8
Citric acid (%)	3	0
Casein (%)	97	100
Catechin (%)	-	17
Flux (l m^{-2} h^{-1})	30	51

Table 6 16: Effect of catechin on steady state rejections in the presence of casein

6.8.3 Effect on feed containing both starch and casein

Catechin was added to a solution containing both starch (1500 mg l^{-1}) and casein (150 mg l^{-1}) It appears that the citric acid rejection decreases but, again, more citric acid was required to obtain the desired pH in the presence of catechin The rejection of catechin is greater, in this case, than when only starch is present, but lower than in the presence of casein This, again, indicates an interaction between the protein and the polyphenol, and the reduced rejection effects of casein with starch in the fouling layer.

	0 mg l^{-1}	50 mg l^{-1}
Ethanol (%)	3	0 5
Glycerol (%)	0	0
Maltose (%)	4	4
Citric acid (%)	10	3
Casein (%)	100	100
Starch (%)		95
Catechin (%)	-	14
Flux (l m^{-2} h^{-1})	32	28

Table 6 17 Effect of catechin on steady state rejections in the presence of both starch and casein

6.8.3 Effect on feed containing starch, casein and calcium

The addition of catechin to the base solution also containing starch (1500 mg l^{-1}), casein (150 mg l^{-1}) and calcium (100 mg l^{-1}) appears to have little effect on the system The flux appears lower but, practically, the fluxes are very close. Even though the fluxes observed are very low, the catechin rejection is lower (8% at a steady state flux of 12 l m^{-2} h^{-1}) than when casein only is present (17% at 51 l m^{-2} h^{-1}). This emphasises that there is an interaction between casein and catechin, and that calcium causes a change in the structure/precipitation of casein.

	0 mg l^{-1}	50 mg l^{-1}
Ethanol (%)	4	3
Glycerol (%)	0	0
Maltose (%)	3	3
Citric acid (%)	0	0
Casein (%)	99	100
Starch (%)	99	98
Calcium (%)	-10	-5
Catechin (%)	-	8
Flux (l m^{-2} h^{-1})	20	12

Table 6 18: Effect of catechin on steady state rejections in the presence of starch, casein and calcium

6.9 ETHYL ACETATE ADDITION

6.9.1 Effect on feed containing starch

Table 6 19 shows the effect of adding 100 mg l^{-1} ethyl acetate to a base solution containing 1500 mg l^{-1} starch It appears to lower the steady state flux and have little effect on component rejection, although it suffers a 20% rejection itself. Ethyl acetate contains a permanent dipole in its C=0 group, which is also capable of hydrogen bonding The lowering of the steady state flux suggests an interaction between the

molecule and the membrane or fouling layer. As will be seen in the next section, interaction with the membrane does not appear to take place

	0 mg l^{-1}	100 mg l^{-1}
Ethanol (%)	2	3
Glycerol (%)	0	0
Maltose (%)	3	4
Citric acid (%)	60	50
Starch (%)	>90	97
Ethyl acetate (%)	-	20
Flux (l m^{-2} h^{-1})	33	20

Table 6 19. Effect of ethyl acetate on steady state rejections in the presence of starch.

6.9.2 Effect on feed containing casein

Table 6 20 shows the effect of adding 100 mg l^{-1} ethyl acetate to a base solution containing 150 mg l^{-1} casein. It appears to have little effect on steady state flux suggesting that it is not altering the membrane structure in any way. Maltose rejections are decreased and it is 20% rejected itself. The fact that maltose rejection is decreased may indicate that hydrogen bonding is occurring between ethyl acetate and casein, taking up potential bonding sites for the sugar

	0 mg l^{-1}	100 mg l^{-1}
Ethanol (%)	2.5	2.5
Glycerol (%)	0.5	0 5
Maltose (%)	8	6
Citric acid (%)	3	0
Casein (%)	97	100
Ethyl acetate (%)	-	20
Flux (l m^{-2} h^{-1})	30	30

Table 6 20: Effect of ethyl acetate on steady state rejections in the presence of casein

6.9.3 Effect on feed containing both starch and casein

Table 6.21 shows the effect of adding 100 mg l^{-1} ethyl acetate to a base solution containing 150 mg l^{-1} casein and 1500 mg l^{-1} starch The steady state flux appears to drop, as does the maltose rejection This may be explained by the comments made in the previous two sections.

	0 mg l^{-1}	100 mg l^{-1}
Ethanol (%)	3	4
Glycerol (%)	0	0
Maltose (%)	4	2 5
Citric acid (%)	10	10
Casein (%)	100	99
Starch (%)	>90	98
Ethyl acetate (%)	-	20
Flux (l m^{-2} h^{-1})	32	17

Table 6 21· Effect of ethyl acetate on steady state rejections in the presence of both starch and casein

6.9.4 Effect on feed containing all components

Catechin was added to a feed containing 1500 mg l^{-1} starch, 150 mg l^{-1} casein, 100 mg l^{-1} calcium and 50 mg l^{-1} catechin It appears from Table 6.22, that it has little effect on steady state flux or rejection

	0 mg l^{-1}	100 mg l^{-1}
Ethanol (%)	3	3
Glycerol (%)	0	0
Maltose (%)	3	4
Citric acid (%)	0	0
Casein (%)	100	100
Starch (%)	98	98
Ethyl acetate (%)	-	20
Catechin (%)	8	10
Calcium (%)	-5	-5
Flux (l m^{-2} h^{-1})	12	13

Table 6 22: Effect of ethyl acetate on steady state rejections with all components present

6.10 EFFECT OF MEMBRANE TYPE

In order to investigate the effect of the membrane material on steady state flux and rejection, experiments were carried out on 0 2 μm rated polymeric membranes made from cellulose nitrate (CN), polyethersulphone (PES), polyamide (PA) and polycarbonate (PC) A solution containing water, ethanol, glycerol, citric acid, maltose, casein, starch, catechin, ethyl acetate and calcium sulphate was used for these experiments, in the same concentrations as used in Section 6 9.4 Flux decline curves are shown in Figure 6 20 and steady state rejections are summarised in Table 6 23

The properties of the membranes used have been investigated using the same methods as Chaudhury (1996) and are given in Table 6 24. All the membrane materials used were hydrophilic. The polycarbonate membrane differed markedly from the other three membrane used in that it is produced by the track etching process and consists of cylindrical pores through a very thin membrane The other membranes are all produced by a casting process that produces thicker membranes with a tortuous asymmetric structure.

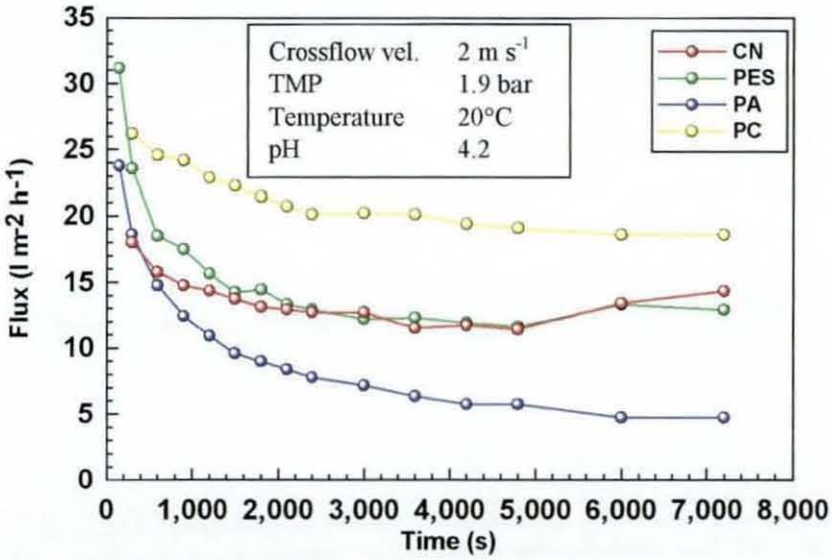

Figure 6.20: Effect of membrane type on flux.

	CN	PES	PA	PC
Ethanol (%)	6	6	13	4
Glycerol (%)	0	0	0	0
Citric acid (%)	0	6	0	0
Maltose (%)	5	4	5	2
Casein (%)	100	100	100	94
Starch (%)	98	85	80	75
Calcium (%)	-5	-10	-10	-3
Ethyl acetate (%)	30	25	50	25
Catechin (%)	9	0	30	7
Flux ($l\ m^{-2}\ h^{-1}$)	14	13	5	19

Table 6.23: Effect of membrane type on steady state rejection.

Figure 6.20 shows the membranes that suffered the greatest loss of flux were polyamide and polyethersulphone. These membranes have the largest pore sizes and this suggests that they may suffer from an internal deposition of matter. They both display greater transmission of starch, indicating that it is passing over the internal structure. It should be noted that the polyamide membranes are used with a coarser surface on the feed side than on the permeate side (as recommended by the manufacturer), utilising a degree of depth filtration to ensure a 0.2 μm cut-off. The final flux displayed by the polyamide membrane is significantly lower than for the others. This is almost certainly due to the coarse layer being on the feed side allowing

Type	Pore size			Thickness	Permeability	Clean water flux (@10psi)	Porosity	Surface charge
	Min	Max.	Mean		(measured)	(measured)	(Chaudhury (1996))	
	µm	µm	µm	µm	m^2	ml cm^{-2} min^{-1}	(%)	
CN	0 260	0 426	0.348	110	$4.3*10^{-15}$	13.1	78	-ve
PES	0 316	0 566	0 437	150	$4\ 2*10^{-15}$	11.5	84	-ve
PC	0 208	0 261	0 237	10	$4\ 0*10^{-16}$	16 7	22	-ve
PA	0 185	0 471	0 363	120	$2.4*10^{-15}$	8.4	69	+ve

Table 6 24· Properties of 0 2µm membranes

material to block its internal structure, although its positive surface charge and the negative charge carried by starch may also be a factor The polycarbonate membrane exhibited the highest fluxes probably due to its much thinner and regular structure minimising internal fouling

The trend in starch rejection appears to follow the mean pore size, with lower rejections at larger pore sizes. The exception to this is for polycarbonate which shows the lowest rejection, yet has the tightest cut off However it is at least a tenth the thickness of the others and has a much lower porosity There is, therefore, a smaller surface area of membrane with which a molecule may interact on passing through the membrane This may lead to both a smaller membrane area onto which the starch may adsorb or may reduce the amount of other adsorbed material with which it may interact. The rejections of ethanol, maltose, casein and ethyl acetate are lower with polycarbonate, higher, yet similar for cellulose nitrate and polyethersulphone and higher still in the case of polyamide This very much follows the trend in the steady state flux and may therefore be due to the flowrate through the fouling layer (Section 6 11).

6.11 EFFECT OF PERMEATE FLUX ON REJECTION.

A general trend observed throughout experimentation with casein was that rejections appeared to be greater when the permeate flux was lower, although different molecules displayed differing degrees of dependence. However, interpreting the effect of permeate flux alone is somewhat difficult as flux itself depends on fouling layer characteristics such as thickness and packing Experiments were performed with a range of mono- and di-saccharides (see Section 6 6) under identical conditions It is reasonable to assume that the fouling layer composition and thickness should be comparable for all five experiments Figure 6 21 shows a plot of rejection against permeate flux for these systems In these cases, there appears to be a clear trend, with higher rejection occurring at lower permeation rates It may also be observed that the

monosaccharides and disaccharides lie on different trendlines, although the molecules within these two series display a close fit to their trendlines.

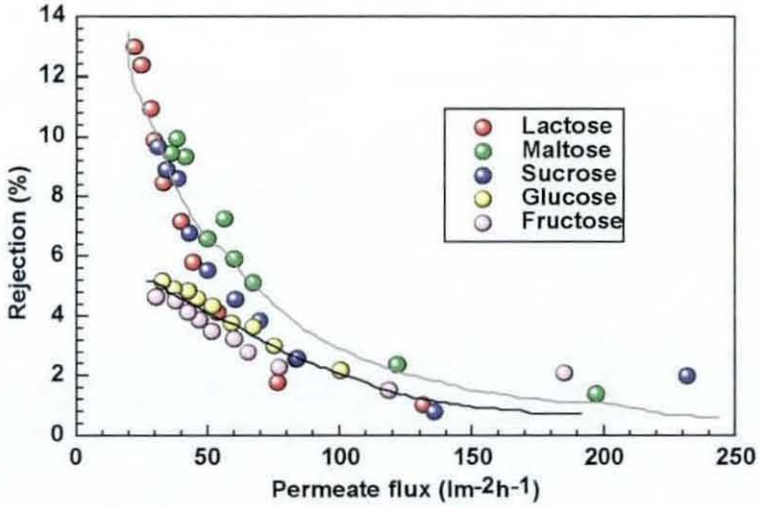

Figure 6.21: Dependence of permeate flux on rejection for sugars with casein.

Data presented by Walla (1994) for the filtration of a lager cellar beer through a 0.45μm alumina membrane at a range of transmembrane pressures (0.5 to 2.5 bar) and crossflow velocities (2 to 4 m s^{-1}) shows a general trend whereby the steady state transmission of components is increased at higher steady state fluxes and is therefore in agreement with data presented here.

The increase in rejections at lower permeate fluxes could still be attributed to a thickening of the fouling layer. This would provide a greater amount of material to "capture" smaller molecules, with the greater thickness resulting in a lower permeability and hence lower permeate flux. However, these lower fluxes occur towards the end of experimentation as equilibrium is approached. At this point the rate of increase in the fouling layer thickness should be small, yet the rate of increase in rejection (as seen in Figure 6.21) appears to be increasing. Therefore it is argued that the increase in component rejection is influenced more by the permeate flux than the fouling layer thickness.

6.12 FOULING MECHANISMS

In this work, fouling is taken to be any process by which the permeability of the membrane is reduced. It may therefore encompass pore blocking, pore bridging, adsorption, concentration polarisation or the formation of a gel layer. The macromolecules starch and casein were added to the system as they are both long chain polymers that have been identified as potential membrane foulants by several authors (Section 2.2.10). The data presented shows that these two molecules are indeed responsible for fouling of the membrane. During filtration both starch and casein initially passed through the membrane, albeit at concentrations much lower (less than 10% transmission) than the feed concentration. On removing the membranes from the crossflow cell after experiments with casein and starch, it was noticeable that the surface was covered in a gel layer. It appeared to be milky in colour for starch and much whiter for the casein. This indicated that high concentrations of the macromolecular components were present on the membrane surface.

It is unlikely that one single mechanism is responsible for the flux decline observed, but more likely a combination as has been observed during the fouling of membranes by proteins (Bowen *et al.* (1995), Prádanos *et al.* (1996), Jonsson *et al.* (1996)). Therefore, data has been analysed using the generalised blocking model (Bowen *et al.* (1995)) in an attempt to understand the fouling steps. Care should be taken when analysing crossflow data using blocking models as the theory has been developed for the dead end case, although the model used by Bowen *et al.* (1995) theoretically accounts for crossflow conditions. However the more simplistic approach as used by Blainpain and Lalande 1996), for the microfiltration of beer, has been used here as plots do show linearity.

Figures 6.22 and 6.23 show casein (150 mg l^{-1}) data plotted on axes of t/V against t and t/V against V, with linearity in the data corresponding to the standard blocking and cake filtration laws. Generally, experiments carried out with casein follow the standard blocking law followed by cake filtration, although intermediate blocking could possibly be argued. This is in agreement with work by Blanpain and Lalande (1996). As they

have highlighted, it is interesting to note that the linear part of the standard blocking plot finishes at a time of 1000 s, which corresponds to a filtrate volume of 0.2 l, the point at which cake filtration appears to begin. Unfortunately, a lack of data at the start of experimentation does not help the differentiation between intermediate and standard blocking, but this was unavoidable. The curve tends to level off at greater volumes and this may be attributed to action of the tangential flow over the cake surface limiting its thickness.

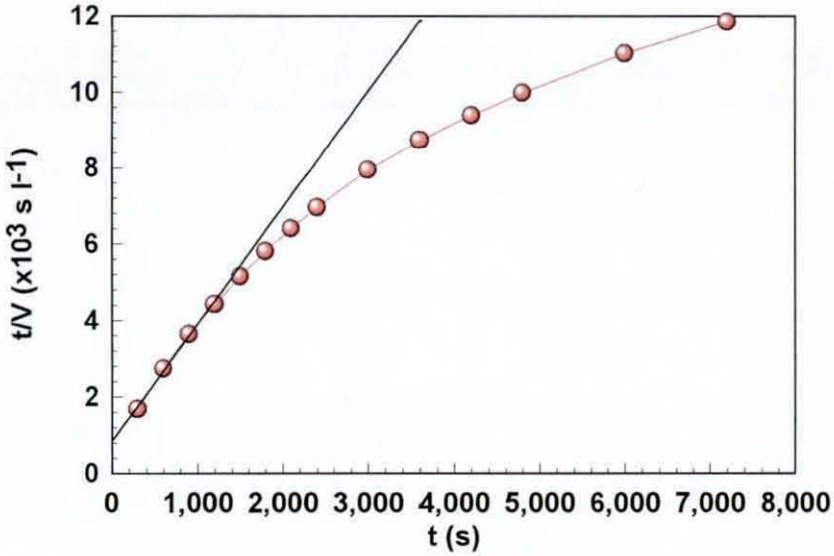

Figure 6.22: A typical standard blocking model plot for casein experiments.

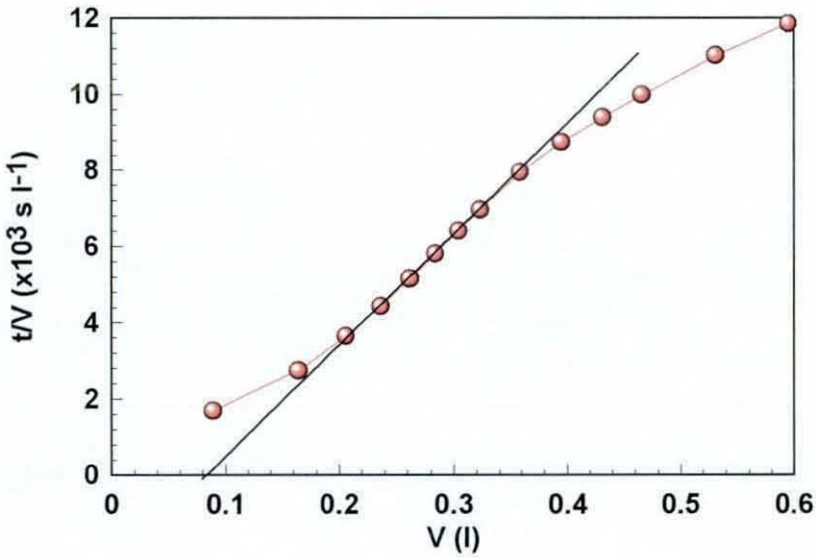

Figure 6.23: A typical cake filtration plot for casein experiments.

Further cake filtration plots have been plotted on axes of $t\text{-}t_i/V\text{-}V_i$ against $V+V_i$ to account for the lack of initial data. Here, t_i is the time that data starts and V_i is the cumulative volume at $t=t_i$. A specific cake resistance may then be calculated from the slope of the linear part of the curve, using equation 6.1, below;

$$\frac{t\text{-}t_i}{V\text{-}V_i} = \frac{\alpha_{av} c \mu}{2A^2 \Delta P}(V + V_i) \qquad (6.1)$$

where α_{av} is the specific cake resistance (m kg^{-1}), c is the solution concentration (kg m^{-3}), μ is the viscosity (Pa s), A is the membrane area (m^2) and ΔP is the pressure difference across the membrane (Pa). It should again be noted that this is a specific cake resistance calculated for the crossflow case and is not therefore a specific cake resistance as in the dead end theory.

Figure 6.24 shows a cake filtration plot for casein with changes in concentration (2.0 m s^{-1}, 1.9 bar). The specific cake resistances calculated are summarised in Table 6.25, along with those calculated for changes in crossflow velocity (150 mg l^{-1}, 3.3 bar). The specific cake resistance increases with concentration, as the likelihood of pore bridging is increased, at least at the low concentrations used here. The decrease in specific cake resistance with crossflow velocity must be due to a change in the structure of the fouling layer at higher shear.

Concentration (mg l^{-1})	α_{av} (m kg^{-1})	Crossflow velocity (m s^{-1})	α_{av} (m kg^{-1})
25	$3.99*10^{14}$	1.1	$4.56*10^{15}$
50	$7.90*10^{14}$	1.6	$2.98*10^{15}$
100	$1.05*10^{15}$	2.0	$7.30*10^{14}$
150	$3.05*10^{15}$	2.4	$6.08*10^{14}$
200	$2.78*10^{15}$	2.8	$7.60*10^{13}$

Table 6.25: Effect of concentration and crossflow velocity on the specific cake resistance of casein deposits.

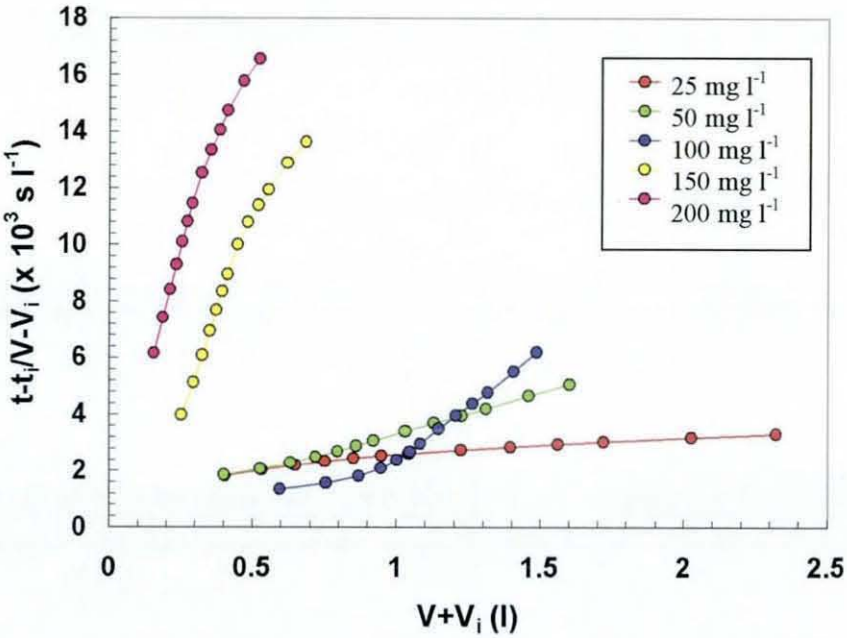

Figure 6.24: Cake filtration plot for increases in casein concentration.

A change in the mode of fouling when filtering casein in the presence of calcium may also be indicated by such plots. $t\text{-}t_i/V\text{-}V_i$ against $V+V_i$ plots for casein (150 mg l^{-1}) with (0, 50, 100 mg l^{-1}) calcium are shown in Figure 6.25. The addition of calcium leads to a dramatic reduction in the slope of the linear part of the curve. The calculated specific cake resistances are $3.05*10^{15}$, $4.74*10^{13}$ and $3.16*10^{13}$ m kg^{-1} at calcium ion concentrations of 0, 50 and 100 mg l^{-1} respectively. This would suggest that the structure of the casein deposit has changed, forming a more open structure possibly due to an increase in particle size. This supports the earlier assumption that flux changes were caused by protein precipitation (Section 6.7.2).

Flux decline data for starch tends not to fit any of the models. An example is shown in Figure 6.26 for changes in starch concentration. Starch containing systems have tended to foul quickly in this work and it appears from Figure 6.26 we are only observing the latter parts of filtration as the shear limits cake/fouling layer growth.

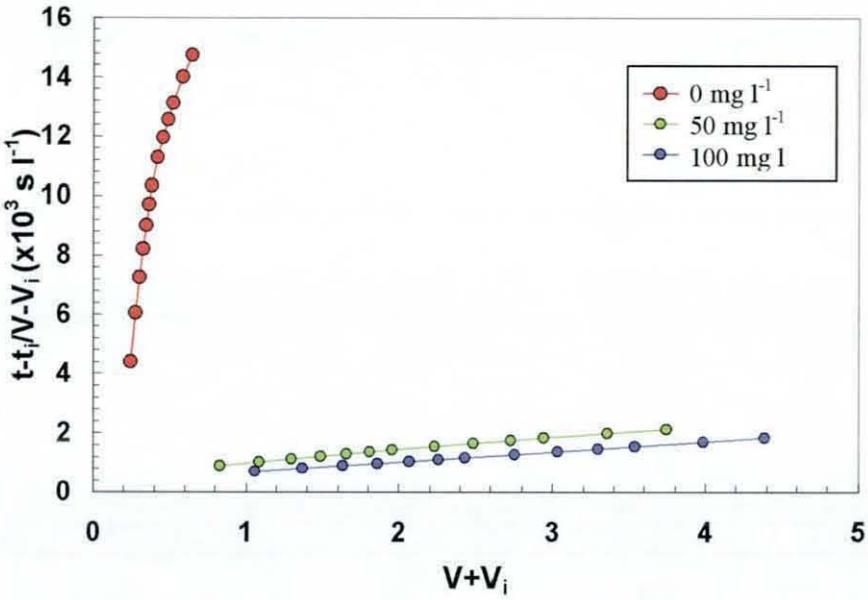

Figure 6.25: Cake filtration plot for casein in the presence of calcium.

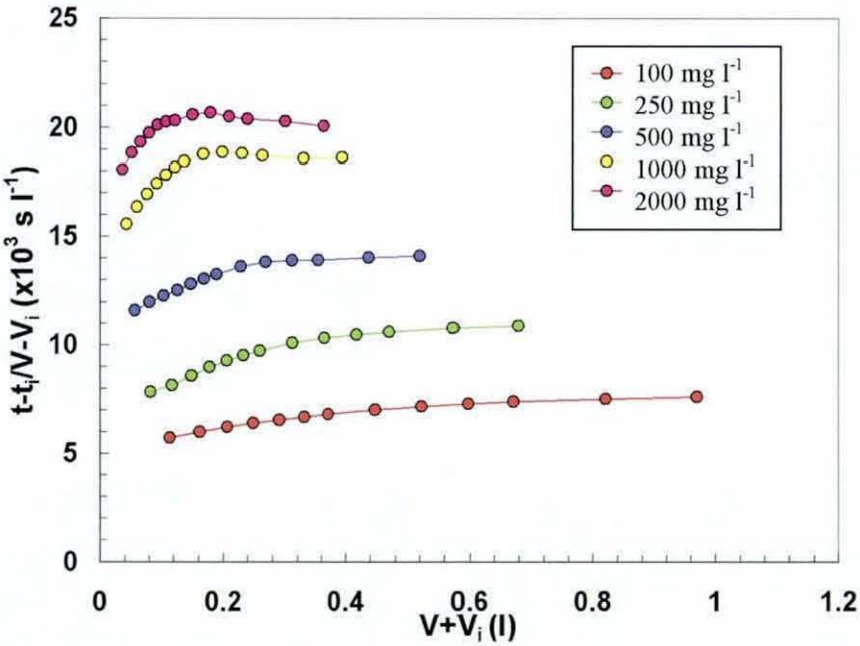

Figure 6.26: Cake filtration plot for increases in starch concentration.

CHAPTER 7
CONCLUSION

The objective of this work was to investigate the rejection of beer components during the microfiltration of beer through membranes with pore sizes less than 0.45 μm. The technique used here, was to filter a model beer solution to which components could be added/removed. A typical beer composition was obtained from an analysis compiled by Moll (1991). Initial experiments investigated a solution containing water, ethanol, glycerol and citric acid, and in later experiments maltose, starch (a model for the longer chain carbohydrate material), casein (a model for the protein fractions), catechin, ethyl acetate and calcium ions were added. Filtration was carried out through 0.2 μm membranes, generally cellulose nitrate, in a crossflow configuration. Operating conditions were crossflow velocities of 1.1 to 2.8 m s^{-1}, a transmembrane pressure of 1.9 to 4.5 bar, a temperature of 20°C and a pH of 4.2.

Citric acid displayed a high rejection (≈50%) when passing through the membrane and this was still the case with starch in the system. However, the rejection was reduced dramatically in the presence of casein. This may be attributed to some kind of charge effect, as both the membrane and starch carry a negative surface charge, whereas the casein has a positive surface charge. Experiments carried out with succincic and acetic acids showed much lower rejections (≈5%). Both these acids have fewer charged species at pH 4.2.

As was expected, starch and casein, large chain macromolecules, were both found to be responsible for dramatic flux decline. Clearly, both molecules were responsible for causing a deposit to form on the surface of the membrane. In both cases, higher concentrations lead to lower initial and steady state fluxes. In systems where both starch and casein were present, starch concentration was the overriding factor in determining the flux, but changes in casein concentration led to changes in component rejection.

Casein was found to be largely responsible for the rejection of maltose and catechin, with rejections increasing from 3-8% and 9-18% respectively. The steady state flux was found to increase with the polyphenol. The interaction between the polyphenol and the protein is not entirely surprising, as the two are widely acknowledged to form insoluble complexes, as appears to be the case here. Further experiments were conducted to investigate the sugar rejection, by filtering solutions containing lactose, sucrose, glucose and fructose. It was found that the monosaccharides (glucose and fructose) displayed half the rejection (≈5%) of the disaccharides (≈10%) (maltose, lactose and sucrose). This may be explained if single sugar rings are adsorbing onto the protein surface and hence two disaccharide rings are adsorbing for every monosaccharide ring.

The addition of calcium ions to the system appeared to reduce the ability of casein to influence the rejections observed. The steady state flux was also increased. This has been attributed to the precipitation of protein. It is therefore likely that soluble protein is responsible for the major flux declines and rejections. In the case of starch, calcium ions were responsible for a further drop in flux, as the increase in ionic strength leads to charge shielding and a more compact starch layer.

Ethyl acetate, the most volatile component present, was found to be rejected (20%) irrespective of the other components present. It may interact with the membrane and appears to interact with the protein causing maltose rejections to drop. However, the mechanism of rejection is somewhat unclear.

Four membranes (polycarbonate, polyethersulphone, polyamide and cellulose nitrate) were challenged with a feed containing all components. The PES and PA membranes, which had the largest pore sizes, showed the largest drop in permeate flux. This suggests the deposition of material within the membrane. Polycarbonate displayed a higher steady state flux and a less marked flux decline. This is due to its thinner structure and well defined cylindrical pores. The rejections of the smaller components were found to be lower at higher fluxes, irrespective of the membrane type.

A general trend observed, throughout, was that lower permeate fluxes resulted in higher rejections. For example, data shows that rejections of ethanol, glycerol and maltose increased at lower fluxes. Once again, this is not surprising, as lower fluxes induce lower forces on the molecules as they pass through the filter. The opposing forces to any capturing/repelling forces are therefore decreased, and rejections appear to increase.

Flux decline data has been analysed using the general blocking laws. Systems containing casein were found to follow a standard blocking model followed by cake filtration, except in the presence of calcium ions, whereby a cake filtration mode was followed. Starch did not appear to fit any of the blocking laws. This may be due to the fact that it quickly fouls the membrane and only the limiting influence of the crossflow shear is observed in t/V against V type plots.

This work provides an insight into the types of interactions that may occur during the microfiltration of beer. It does, however, represent a worst case scenario in terms of component rejections observed. As the data shows, the introduction of further molecules may mask interactions leading to lower rejections. Beer is a much more complex system than can be modelled with ten components, making this system a rather simplistic starting point.

REFERENCES

Atkinson, B., Reed, R.J.R. and Leeder, G.L, "The application of membranes and deep bed methods in the filtration of beer", Inst. Brew. Conv., Central and Sth. African Sec., 1985, pp 141-159.

Balakrishnan, M., Agarwal, G.P. and Cooney, C.L., "Study of protein transmission through ultrafiltration membranes.", J. Membr. Sci., 85, 1993, pp 111-128.

Bamforth, C.W. and Reed, R.J.R., "Process developments in brewing: the need for change", Food Tech. Int. Eur., 1994, pp 74-76.

Bauser, H., Chmiel, H., Stroh, N. and Walitza, E., "Interfacial effects with microfiltration membranes.", J. Membrane Sci, 11, 1982, pp 321-332.

Blanpain, P., Hermia, J. and Lenoèl, M., "Mechanisms governing permeate flux and protein rejetion in the microfiltration of beer with a cyclopore membrane.", J. Membrane Sci., 84, 1993, pp 37-51.

Blanpain, P. and Lalande, M., "Investigation of fouling mechanisms governing permeate flux in the crossflow microfiltration of beer.", 7th World Filtration Congress, 1996, pp 561-565.

Blanpain-Avet, P., Fillaudeau, L. and Lalande, M., "Investigation of mechanisms governing membrane fouling and protein rejection in the sterile microfiltration of beer with an organic membrane", Proc. IChemE fouling and cleaning in food processing, 6-8 April, 1998, ppII.4.a-II.4.h.

Bio-rad bulletin 1833, 1995.

Bio-rad bulletin 1928, 1995.

Bowen, W.R. and Cooke, R.J., "Properties of microfiltratio membranes. Computer automated determination of the zeta-potential of cellulose nitrate membranes.", 5th World filtration Congress, 1992, pp231-239.

Bowen, W.R. and Gan, Q., "Properties of microfiltration membranes: The effects of adsorption and shear on the recovery of an enzyme.", Biotechnol. Bioeng., 40, 1992, pp 491-497.

Bowen, W.R. and Hall, N.J., "Properties of microfiltration membranes: Mechanisms of flux loss in the recovery of an enzyme.", Biotechnol. Bioeng., 46, 1995, pp 28-35.

Bowen, W.R., Calvo, J.I. and Hernández, A., "Steps of membrane blocking in flux decline during protein microfiltration.", J. Membr. Sci., 101, 1995, pp153-165.

Brink, L.E.S., Elbers, S.J.G., Robbertsen, T. and Both, P., "The anti-fouling action of polmers preadsorbed on ultrafiltration and microfiltration membranes.", J. Membr. Sci., 76, 1993, pp 281-291.

Bühler, T.M., Burrell, K., Eggars, H.U. and Reed, R.J.R., "The application of membranes for new approaches to brewery operations.", Proc. Eur. Brew. Conv., Oslo, 1993, pp 691-700.

Burrell, K.J. and Reed, R.J.R., "Crossflow micorfiltration of beer: Laboratory-scale studies on the effect of pore size.", Filtr. Sep., 31, June 1994a, pp 399-405.

Burrell, K.J., Gill, C., McKechnie, M., and Murray, J., "Advances in separations technology for the brewer: Ceramic crossflow microfiltration of rough beer", Tech. Q. Master Brew. Assoc. Am., 31, 1994b, pp42-50.

Burrell, K., Kotzian, R., and O'Sullivan, P., "Progress in the crossflow microfiltration of beer", Brew. Distill. Int, July, 1994c, 22-23.

Cantrell, I.C., Dickenson, C.J., Homer, K. and Lowe, C.M., "The recovery of beer from yeast and other processing residues by ultrafiltration.", J. Inst. Brew., 91, 1985, pp 132-.

Chaudhury, M.S.S.L.T., "Mechanisms of membrane fouling.", Ph.D Thesis, Exeter University, 1996.

Chimiel, H., McDonogh, R.M., Bauser, H. and Stroh, N., "Aspecific interaction of proteins with polymer surfaces.", J. Disp. Sci. Tech., 12, 1991, pp161-177.

Clark, W.M., Bansal, A., Sontakke, M. and Ma, Y.H., "Protein adsorption and fouling in ceramic ultrafiltration membranes.", J. Membrane Sci., 55, 1991, pp 21-38.

Collison, R., "Starch retrogradation" in "Starch and its derivatives", Chapman and Hall Ltd. 1968, London.

Curioni, A., Pressi, G., Furegon, L. and Peruffo, A.D.B., "Major proteins of beer and their precursors in barley: Electrophoretic and immunological studies.", J. Agric. Food Chem., 43, 1995, pp 2620-2626.

Czech, B., "Crossflow filtration of beer-experiences within the brewery", Brewer, 81, 1995, pp103-110.

Dale, C.J. and Young, T.W., "Apllications of fast protein liquid chromatography (FPLC) to the analysis of the nitrogenous constituents of beer.", J. Inst. Brew., 98, 1992, pp 117-121.

de Clerk, J., "Determinations of tannin in brewing.", Chem. Abst., 42, 1947, pp3530.

Doyen, W., Adriansens, W., Molenberghs, R. and Leysen, R., "A comparison between polysulfone, zirconia and organo-mineral membranes for use in ultrafiltration.", J. Membrane Sci., 113, 1996, pp 247-258.

Dumon, S. and Barnier, H., "Ultrafiltration of portein solutions on ZrO_2 membranes. The influence of surface chemistry and solution chemistry on adsorption.", J. Membrane Sci., 74, 1992, pp 289-302.

Fauchille, S. and Gachelin, D., "Human albumin ultrafiltration comparison of different devices and operating conditions.", 7th World filtration congress, 1996, pp 604-608.

Finnigan, T., Shackleton, R. and Skudder, P., "Using ceramic microfiltration for the filtration of beer and recovery of extract.", Filtr. Sep., 26, May/June 1989, pp 198-200.

Freeman, G J., McKechnie, M.T., Smedley, S.M., Hammond, R.V., and Napper, P.W., "Determination and use of process characteristics for optimization of the beer filtration operation", Trans. IChemE, 73, C, 1995.

Frieling, J., "Crossflow microfiltration as an alternative to customary sheet filtration respectively kieselguhr- and sheet filtration?", Eur. Brew. Conv. Monogr. XVI, Leuven, 1990, pp160-170.

Gan, Q., Field, R.W., Bird, M.R., England, R., Howell, J.A., McKechnie, M.T. and O'Shaughnessy, C.L., "Beer clarification by cross-flow microlfiltation: Fouling mechanisms and flux enhancement", Trans. IChemE, 75, A, 1997, pp 3-8.

Gans, U. and Denk, V., "Die wirtschaftliche crossflow-mikrofiltration von bier", Brauwelt, 134, 1994, pp2000-2004, 2013-2014.

Gekas, V. and Hallström, B., "Microfiltration membranes, cross-flow transport mechanisms and fouling studies.", Desalination, 77, 1990, pp 195-218.

Grund, G., Robinson, C.W. and Glick, B.R., "Protein type effects on steady-state crossflow membrane ultrafiltration fluxes and protein tranmission.", J. Membr. Sci., 70, 1992, 177-192.

Heinemann, P., Howell, J.A. and Bryan, R.A., "Microfiltration of protein solutions: Effect of fouling on rejection.", Desalination, 68, 1988, pp 243-250.

Hermia, J. and Brocheton, S., "Comparison of modern beer filters", Filtr. Sep., November, 1994, pp721-725.

Hough, J.S., Briggs, D.E., Stevens, R. and Young, T.W., "Malting and brewing science.", Volume 1, Second edition, Chapman and Hall, London, 1982a.

Hough, J.S., Briggs, D.E., Stevens, R. and Young, T.W., "Malting and brewing science.", Volume 2, Second edition, Chapman and Hall, London, 1982b.

Hough, J.S., "The biotechnology of malting and brewing.", University press, Cambridge, 1985.

Hug, H., Pfenninger, H.B., Meier, J., Girr, M. and Treptau, B., "Erste praktische Ergebnisse zur Bierrückgewinnung mit einer grosstechnischen Crossflow-Mikrofiltrationsanlage", Proc. Eur. Brew. Conv., Zurich, 1989, pp 453-460.

Ingham, K.C., Busby, T.F., Sahlestrom, Y. and Castino, F., "Separation of macromolecules by ultrafiltration: Influence of protein adsorption, protein-protein interactions, and concentration polarization.", Polymer Science and Technology, 13, 1980, pp 141-158.

Iordanskii, A.L., Markin, V.S., Razumovskii, L.P., Kosenko, R.Y., Tarasova, N.A. and Zaikov, G.E., "Diffusion model of protein adsorption and effect of protein layer composition on water permeability for ultrafiltration membranes.", Desalination, 104, 1996, pp 113-118.

Iritani, E., Mukai, Y. and Murase, T , "Separation mechanism in filtration of binary protein mixtures.", 7th World filtration congress, 1996, pp 581-585.

Jonsson, G., Prádanos, P. and Hernández, A., "Fouling phenomena in microporous membranes. Flux decline kinetics and structural modifications.", J. Membr. Sci., 112, 1996, pp 171-183.

Joslyn, M.A., "Methods in food analysis: physical, chemical and instrumental methods of analysis.", 2nd edition, Academic Press, London, 1970.

Kelly, S.T. and Zydney, A.L., "Mechanisms for BSA fouling during microfiltration.", J. Membr. Sci., 107, 1995, pp 115-127.

Kiefer, J., "Crossflow filtration of beer.", Proc. Eur. Brew. Conv., Lisbon, 1991, pp 657-664.

Kim, K.J., Fane, A.G., Fell, C.J.D. and Joy, D.C., "Fouling mechanisms of membranes during protein ultrafiltration.", J. Membr. Sci., 68, 1992, pp 79-91.

Kim, K.J., Chen, V. and Fane, A.G., "Some factors determining protein aggregation during ultrafiltration.", Biotech. Bioeng., 42, 1993, pp 260-265.

Kirk, R.E., and Othmer, D.F., "Kirk-Othmer Encyclopedia of Chemical Technology - Volume 5.", 3rd edition, Wiley, New York, 1979a.

Kirk, R.E., and Othmer, D.F., "Kirk-Othmer Encyclopedia of Chemical Technology - Volume 6.", 3rd edition, Wiley, New York, 1979b.

Kirk, R.E., and Othmer, D.F., "Kirk-Othmer Encyclopedia of Chemical Technology - Volume 16.", 3rd edition, Wiley, New York, 1979c.

Ko, M.K., Pellegrino, J.J., Nassimbene, R. and Marko, P., "Characterisation of the adsorption-fouling layer using globular proteins on ultrafiltration membranes.", J. Membr. Sci., 76, 1993, pp101-120.

Kontturi, K. and Vuoristo, M., "Adsorption of globular proteins on polymeric microfiltration membranes.", Desalination, 104, 1996, pp 99-105.

Le, M.S., "Recovery of beer from tank bottoms with membranes.", J. Chem. Tech. Biotechnol., 87, 1987, pp 59-66.

Le Berre, O. and Daufin, G., "Fouling and selectivity of membranes during separation of β-casein.", J. Membrane Sci., 88, 1994, pp 263-270.

Leeder, G.I. and Houldsworth, D.W., "Cost benefits of crossflow microfiltration", Brew. Distill. Int., 19, October, 1988, pp14, 16-17.

Leeder, G. and Girr, M., "Cross-flow micro filtration for processing brewery tank bottoms", Tech. Q. Master Brew. Assoc. Am., 31, 1994, pp58-63.

Lenoël, M., "Beer recovery from yeast slurries and tank bottoms from pilot to industrial results", Eur. Brew. Conv. Monogr. XVI, Leuven, 1990, pp128-139.

Lenoël, M., Blanpain, P., Weishaupt, R. and Shingleton, M., "Modélisation de la microfiltration tangentielle de bière sur membranes - compréhension du mécanisme de colmatage", Proc. Eur. Brew. Conv. Oslo, 1993, pp683-690.

Lenoël, M., Blanpain, P. and Taylour, J., "Rational design of cleaning procedure for microfiltration membranes", Tech. Q. Master Brew. Assoc. Am., 31, 1994, pp134-137.

Letters, R., "Carbohydrate gels. A problem with newer brewing technologies", Proc. Inst. Brew. Central Sth. African Sect., Victoria Falls, March, 1995, pp115-121.

McKechnie, M.T., "Filtration or solid/liquid separation? The future for beer clarification.", Brew. Guardian, 124, July, 1995, pp36-43.

Millesime, L., Dulieu, J. and Chaufer, B., "Protein retention with modified and unmodified inorganic ultrafiltration membranes: model of ionic strength controlled retention.", J. Membr. Sci., 108, 1995, pp 143-159.

Meier, J., "Applied crossflow microfiltration for waste beer treatment", Brauwelt Int., 1990, pp120-124.

Mochizuki, S. and Zydney, A.L., "Effect of protein adsorption on the transport charteristics of assymetric ultrafiltration membranes.", Biotech. Prog., 8, 1992, pp553-561.

Moll, M., "Beers and coolers.", Intercept Ltd., Andover, 1994.

Müller, W., "More than two years of practical experience with tangential flow filtration for recovery from spent yeast", Tech. Q. Master Brew. Assoc. Am., 29, 1992, pp42-47.

Mylius, U.v. and Reiter, A., "Waste beer recovery and yeast concentration by cross-flow microfiltration", Brauwelt Int., 1988, pp68-71.

Nielsen, C.E., "Microfiltration route to recovering beer fromtank bottoms", Brew. Distil.Int., 20, 1989, pp20-21.

Noble, C.S., "Beer filtration. Current practice and future technologies", Ferment, 1, April, 1988, pp35-39.

Norde, W., "Adsorption of proteins from solution at the solid-liquid interface.", Adv. Coll. Int. Sci., 25, 1986, pp267-340.

Obermeyer, H.D., Kulozik, U. and Kessler, H.G., "Controlled deposit formation to influence the retention of solutes in reverse osmosis and ultrafiltration.", Desalination, 90, 1993, pp 161-172.

O,Reilly, S.M.G., Lummis, D.J., Scott, J. and Molzahn, S.W., "The application of ceramic filtration for the recovery of beer from tank bottoms and in beer filtration.", Proc. Eur. Brew. Conv., Madrid, 1987, pp 639-646.

O'Shaughnessy, C. and McKechnie, M.T., "The future of separations technology", The Brewer (http://WWW.BREWORLD.COM/the_brewer/9603/br1.html), March, 1996.

Palecek, S.P. and Zydney, A.L., "Hydraulic permeability of protein deposits formed during microfiltration: effect of solution pH and ionic strength.", J. Membrane Sci., 95, 1994a, pp 71-81.

Palecek, S.P. and Zydney, A.L., "Intermolecular electrostatic interactions and their effects on flux and protein deposition during protein filtration.", Biotehnol. Prog., 10, 1994, pp 207-213.

Peachey, B.W., "Crossflow filtration in brewing - a critical review", Ferment, 4, Dec., 1991, pp362-365.

Persson, K.M., Capanelli, G., Bottino, A. and Trägårdh,G., "Porosity and protein adsorption of four polymeric microfiltration membranes.", J. Membr. Sci., 76, 1993, pp61-71.

Pincet, F., Perez, E. and Belfort, G., "Molecular interactions between proteins and synthetic membrane polymer films.", Langmuir, 11, 1995, pp 1229-1235.

Pollock, J.R.A., "Brewing science.", Volume 2, Academic press, London, 1981.

Pouliot, M., Pouliot, Y., Britten, M. and Ross, N., "Effects of pH and ionic environment on the permeability and rejective properties of an alumina microfiltration membrane for whey proteins.", J. Membrane Sci., 95, 1994, pp 125-134.

Prádanos, P., Hernández, A., Calvo, J.I. and Tejerina, F., "Mechanisms of protein fouling in cross-flow UF through an asymmetric inorganic membrane.", J. Membr. Sci , 114, 1996, pp 115-126.

Pujar, N.S. and Zydney, A.L., "Electrostatic and electrokinetic interactions during protein transport through narrow pore membranes.", Ind. Eng., Chem. Res., 33, 1994, pp 2473-2482.

Quiocho, F.A., "Probing the atomic interactions between proteins and carbohydrates.", Biochem. Soc. Trans., 21, 1993, pp442-448.

Randon, J., Blanc, P. and Paterson, R., "Modification of ceramic membrane surfaces using phosphoric acid and alkyl phosphonic acids and its effects on ultrafiltration of BSA protein.", J. Membrane Sci., 98, 1995, pp 119-129.

Reed, I.M. and Sheldon, J.M., " Investigation of protein fouling characteristics of ultrafiltration membranes.", Effective industrial membrane processes - Benefits and opportunities, 1991, pp 91-99.

Reed, R., Grimmett, C.M. and Leeder, G.I., "Beer filterability – evaluation and alternative approaches to processing.", EBC Congress, London, 1983, pp 225-232.

Reed, R.J.R., "Centenary review article – Beer filtration.", J. Inst. Brew., 92, 1986, pp 413-419.

Reed, R.J.R. and Leeder, G.I., "Cross-flow filtration in brewing", Brew.Gaurd., 115, 1986, pp15-18.

Reed, R.J.R., Evans, S.P., Taylor, D.G. and Anderson, H.J., "Single stage processing of beer using pulsed crossflow filtration", EBC Congress, 1989, pp 413-424.

Reed, R.J.R., "Advances in filtration", The Brewer, Sept., 1989, pp 965-970.

René, F. and Maingonnat, J-F., "Microfiltration de la bière: Revue bibliographique", Ind. Aliment. Agric., 110, 1993, pp 721-729.

Ricq, L., Pierre, A., Reggiani, J., Zaragoza-Piqueras, S., Pagetti, J. and Daufin, G., "Effects of proteins on electrokinetic properties of inorganic membranes during ultra- and micro-filtration.", J. Memrane Sci., 114, 1996, pp 27-38.

Ryder, D.S., Davis, C.R., Anderson, D., Glancy, F.M. and Power, J.N., "Brewing experience with cross-flow filtration", Tech. Q. Master Brew. Assoc. Am., 25, 1988, pp67-79.

Sayed Razavi, S.K., Harris, J.L. and Sherkat, F., "Fouling and cleaning of membranes in the ultrafiltration of aqueous extract of soy flour.", J. Membrane Sci., 114, 1996, pp 93-104.

Schlenker, R.W., "Tangential flow filtration for beer recovery from spent yeast.", Filtr. Sep., Nov. 1998, pp 863-865.

Schoenmakers, P.J., "Optimization of chromatographic selectivity – a guide to mehtod development.", Elseveir, Amsterdam, 1986.

Siebel, R.E., Davis, C.R. and Ryder, D.S., "Frontiers in cross-flow filtration", Proc. Conv. Inst. Brew. (Aust. N.Z. Sect.), Brisbane, 1988, pp49-56.

Sudarmana, D.L., Goldsmith, M.R., Hinh, A.H., Pecar, M.A., Hawthorne, D.B. and Kavanagh, T.E., "Microfiltration tudies with a modified membrane filterability procedure", Tech. Q. Master Brew. Assoc. Am., 33, 1996, pp63-72.

Tandon, A., Gupta, S.K. and Agarwal, G.P., "Modelling of protein transmission through ultrafiltration membranes.", J. Membr. Sci., 97, 1994, pp83-90.

Taylor, G., Levesley, J.A. and Hoare, M., "Pilot-scale ultrafiltration of concentrated protein precipitate suspensions: The effect of concentration and fluid dynamics.", Chem. Eng. Comm., 129, 1994, pp 227-250.

Tracey, E.M. and Davis, R.H., "Protein fouling of track-etched polycarbonate microfiltration membranes.", J. Coll. Int. Sci., 167, 1994, pp 104-116.

Tsapyuk, E.A. and Mank, V.V., "Effect of the structure of starch and gelatin macromolecules on the properties of dynamic membranes formed from them.", Coll. J. USSR., 49, 1987, pp 354-358.

Vandanjon, L., Jaouen, P., Robert, J.M. and Quemeneur, F., "Cell damage caused by shear in tangential flow filtration systems.", 7th World filtration congress, 1996, pp 614-618.

van Eijndhoven, R.H.C.M., Saskena, S. and Zydney, A.L., "Protein fractionation using electrostatic interactions in membrane filtration.", Biotech. and Bioeng., 48, 1995. pp 406-414.

van Oers, C.W., Vorstman, M.A.G. and Kerkhof, P.J.A.M, "Solute rejectionin the presence of a deposited layer during ultrafiltration.", J. Membr. Sci., 107, 1995, pp 173-192.

Wagner, D., Donhauser, S. and Walla, G., "Crossflow-Mikrofiltration (CMF) von Hefe und Bier. Filtration ohne Kieselguhreinsatz", Proc. Eur. Brew. Conv., Madrid, 1987, pp631-638.

Walla, G.E., "Yeast beer recovery with crossflow-microfiltration", Inst. Brew. Conv., Asia Pacific sect., 1994, pp190-195.

Weast, R.C., "CRC handbook of chemistry and physics.", 62nd edition, CRC press Inc., Florida, 1982.

Williams, K.M., Fox, P. and Marshall, T., "A comparison of protein assays for the determination of the protein concentration of beer.", J. Inst. Brew., 101, 1995, pp 365-369.

Xu, Y., Dodds, J., Leclerc, D. and Lenoel, M., "A technique for the study of the fouling of microfiltration membranes using two membranes in series.", J. Membrane Sci., 105, 1995, pp 23-30.

Xu, Y., Dodds, J., Leclerc, D.and Lenoèl, M., "Influence of the nature of the membrane on microfiltration of beer.", 7th World Filtration Congress, 1996, pp 556-560.

APPENDIX 1:
ANALYTICAL METHODS

A1:0 INTRODUCTION

This appendix contains the exact details of analytical methods, including any experimentation performed to justify their use and accuracy.

A1:1 HPLC

When analysing the system containing ethanol, glycerol, citric acid and water, integrator method file 1 was used. The full method is given in Table A1:1. The retention times of the components where; 9.10 mins - citric acid, 13.71 mins - glycerol, 22.61 mins- ethanol.

METHOD	:	1			
DELAY	:	6.50			
RUN TIME	:	26 00			
PLOT Y/N	:	Y			
CHART SPEED	:	4			
ATTEN. ^2	:				
TIME	:	0.1	VALUE	:	7
OFFSET	:	1 0			
ANNOTATE Y/N	:	Y			
MARK Y/N	:	Y			
DRAW Y/N	:	Y			
AUTOZERO	:				
SET	:	0 1			
INIT PKW	:	10.0			
MEM SAVE Y/N	:	Y			

Table A1:1: Integrator settings for analysis without maltose (cont.).

DISC SAVE Y/N	:	N			
DRIVE NO. 0/1	:	0			
DIVISOR	:	1			
MIN AREA	:	10000			
OVERLOAD	:	1000			
CUM DIG Y/N	:	N			
NOISE	:				
TIME	:	0.1	VALUE	:	2711
THRESHOLD	:				
TIME	.	0.1	VALUE	:	4000
SKIM RATIO	:				
TIME	:	0.1	VALUE	:	8
PKW CHANGE 2^	:				
TIME	:	0.00	VALUE	:	0
BASELINE	:				
SET	:	0 50			
VALLEY/VALLEY	:				
SET	:	0 00	RESET	:	0 00
HORZ BASE	:				
SET	:	0 00	RESET	:	0 00
INTEGRATE	:				
SET	:	0.00	RESET	:	0.00
INHIBIT-INT	:				
SET	:	0 00	RESET	:	0.00
NEGATIVE PEAK	:				
SET	:	0 00	RESET	:	0.00
DIGITISE	:				
SET	:	0.00	RESET	:	0.00
XCOM1	:				
SET	:	0 00	RESET	:	0 00
XCOM2	:				
SET	:	0 00	RESET	:	0.00
XCOM3	:				
SET	:	0.00	RESET	:	0 00
XCOM4	:				
SET	:	0.00	RESET	.	0 00

Table A1:1 (cont.): Integrator settings for analysis without maltose.

XCOM5	:				
SET	:	0.00	RESET	:	0.00
XCOM6	:				
SET	:	0.00	RESET	:	0 00
AREA/HT Y/N	:	Y			
CAL CYCLE	:	0			
RF TOL%	:	0			
NORM Y/N	:	N			
INT STD Y/N	:	N			
EXT STD Y/N	:	Y			
SMP/IS	:	1.0000000E0			
CAL AMT	:	1 0000000E0			
PK TIME TOL%	:	5			
PEAK TIME	:				
TIME	:	0.00	AMOUNT	:	1.000000000E0
	:		RF	:	0 000000000E0
TIME	:	9.10	AMOUNT	:	2.500000000E-2
	:		RF	:	6 253741000E-7
TIME	.	13 71	AMOUNT	:	1.600000000E2
			RF	:	2.927782700E-7
TIME	:	22 61	AMOUNT	:	4 080000000E1
	:		RF	:	5 563305000E-7
REF PEAK	:				
TIME	:	0.00			
PRINT CALC Y/N	:	Y			
IS PEAK	:	0 00			
PEAK GROUP	:				
SET	·	0 00	RESET	.	0.00

Table A1:1 (cont.): Integrator settings for analysis without maltose.

In the case of a system containing ethanol, maltose, glycerol, citric acid and water, integrator method file 2 was used. The method is given in Table A1:2 below. Large

sections of the method, that remain at the instruments default values, have been omitted, but were the same as in Table A1:1. The retention times of the components where; 10.71 mins - maltose, 11.70 mins - citric acid, 12.73 mins - glucose (impurity), 19.08 mins - glycerol, 29.93 mins - ethanol. In several experiments, citric acid was replaced by acetic or succinic acid and maltose was replaced by lactose, sucrose, glucose or fructose. In this case retention times and response factors for these components were used instead. These values are given in Table A1:3.

METHOD	:	2			
DELAY	:	10.00			
RUN TIME	:	33.00			
PLOT Y/N	:	Y			
CHART SPEED	:	2			
ATTEN. ^2	:				
TIME	.	0 1	VALUE	.	11
OFFSET	:	1 0			
ANNOTATE Y/N	:	Y			
MARK Y/N	:	Y			
DRAW Y/N	:	Y			
AUTOZERO	:				
SET		0 1			
INIT PKW	·	10.0			
MIN AREA		10000			
OVERLOAD	.	9999			
CUM DIG Y/N	:	N			
NOISE	.				
TIME	:	0.1	VALUE		500
THRESHOLD	.				
TIME	:	0.1	VALUE	:	4000
AREA/HT Y/N	:	Y			
CAL CYCLE	:	0			
RF TOL%	:	5			
NORM Y/N	:	N			

Table A1:2: Integrator settings for analysis with maltose (cont.).

INT STD Y/N	:	N			
EXT STD Y/N	:	Y			
SMP/IS	.	1 0000000E0			
CAL AMT	:	1 0000000E0			
PK TIME TOL%	:	5			
PEAK TIME	:				
TIME	:	0.00	AMOUNT	:	1.000000000E0
	:		RF	:	0.000000000E0
TIME	:	10.71	AMOUNT	:	1.600000000E0
	:		RF	:	2.157364600E-7
TIME	:	11.70	AMOUNT	:	2.500000000E-2
	:		RF	:	4.365287200E-7
TIME	:	12.73	AMOUNT	:	1.600000000E-2
	:		RF	:	3 024231600E-7
TIME	:	19.08	AMOUNT	:	1.600000000E0
	:		RF	:	2.377809200E-7
TIME	:	29.93	AMOUNT	:	4 080000000E1
	:		RF	.	4 530676000E-7

Table A1:2 (cont.): Integrator settings for analysis with maltose.

Component	Retention time	Response factor
Acetic acid	22.66	2.56404E-8
Succinic acid	17.10	2.59237E-7
Glucose	12.31	1.85780E-7
Fructose	13.46	1.88127E-7
Lactose	10.58	1.86821E-7

Table A1:3: Retention times and response factors for alternative components.

In the case of a system containing ethyl acetate, with or without other components, integrator method file 3 was used. The method is given in Table A1:4 below. Large sections of the method, that remain at the instruments default values, have been omitted, but were the same as in Table A1:1. The retention time of ethyl acetate is 28.30 mins. This method may only be used to quantify ethyl acetate, even though the

integrator shows the other peaks. This is because its low concentration requires the detector settings to be more sensitive and this in turn causes an overload on the larger peaks.

METHOD	:	3			
DELAY	:	20.00			
RUN TIME	:	32.00			
PLOT Y/N	:	Y			
CHART SPEED	:	2			
ATTEN. ^2	:				
TIME	:	0.1	VALUE	:	9
OFFSET	:	1.0			
ANNOTATE Y/N	:	Y			
MARK Y/N	:	Y			
DRAW Y/N	:	Y			
AUTOZERO	:				
SET	:	0 1			
INIT PKW	:	10 0			
MIN AREA	:	20000			
OVERLOAD	:	9999			
CUM DIG Y/N	:	N			
NOISE	:				
TIME	:	0.1	VALUE	:	184
THRESHOLD	:				
TIME	:	0 1	VALUE	:	4000
AREA/HT Y/N	:	N			
CAL CYCLE	:	0			
RF TOL%	:	0			
NORM Y/N	:	N			
INT STD Y/N	:	N			
EXT STD Y/N	:	Y			
SMP/IS	:	1.0000000E0			

Table A1:4: Integrator settings for ethyl acetate analysis (cont.).

CAL AMT	:	1 0000000E0			
PK TIME TOL%	:	5			
PEAK TIME	:				
TIME	:	0.00	AMOUNT	:	1.000000000E0
	:		RF	:	0.000000000E0
TIME	:	28.30	AMOUNT	:	1.000000000E2
	:		RF	.	1.177995000E-2

Table A1:4 (cont.): Integrator settings for ethyl acetate analysis.

A1:2 STARCH ANALYSIS

The reaction used in the identification of starch is that between starch and iodine. The reaction involves the adsorption of iodine onto the surface of the starch molecule and within the helix. It is known that amylose and amylopectin stain different colours (one blue the other red) and starch is a mixture of the two. The method was investigated in detail to ensure that other components within the sample would not interfere with the reaction.

Only small quantities of sample were required (250 µl) to produce the colour reaction. By scanning the stained feed between 250 and 1000 nm, changes in absorption with concentration were apparent. Experiments showed the method to be linear between concentrations of 250 to 2000 mg l^{-1}. The most sensitive wavelength appeared to be about 600 nm. It should, however, be noted that this method was developed by changing starch concentration alone, whilst composition (amylose:amylopectin ratio) remained the same. The absorption peak may change shape with composition and therefore any concentrations deduced should be treated carefully. However, the size and shape of the peak may be used to trace any changes in the starch concentration or composition.

The method development and validation is given below. The operating parameters for the Perkin Elmer lambda 2 spectrometer are given in Table A1:5.

ORDINATE	ABS	:	GRAPHICS PLOT	YES
WAV. MAX	1100 NM	:	ORD. MAX	1 ABS
WAV. MIN	380 NM	:	ORD. MIN	0 ABS
SPEED	960 NM/MIN	:	SCALE	50.0 NM/CM
SMOOTH	2 NM	:	GRID	YES
LAMP	UV+VIS	:	OVERLAY	NO
BACK CORR	&YES	:	PRINT DATA	YES
ACCESSORY	MANUAL	:	THRESHOLD	0.1 ABS
SAMPLES/BATCH	3	:	AUTOMETHOD	ON
START SAMPLE	1	:	OPER. ID	0000
CYCLES	1	:	SAMPLE ID	
CYCLE-TIME	1.2 MIN	:		

Table A1:5: Spectrometer settings for starch analysis.

Initial trial-

A sample of 0.001M iodine solution was obtained, as detailed in the analysis chapter, resulting in a pale straw coloured solution. A stock solution of 1500 mg l^{-1} starch solution was then prepared. Three samples were prepared containing 250 µl starch solution and/or 1 ml iodine solution with their volumes made up to 4 ml with DI water. These solutions were poured into quartz cuvettes and the absorption measured from 1000 down to 190 nm on a Perkin Elmer lambda 2 UV/vis spectrophotometer, with background correction.

The results of the initial trial are shown in Figure A1:1. It can clearly be seen that starch solution showed little/no absorbance down to 300 nm and iodine solution showed little/no absorbance down to 500 nm, but produced two peaks between 275 and 500 nm, with further peaks below this value. The stained starch gave a broad peak between 400 and 900 nm and then displayed the iodine peaks. This suggested that there was excess iodine present.

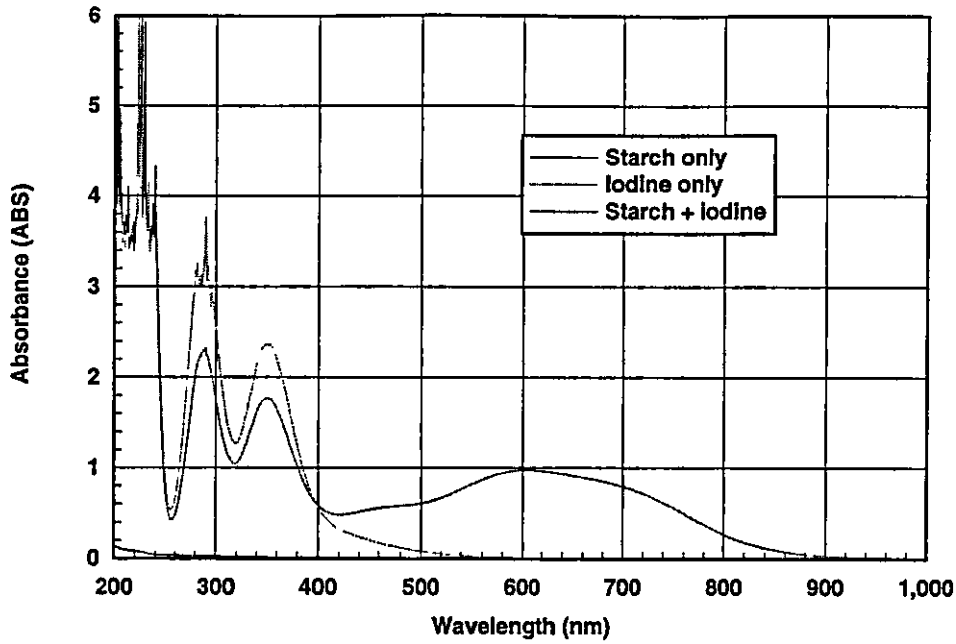

Figure A1:1: Absorbance measurements - initial trial.

Effect of iodine concentration-

In order to investigate the effect of iodine concentration, four samples were prepared, each containing 250 µl of starch solution. Volumes of 200, 400, 600 and 800 µl 0.001M iodine solution were added to each sample and the total volume made up to 4 ml with DI water.

The effect of iodine concentration is shown in Figure A1:2. As expected the iodine peaks increased with concentration. However, it was also clear that the stained starch peaks also increased, indicating that the presence of more iodine shifted the equilibrium of the reaction.

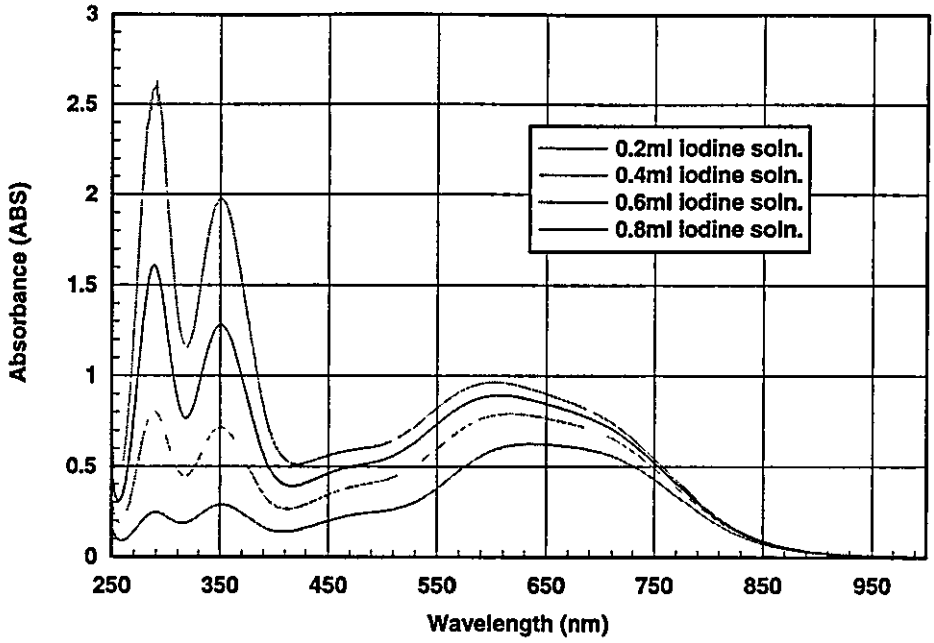

Figure A1:2: Absorbance measurements - effect of iodine concentration.

Effect of starch concentration-

In order to investigate the effect of iodine concentration, four samples were prepared, each containing 1 ml of 0.001M iodine solution. Volumes of 50, 100, 150 and 200 µl starch solution were added to each sample and the total volume made up to 4 ml with DI water.

The effect of starch concentration is shown in Figure A1:3. It can be seen that the stained starch peak increased with concentration, whilst the iodine peak remained constant. Overall, these results indicated that the method was suitable and that enough iodine was present.

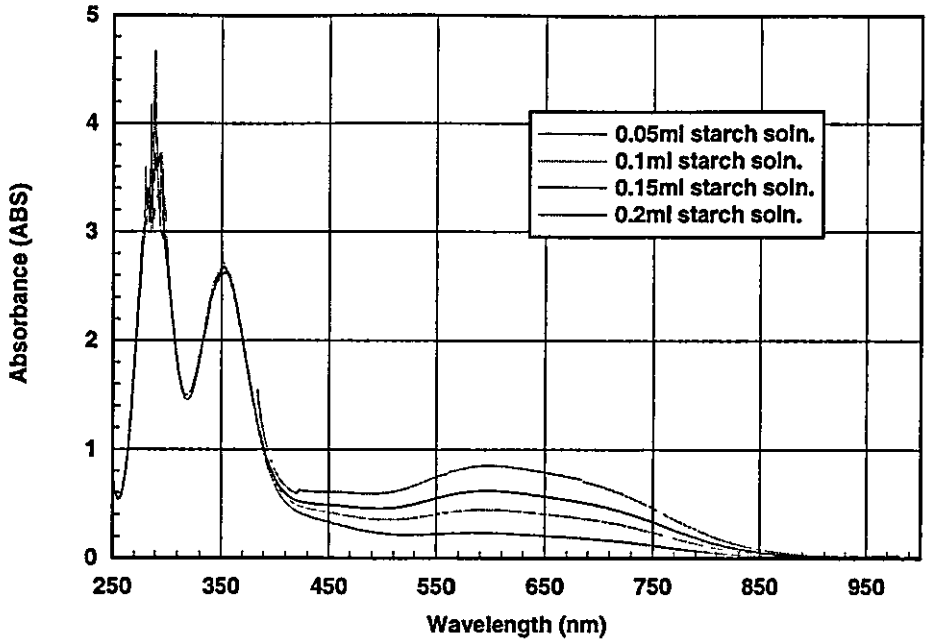

Figure A1:3: Absorbance measurements - effect of starch concentration.

Potential interferences and linearity-

A set of samples were produced at starch concentrations of 250, 500, 1000 and 1500 mg l^{-1} in both starch free feed and DI water. 250 µl aliquots were diluted with 2750 µl DI water in a test tube, with 1 ml iodine solution added prior to absorbance measurements.

The results in Figure A1:4 suggest that other components in the model beer stream did not interfere significantly with this test method. The absorbance figures were obtained by measuring the peak height from a paper copy of the absorbance - wavelength plot. It may also be seen that measuring absorbance at 600 nm is more sensitive to concentration than measuring at 500 nm.

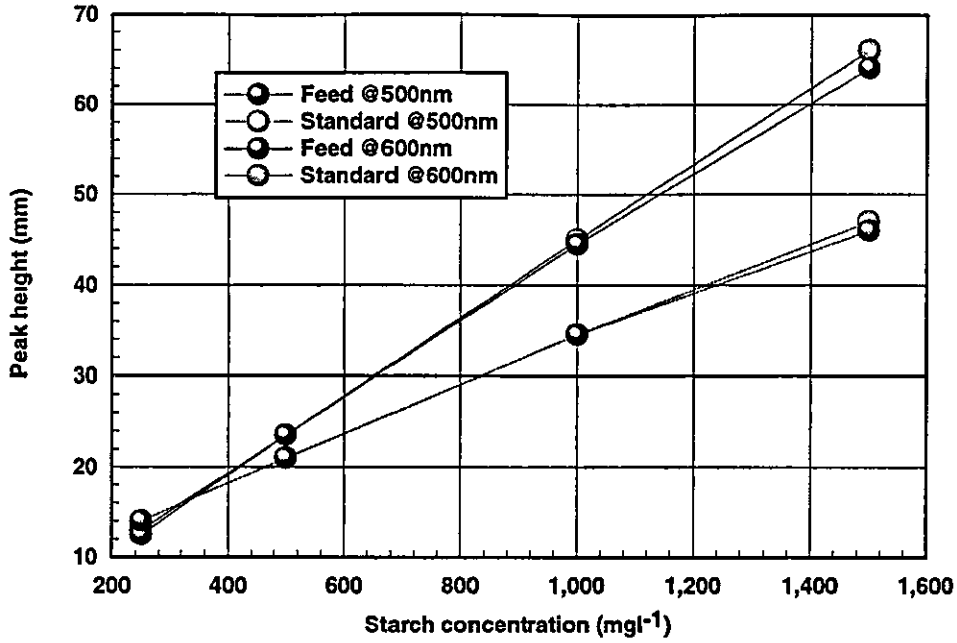

Figure A1:4: Absorbance measurements - linearity and optimisation.

Conclusion:

These results suggest that measuring the absorbance at 600 nm of 250 µl of sample in 2750 µl DI water with 1 ml 0.001M iodine added should give an indication of the starch concentration. It should however be noted that the effect of changing starch composition or molecular weight are not known. Hence care must be taken with results, although any changes in size or shape of the stained starch peak would indicate changes in the starch component of samples.

A1:3 PROTEIN ANALYSIS

The method of protein analysis, namely the Microprotein-PR™ kit supplied by Sigma, did not require validation as it is stated that the kit is linear from 1-2000 mg l^{-1} with a list of interfering substances provided. They are phosphate (inorganic), Ca^{2+}, Mg^{2+}, creatine, urea, glucose, uric acid, citrate (sodium), oxalate (sodium) and ascorbate (sodium), all of which affect the total protein measurement by less than 5%. This value was insignificant with respect to the data obtained.

A1:4 CALCIUM ANALYSIS

Calcium analysis was performed on a Perkin Elmer 3030 atomic adsorption spectrophotometer. The instrument works by burning the sample and measuring the adsorption of a discrete wavelength of light, characteristic of the metal in question. It was therefore unlikely that other components would affect the method, but this was checked. A series of standards (25, 50, 100, 125 and 150 mg l^{-1}) were prepared in both de-ionised water and feed solution using $CaCl_2$ as the source of calcium ions. 200 µl aliquots of these standards were then diluted in 5ml of DI water prior to analysis. The plot of feed adsorption against standard adsorption are shown in Figure A1:5. It may be seen that the line through the data has a gradient of 1 indicating that other components do not interfere.

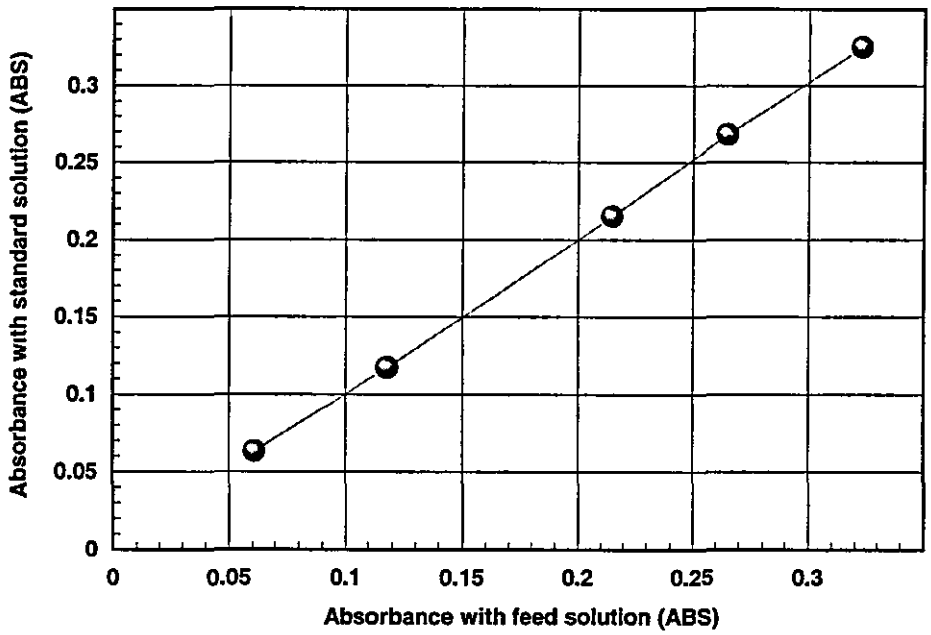

Figure A1:5: Validation of Ca^{2+} measurement by AA.

A1:5 CATECHIN ANALYSIS

Methods of polyphenol analysis used in the brewing industries tend to involve a separation step, removing the polyphenol from the other components, redissolving it and finally determining its concentration. Although the model solution contains several components, there is generally only one component with a given chemistry. The method using ferric chloride ($FeCl_3$) was used here. It does not require a separation step. The method viability and subsequent validation is given below.

Initial investigation-

Initially four samples were prepared (DI water, 100 mg l^{-1} catechin, feed without casein and 100 mg l^{-1} casein) and their pH set to 10 with 0.25M Na_2CO_3 solution. 2 ml aliquots were then added to a set of test tubes containing 1ml DI water. Five minutes prior to analysis, 500 µl of 0.15M $FeCl_3$ solution was added to each tube. The samples were poured into quartz cuvettes and placed in a Perkin-Elmer lambda 2 UV/vis spectrophotometer. Their absorbance was measured from 1000 nm to 190 nm against a DI water blank. In all cases there was considerable absorbance below 400 nm. Table A1:6 summarises the results.

Sample	Observation
DI water	v. little/no absorbance above 600 nm, rising below 600 nm.
100 mg l^{-1} catechin	obvious absorbance, rising slowly 1100-550 nm, then more sharply 550-400 nm.
feed without casein	slight absorbance below 600 nm (probably scattering), then as for DI water.
100 mg l^{-1} casein	slightly greater absorbance than DI water (but v. little) above 600 nm, then as for DI water.

Table A1:6: Observed absorbance of the four samples.

The data suggest that the method was of use but any absorbance due to scattering would have to be removed, i.e. by measuring against a blank feed sample or spinning solids out. It appeared that the best region to measure the absorbance was around 600-650 nm as the $FeCl_3$ blank showed no absorbance at these wavelengths, whilst the catechin containing sample showed an appreciable absorbance.

Effect of $FeCl_3$ conc.-

In order to investigate the effect of $FeCl_3$ concentration, four samples were studied. Each sample contained 20 µl 0.25M Na_2CO_3 solution and 2 ml 200 mg l^{-1} catechin solution. 1.5 ml $FeCl_3$ at concentrations of 0.15, 0.125, 0.1 and 0.75M were then added to each tube five minutes prior to absorbance measurements. The results at 600 and 650 nm are shown in Figure A1:6.

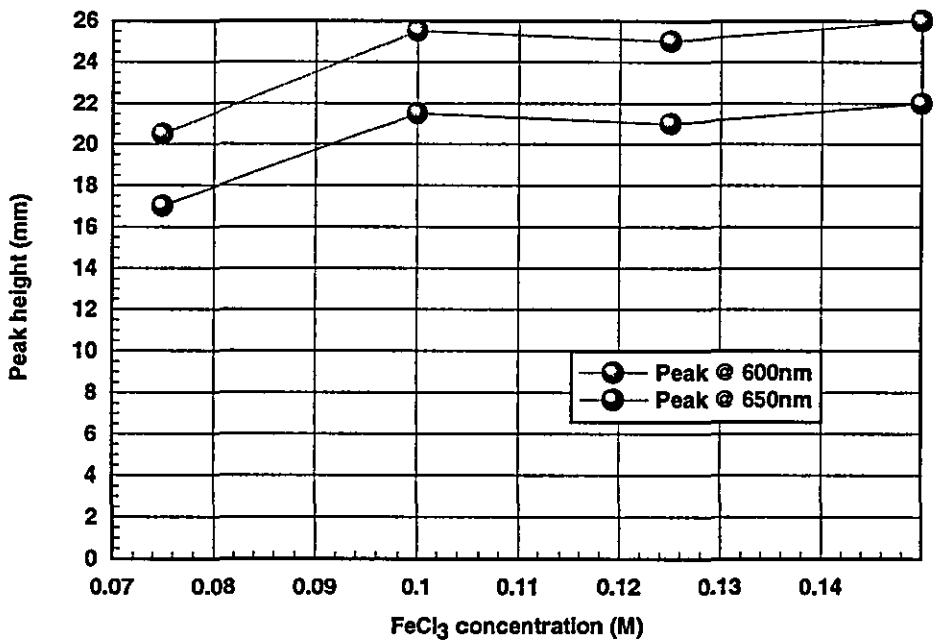

Figure A1:6: Effect of $FeCl_3$ on absorbance.

There appeared to be little effect of $FeCl_3$ concentration on absorbance between concentrations of 0.1-0.125M.

Effect of reaction time-

In order to investigate the effect of reaction time a single sample was prepared using 0.2 µl 0.25M Na_2CO_3 solution, 500 µl 0.15M $FeCl_3$ solution 2 ml 100 mg l^{-1} catechin solution and 1 ml DI water. The sample was then placed in a quartz cuvette and its absorbance measured after 1, 2, 3, 5, 10 and 15 minutes. The results at 600 and 650 nm are shown in Figure A1:7. It highlights the need to specify a reaction time. If the samples were left for too long particulates formed and dropped out of solution.

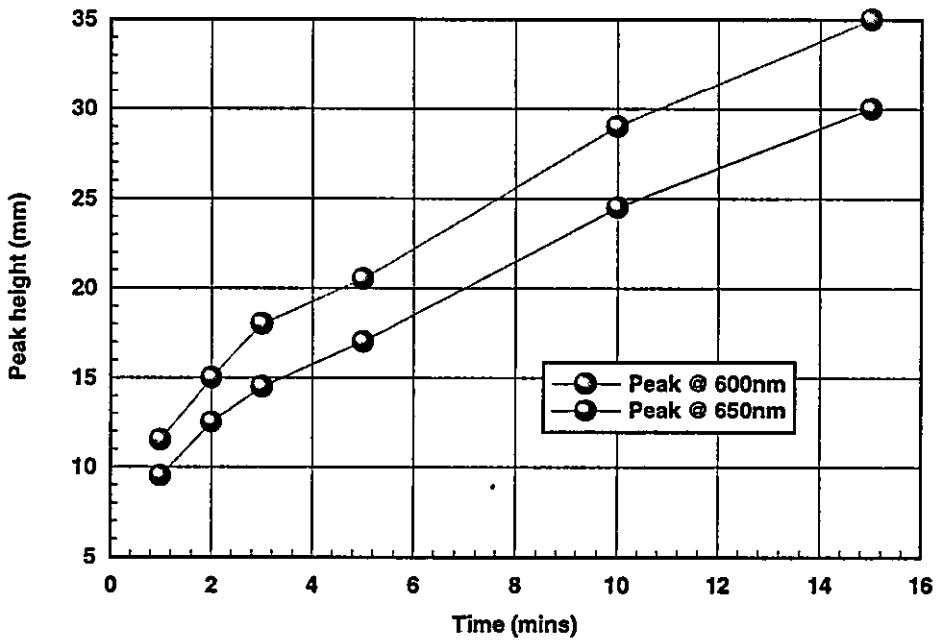

Figure A1:7: Effect of reaction time on absorbance.

Effect of Na_2CO_3 conc.-

In order to investigate the effect of Na_2CO_3 concentration, four samples were studied. Each sample contained 2ml 100 mg l^{-1} catechin solution, 1 ml DI water and 500 µl 0.15M $FeCl_3$ solution. 40 µl sample at concentrations of 0, 0.0625, 0.1875, 2.5M Na_2CO_3 solution were then added to each tube five minutes prior to absorbance measurements. The results at 600 and 650 nm are shown in Figure A1:8.

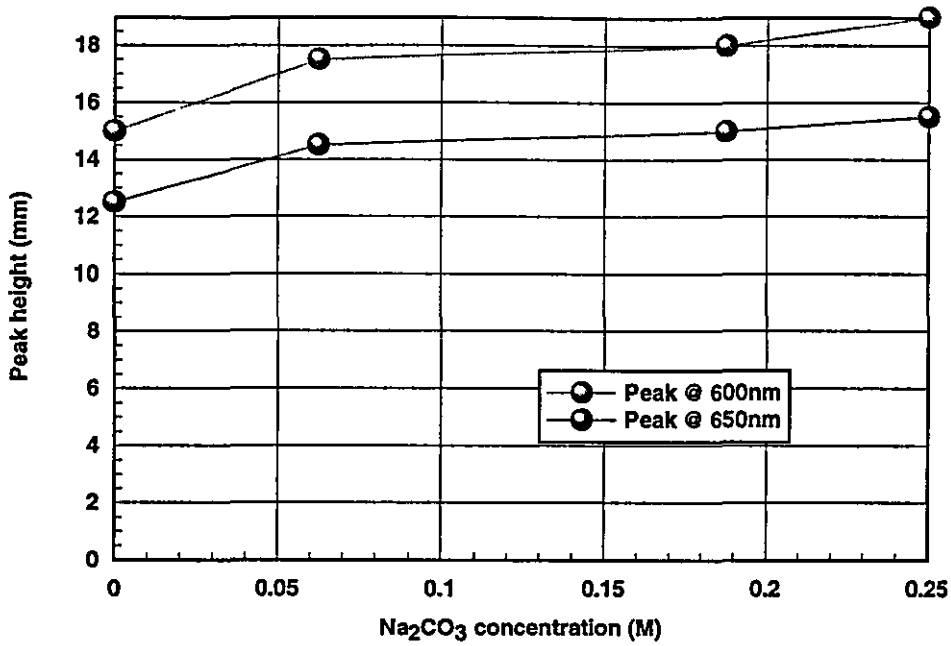

Figure A1:8: Effect of Na_2CO_3 concentration on absorbance.

Calibration-

A calibration curve was prepared by reacting 3 ml of sample (@ pH 10) with 500 µl 0.15M $FeCl_3$ with the absorbance of the resultant mixture measured at 600 and 650 nm after a reaction time of 3 minutes. The resulting curve is shown in Figure A1:9.

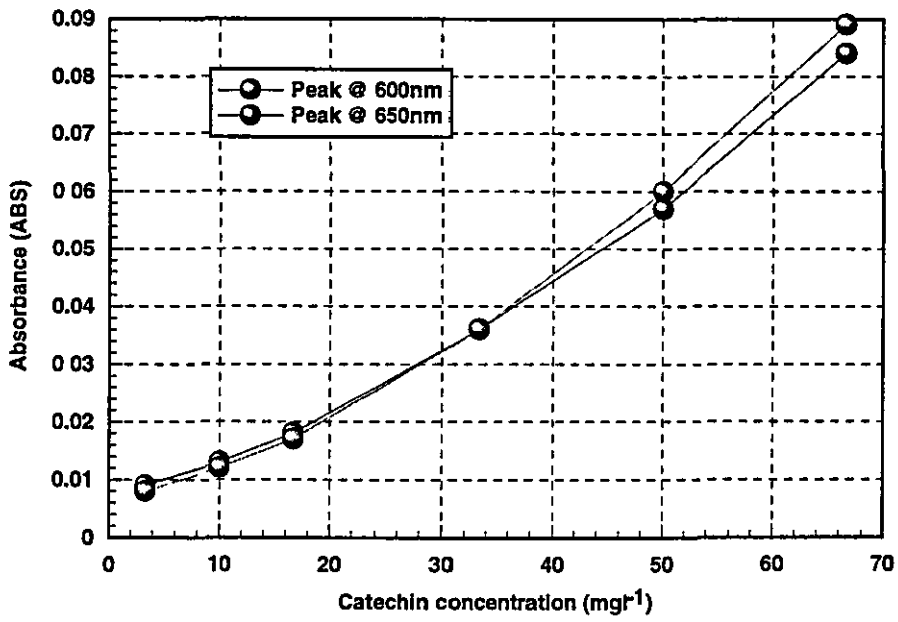

Figure A1:9: Effect of sample concentration.

A1:6 SUCROSE ANALYSIS

The method used for sucrose analysis is for the determination of total carbohydrate content of food such as cereals and jams. It consists of hydrolysing the polysaccharides/saccharides into their constituent monosaccharides, i.e. glucose and fructose. Disaccharides such as maltose consist solely of glucose rings as does starch, whilst lactose contains both glucose and galactose However, sucrose consists of a glucose and fructose ring combined, so hydrolysis will result in the formation of both these monosaccharides.

The reason for attempting this method was that the aminex HPX-87H column would not detect the sucrose molecule (it inverts). It would, however, detect both glucose and fructose. Therefore, sucrose could be analysed indirectly after complete hydrolysis. The colour reaction employed here was used to ensure total hydrolysis.

Method:

Two 10 ml of samples of sucrose standard were pipetted into boiling tubes. 1 ml of 1.5M sulphuric acid was added to one (tube 1) and 0.5 ml to the other (tube 2). Both boiling tubes were placed in a boiling water bath for 25 minutes and allowed to cool. 1.2 ml of 10% NaOH was added to tube 1 and 0.6 ml to tube 2 and both tubes mixed. The tubes were then made up to 20 ml with DI water. 2 ml samples from each tube were then pipetted into clean test tubes. 1.0 ml of DNS reagent (3,5-dinitrosalicyclic acid) was added to each tube. The tubes were heated in a boiling water bath for 5 minutes, cooled, their volumes adjusted to 20 ml and mixed. The absorbance was then measured at 540 nm on a Perkin Elmer lambda 2 spectrometer.

To calibrate the method, a set of glucose standards were produced at concentrations of 0, 0.25, 0.5, 1.0, 1.25, 1.5 mg ml^{-1}. 1ml aliquots were pipetted into a series of boiling tubes. 1.0 ml DNS and 3 ml DI water were added to each and boiled for 5 minutes. They were then cooled and made up to 20 ml with DI water. The absorbance was again read at 540 nm.

The calibration graph is shown in Figure A1:11. As the two hydrolysed samples gave the same absorbance values, they were proved to be fully hydrolysed. Therefore the smaller quantities of acid and base were sufficient.

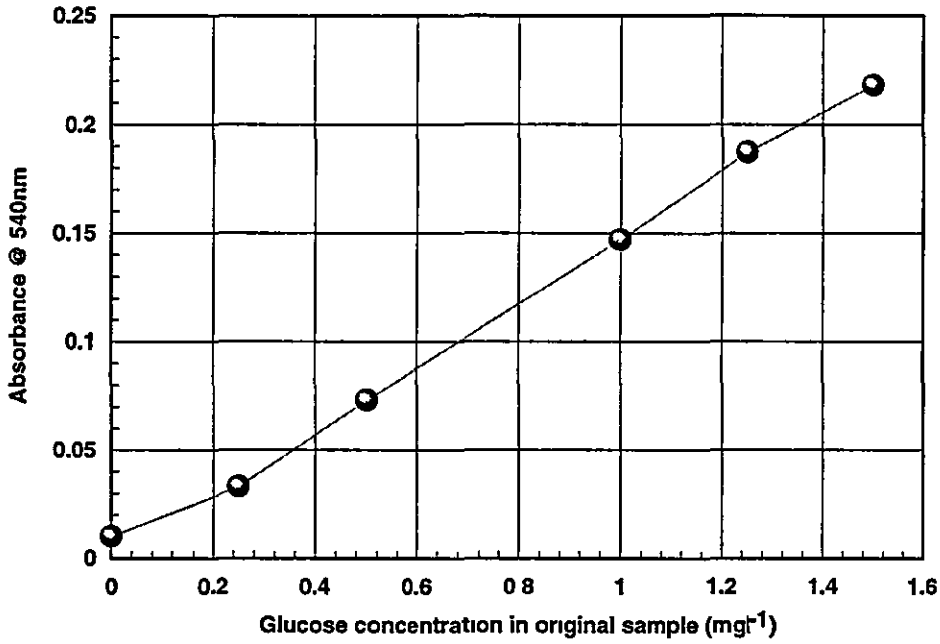

Figure A1:11: DNS method calibration.

On injection into the HPLC column, two clear peaks for glucose and fructose were observed (Figure A1:12). A noticeable difference between this chromatogram and those previous was the large thin spike where there was previously a small negative peak. The reason for this was that usually the negative peak was merely the water in which the samples are dissolved. However, with the hydrolysates the thin spike was almost certainly due to the Na^+ and SO_4^{2-} ions , used for acidification and subsequent neutralisation, passing straight through the column.

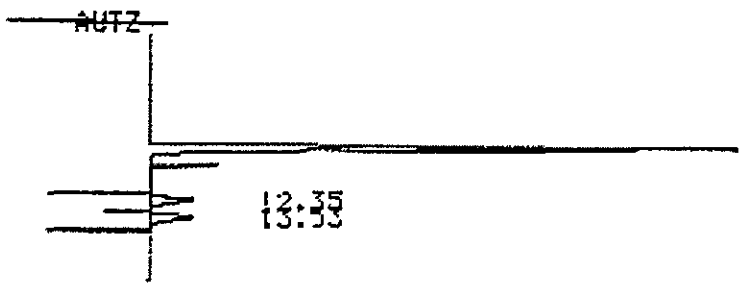

Figure A1:12: Sample chromatogram.

APPENDIX 2:
CALCULATIONS

A2.0 INTRODUCTION

This section contains an outline of the theory and equations used for various calculations in the body of the thesis

A2.1 VARIATION OF ACID SPECIES WITH pH

The fraction of acid species present in solution may be calculated from a knowledge of the equation(s) of dissociation, the pH and the acid dissociation constants. For example, take the acid HA in aqueous solution, such that;

$$HA \Leftrightarrow H^+ + A^- \qquad \text{(A2.1)}$$

The acid dissociation constant K_a is defined as;

$$K_a = \frac{[H^+][A^-]}{[HA]} \qquad \text{(A2.2)}$$

whereby square brackets denote concentrations. It should be noted that an acid with more than one acid group will have more than one K_a value. The pH and pK_a are then defined by;

$$pH = -\log_{10}[H^+] \qquad pK_a = -\log_{10}[K_a] \qquad \text{(A2.3)}$$

By rearranging equations A2.2 and A2.3 the ratio of acid species to unionised acid may be calculated;

$$\frac{[A^-]}{[HA]} = \frac{10^{(-pK_a)}}{10^{(-pH)}} \tag{A2.4}$$

If it is assumed that there is 1mol of solid is dissolved in1dm^{-3} then,

$$[HA] = 1 - [A^-] = 1 - \left(\frac{10^{(-pK_a)}}{10^{(-pH)}}[HA]\right) = 1 - [HA]x \tag{A2.5}$$

$$[HA] = \frac{1}{1+x} \tag{A2.6}$$

Hence [HA] may be calculated at a given pH from equation A2.6 and [A$^-$] may be deduced from equation A2.5.

A2.1.1 Acid dissociation constants

The table below summarises the dissociation constants for acetic, succinic and citric acids (Kirk-Othmer (1979) and Weast (1982)).

	pK_a
Acetic acid	4.75
Succinic acid	4.16
	5.61
Citric acid	3.14
	4.77
	6.39

Table A2.1: Acid dissociation constants.

A2.1.2 Sample calculation

Citric acid contains three acids groups and therefore has three dissociation constants, as detailed below;

$$H_3Cit \Leftrightarrow H^+ + H_2Cit^- \qquad K_1 = \frac{[H^+][H_2Cit^-]}{[H_3Cit]} \qquad (A2.7)$$

$$H_2Cit^- \Leftrightarrow H^+ + HCit^{2-} \qquad K_2 = \frac{[H^+][HCit^{2-}]}{[H_2Cit^-]} \qquad (A2.8)$$

$$HCit^{2-} \Leftrightarrow H^+ + Cit^{3-} \qquad K_3 = \frac{[H^+][Cit^{3-}]}{[HCit^{2-}]} \qquad (A2.9)$$

By rearranging and combining these equations;

$$\frac{[H_2Cit^-]}{[H_3Cit]} = \frac{K_1}{[H^+]} \qquad (A2.10)$$

$$\frac{[HCit^{2-}]}{[H_3Cit]} = \frac{K_1K_2}{[H^+]^2} \qquad (A2.11)$$

$$\frac{[Cit^{3-}]}{[H_3Cit]} = \frac{K_1K_2K_3}{[H^+]^3} \qquad (A2.12)$$

Hence, the ratios of the species may be calculated at any pH. A simple mass (mole) balance on the system, as in equation A2.5, gives;

$$[H_3Cit] = 1 - [H_2Cit^-] - [HCit^{2-}] - [Cit^{3-}] \qquad (A2.13)$$

Dividing equation A2.13 by $[H_3Cit]$, substituting equations A2.10-A2.12 .for the resulting species ratios and rearranging gives;

$$[H_3Cit] = \frac{1}{1 + \frac{K_1}{[H^+]} + \frac{K_1K_2}{[H^+]^2} + \frac{K_1K_2K_3}{[H^+]^3}} \qquad (A2.14)$$

K_a and $[H^+]$ may then be deduced from pK_a and pH using equation A3.3. Once $[H_3Cit]$ has been calculated, it may be substituted into equations A3.10-A3.12 to give the concentration of the other species.

A2.2 CALCULATION OF MOLECULAR RADIUS, SURFACE AREA AND VOLUME.

In order to give an approximate molecular radius, the volume of a molecule may be calculated from its molecular weight and molar density and then dividing by Avogadro's number to give a volume for a single molecule (equation A2.15). However, available density values are for acetic and succinic acids in the liquid form and citric acid in the solid form. Therefore, the molar volumes, V_m, calculated by partial group methods were used. The molecular volume may be calculated by dividing the molar volume by Avogadro's number (equation A2.16). The molecular radius may then be deduced from simple geometry (equation A2.17).

$$V = \frac{M}{\rho N_A} \qquad (A2.15)$$

$$V = \frac{V_m}{N_A} \qquad (A2.16)$$

$$V = \frac{4\pi}{3} r^3 \qquad (A2.17)$$

where V is the molecular volume, M is the molecular weight (kg), ρ is the density (kgm^{-3}), N_A is avogadro's number ($6.022 \times 10^{26} mol^{-1}$) and r is the molecular radius (m). Rearranging the latter equations yields;

$$r = \sqrt[3]{\frac{3V}{4\pi}} \qquad \text{(A2.18)}$$

The surface area, A_s, may then be calculated by simple geometry (equation A2.19);

$$A_s = 4\pi\ r^2 \qquad \text{(A2.19)}$$

The charge density, σ (Cm^{-2}), may then be taken as the charge on the molecule divided by the surface area (equation A2.20);

$$\sigma = \frac{ke}{A_s} \qquad \text{(A2.20)}$$

where k is the charge on the molecule (i.e., -1, -2, -3) and e is the charge on an electron (1.602×10^{-19}C). A comparison of calculated charge density by density and group contribution methods is shown in Table A2.2.

	Charge density ($C\ m^{-2}$)	
	Density	Group contributions
Ac^-	-0.159	-0.169
$HSuc^-$	-0.133	-0.134
Suc^{2-}	-0.265	-0.268
H_2Cit^-	-0.095	-0.121
$HCit^{2-}$	-0.189	-0.243
Cit^{3-}	-0.284	-0.364
Ca^{2+}	+0.541	+0.538

Table A2.2: Summary of charge densities.

A2.3 CALCULATION OF CHANGE IN PORE SIZE.

Assuming the membranes to consist of a series of cylindrical pores, the flow/pressure drop/pore size dependence could be approximated by the equation for streamline flow in a cylindrical pipe;

$$u = \frac{d^2}{32\mu}\frac{\Delta P}{l} \qquad \text{(A2:21)}$$

where u is the pore velocity (m s^{-1}), d is the pore diameter (m), l is the pore length (m) and ΔP is the pressure drop across the membrane (N m^{-2}). Assuming all pores to be of the same diameter, the total number of pores through a membrane of area A is;

$$N = A \times \varepsilon \times \frac{4}{\pi \times d^2} \qquad \text{(A2.22)}$$

where A is the total membrane area (m^2) and ε is the porosity The volumetric flow rate (m^3 s^{-1}) through the membrane is;

$$Q = J \times A \qquad \text{(A2.23)}$$

where J is the permeate flux (m^3 m^{-2} s^{-1}). The pore velocity may then be calculated from the volumetric flow rate through the membrane, Q (m^3 s^{-1}), the pore diameter and the number of pores, N;

$$u = \frac{Q}{N} \times \frac{4}{\pi d^2} \qquad \text{(A2.24)}$$

Substituting equations A2.22 and A2.23 into A2.24 yields;

$$u = \frac{J}{\varepsilon} \qquad \text{(A2.25)}$$

Combining equations A2.25 and A2.21 and rearranging;

$$d = \sqrt{\frac{32\mu l J}{\varepsilon \times \Delta P}} \qquad \text{(A2.26)}$$

For a steady state flux of 250 l m^{-2} h^{-1}, a membrane thickness of 120 μm, a porosity of 0.78 and a pressure drop of 1.9 bar, the calculated pore size is 0.044 μm. Calculating the molecular radius of citric acid as in Section A2.2, using a molecular weight of 192.14 kg and a density of 1665 kg m^{-3}, yields a radius of 0.36 nm. To check the validity of this method the clean water flux at 10 psi was calculated for the same membrane as above. The calculated value of 15 ml cm^{-2} min^{-1} compares favourably with the experimental value of 13.1 ml cm^{-2} min^{-1}.

APPENDIX 3:
MEMBRANE CHARACTERISATION

A3.0 INTRODUCTION

This section contains the procedures used to characterise the membrane thickness, pore size, permeability and clean water flux.

A3.1 MEMBRANE THICKNESS

Samples of membrane were cut in the usual way as used during experimentation. Their thickness was then carefully measured at five different places on the sample using a micrometer. It was not found that the thickness varied. The results are given in Table A3.1.

Membrane	Thickness (μm)
PES	150
CN	110
PA	120
PC	10

Table A3.1: Membrane thickness.

A3.2 MEMBRANE PORE SIZE

Membrane pore size and pore size distributions, amongst others, may be measured with a porometer (Coulter porometer II, Coulter Electronics Ltd). The membrane sample was cut into a 35mm disc and wetted with a low surface tension, low vapour pressure and low reactivity wetting agent, such as Coulter porofil or 3M Fluorinert™. After 60 seconds soaking, the membrane was placed in the 35mm membrane holder

on the porometer. All membranes were then analysed for pores in the range 0.1 to 0.6 μm.

The instrument works by displacing the wetting agent from the pores by means of compressed air. The air pressure is increased so as to displace the fluid from smaller and smaller pores. The flow rate of air passing though the sample is measured as a function of pressure. Finally the same sample is tested dry. The instrument then calculates the pore size distribution from these values. It should be noted that the model used assumes that the pores are continual cylinders through the membrane. This is only the case for the polycarbonate membrane as the others have tortuous structures. Also, it does not take into account the orientation of the membrane being tested. The results are given in Table A3.2.

Membrane	Min.	Max.	Mean	Pore density
	μm	μm	μm	$*10^9$ cm^{-2}
PES	0.316	0.566	0.437	10.0
CN	0.260	0.426	0.348	16.6
PA	0.185	0.471	0.363	23.8
PC	0.208	0.261	0.237	7.4

Table A3.2: Membrane pore size and density.

A3.3 CLEAN WATER FLUX AND PERMEABILITY

The permeability and clean water fluxes of the membranes were tested using a permeameter. Membrane samples were placed in a sample holder, in this case 47mm in diameter. The sample cell was then filled with deionised water that had been passed through a 0.45 μm membrane to remove any particulates. In this way the permeability of an unfouled membrane could be measured. The system was then pressurised to the required pressure (10 psi for clean water flux measurement). The inlet to the test cell was opened and the time to collect a measured volume was recorded. The results are

given in Table A3.3. The permeability was calculated from Darcy's law, below. All tests were carried out at room temperature.

$$k = \frac{u\mu dz}{dP} \qquad \text{A3.1}$$

where k is the permeability, dP the pressure drop across the filter, dz the thickness of the membrane, μ the viscosity of water at the test temperature and u is the superficial velocity (volume flow rate per cross sectional area of membrane) of the water.

Membrane	Permeability	Clean water flux (@10psi)
	m^2	$ml\ cm^{-2}\ min^{-1}$
CN	$4.3*10^{-15}$	13.1
PES	$4.2*10^{-15}$	11.5
PC	$4.0*10^{-16}$	16.7
PA	$2.4*10^{-15}$	8.4

Table A3.3: Permeability and clean water flux of membranes used.

APPENDIX 4:
DEFINITION OF UNITS

A4.0 INTRODUCTION

This section contains definitions of the units used throughout the thesis. Most units are defined by standard methods laid down by the European Brewery Convention (EBC).

A4.1 Degrees Plato (°Pl):

Degrees Plato are a unit of wort strength/density. Specific gravity measurements may be converted into % extract or degrees Plato using tables calculated by F. Plato, for sucrose solutions. Such a table is shown below;

SG @ 20°C	% extract/°Pl
1.00250	0.641
1.00748	1.918
1.01247	3.185
1.01745	4.439
1.02242	5.682
1.02740	6.917
1.03238	8.140
1.03736	9.352
1.04234	10.554
1.04731	11.745
1.05227	12.925

Table A4:1: Table for conversion from SG to % extract/°Pl.

A4.2 Bitterness (EBU):

The EBC method for the determination of bitter substances is as follows. 10.0 ml of degassed acidified beer is mixed with 20 ml of isooctane (2, 2, 4-trimethylpentane) and centrifuged. The absorbance of the isooctane layer is then read in a 1 cm cell at 275 nm against a pure isooctane blank. The bitterness is then given by;

$$\text{Bitterness (EBU)} = 50 \times \text{Absorbance}$$

A4.3 Colour (EBC):

To determine the colour of a beer following the EBC method, beers must firstly be turbidity free (less than 1 EBC). This may be achieved by filtering through a membrane. The absorbance is then read in a 10mm cell at 430 nm against a DI water blank. Samples should be diluted if the absorbance exceeds 0 8. The colour is then given by;

$$\text{Colour (EBC)} = \text{Absorbance} \times \text{dilution factor} \times 25$$

A4.4 Haze (EBC):

The EBC method for measuring haze is based on a diluted formazin haze standard. 1.00 g of hydrazinium sulphate is dissolved in 100 ml of DI water and allowed to stand for 4 hours. 10.00 g of hexamine are then dissolved in 100 ml of DI water. Equal quantities of the two solution are then mixed by gentle stirring in a stoppered bottle. The solution is then left to stand for 24 hours in a water bath at 25 ± 3°C. This results in a 1000 formazin haze unit standard. 10 ml of this standard are then diluted to 100 ml with DI water to produce a 100 formazin haze unit standard. A series of standards may then be made by diluting V1, V2....Vi ml of the 100 formazin haze unit standard to 100 ml with DI water. This produces solutions containing V1, V2....Vi EBC formazin haze units. These standards may then be used to calibrate a

nephelometer type haze meter. Subsequent analysis of samples may then be expressed in EBC formazin haze units.